universität wien

MASTERARBEIT / MASTER'S THESIS

Titel der Masterarbeit / Title of the Master's Thesis

„Examination of some subcellular structures of *Physcomitrella patens* using confocal microscopy"

verfasst von / submitted by

Katrin Thiering BSc

angestrebter akademischer Grad / in partial fulfilment of the requirements for the degree of

Master of Science (MSc)

Wien, 2018 / Vienna 2018

Studienkennzahl lt. Studienblatt / degree programme code as it appears on the student record sheet:	A 066 832
Studienrichtung lt. Studienblatt / degree programme as it appears on the student record sheet:	Masterstudium Botanik
Betreut von / Supervisor:	ao. Univ.-Prof. Mag. Dr. Ingeborg Lang
Mitbetreut von / Co-Supervisor:	

Acknowledgements

Thanks to all the members of the Core Facility Cell Imaging and Ultrastructure Research Team (University of Vienna, Faculty of Life Sciences), which were supporting me so nicely and giving advice every time when needed. A great thank you to my supervisor Mag. Dr. Ingeborg Lang (Core Facility Cell Imaging and Ultrastructure Research, Faculty of Life Sciences. University of Vienna), because she helped me a lot and encouraged me to improve myself. A special thanks to Dr. Magdalena Bezanilla (Department of Biological Sciences, Dartmouth College, Hanover, USA) for providing the cell lines, without them my work would not have been be possible.

Contents

Abstract

Mosses are the first land plants and therefore differ from algae and they are evolutionary separated from the vascular plants. In comparison to the vascular plants, the gametophytic plant is dominant in mosses. This gametophyte can be easily investigated and because of its haploidy, genetic modifications are easily done. For *Physcomitrella patens* are GFP cell lines available; these can be used to study some subcellular structures with confocal microscopy, as done in the present work.

The aim of this study was to analyse the subcellular structures in *P. patens*, how they look like and how they respond to osmotic stress meaning that those strands contain ER, actin and tubulin.

The Endoplasmic reticulum (ER) cell line showed the ER near the plasma membrane; this was proven by labelling with the styryl dyes FM 1-43 and FM 4-64. Furthermore, the nuclear envelope and the dynamic network of cisternae and tubules formed by the ER were seen. Under osmotic stress, the cisternae were aggregating and getting fewer.

The Life-act cell line showed the actin in the cortex of the cell, around the nucleus and a network between chloroplasts. Unfortunately, labelling the actin filaments with the Rhodamine phalloidin did not work in living cells. During plasmolysis, the actin filaments formed ring structures near the chloroplasts and enclosed them within the actinfilaments.

The GFP-Tub cell line showed that the microtubules enclosed the chloroplasts within the microtubules. Furthermore, it was also shown in close vicinity to the plasma membrane and around the nucleus. Under plasmolysis the tubulin was aggregating around the chloroplasts and formed rings around them.

The Myosin VIII, Reticulon and Calnexin cell lines did not show the structures known from literature.

When plasmolysed, the cell lines of ER, Life-act and GFP-Tub of *P. patens* showed in the leaflets and protonemata the Hechtian strands.

Zusammenfassung

Moose sind die ersten Landpflanzen und unterscheiden sich deshalb von Algen und sie sind evolutionär von den Gefäßpflanzen getrennt. Im Unterschied zu den Gefäßpflanzen ist in Moosen die gametophytische Pflanze dominant. Dieser Gametophyt eignet sich gut für zelluläre Untersuchungen und aufgrund seiner Haploidität sind genetische Modifikationen leicht zu erreichen. Für *P. patens* sind GFP-markierte Zelllinien vorhanden; diese können benutzt werden um spezifische Strukturen im Zellinneren mit Konfokal-Mikroskopie zu untersuchen, wie es in dieser Arbeit mit vielen Zelllinien durchgeführt wurde.

Das Ziel dieser Arbeit war es die subzellulären Strukturen in *P. patens* zu analysieren, zu dokumentieren und zu dokumentieren wie sie auf osmotischen Stress reagieren.

Die Endoplasmatische Reticulum (ER) Zelllinie zeigte das ER in der Nähe der Plasmamembran, dies wurde durch Färben mit den Styryl Färbungen FM 1-43 und FM 4-64 überprüft. Weiters sieht man die vom ER geformte Kernhülle und das dynamische

Netzwerk aus Zisternen und Röhren. Unter osmotischem Stress fügten sich die Zisternen zusammen und wurden weniger.

Die Life-act Zelllinie zeigte das Aktin im Cortex der Zelle, um die Kernhülle und als Netzwerk zwischen den Chloroplasten sichtbar. Leider funktionierte das Färben der Aktinfilamente mit Rhodamine phalloidin in lebenden Zellen nicht. Während der Plasmolyse formten die Aktinfilamente eine Ring-Struktur nahe der Chloroplasten und umschlossen sie zwischen den Aktinfilamenten.

Die GFP-Tub Zelllinie zeigte, dass die Mikrotubuli die Chloroplasten zwischen den Mikrotubuli umschlossen. Weiters wurde es auch in der Nähe zu der Plasmamembran und um den Kern gezeigt.

Die Myosin VIII, Reticulon und Calnexin Zelllinie zeigten nicht die aus der Literatur bekannten Strukturen.

Wenn plasmolisiert, zeigten die Zelllinien von ER, Life-act und GFP-Tub von *P. patens* in den Blättchenzellen und im Protonemata die Hecht'schen Fäden, was darauf hinweist, dass ER, Aktin und auch Tubulin in den Fäden vorhanden ist.

1 Introduction

1. 1 Bryophytes

Bryophytes are evolutionary located between algae and the vascular plants. They are the first land plants and therefore have some features which neither belong to the algae nor to the vascular plants. Bryophytes comprise three major groups: the hornworts, the liverworts and mosses. Through genome duplication diversification occurs in the evolution of organism, this is also true for mosses like *P. patens* (Rensing et al. 2007). The evolution of mosses is different to *Arabidopsis thaliana*, but there are some genes which have the same function (tip growth), but different expression in *P. patens* and *A. thaliana* (Ortiz-Ramírez et al. 2016*)*. Therefore, morphological appearance differs, also concerning the subcellular structures. In mosses, the gametophytic generation dominates; they develop a long living gametophyte and a short living sporophyte. The haploid gametophyte produces leaflets, a stem and rhizoids. The gametophyte of protonema mosses also forms protonemata with caulonema cells with diagonally cell walls and less chloroplasts and chloronema cells with perpendicular cell walls and many chloroplasts. In this study the protonema cells were examined and also the leaflets.

P. patens belongs to the family of Funariaceae. This moss is just some millimetres high, so it can grow very fast on a small space, it is a cleistocarpous, ephemeric earth moss with lanceolate leaflets with a leaf-vein. Its upper leaflets are bigger, and its marginal is dentate (Frahm et al. 2004). It can also live in a variety of ecological conditions and is able to grow under laboratory conditions. *P. patens* is a model organism and is often used in genomic and plant development studies (Schaefer and Zrÿd 1997). Its genome was sequenced in 2007 and therefore can be used in genetic analysis (Quatrano et al. 2007). *P. patens* has an alternation of generations like seed plants, but its gametophyte, the haploid phase of the life cycle, is dominant, making it ideal for genetic studies (Cove 2005). In a genome study, it was shown that the mitochondrial genome remains a prototype in comparison to the land plant evolution (Terasawa et al. 2007). Many genetically alternated cell lines exist, for instance **GFP**-marked cell lines. Some of these cell lines were used in this study to investigate the ER and cytoskeleteon with specific labelling of subcellular structures and rearrangements in there of living cell lines. GFP stands for green fluorescent protein and is a commonly used reporter sequence, which is originally produced by the jellyfish *Aequorea victoria*. The sequence of interest (e.g. actin) is linked to the GFP-reporter sequence and then inserted into the moss genome. The transgenic organism then expresses the gene in an appropriate time and space. The product of the gene, the GFP-labelled protein, can then be easily observed with fluorescence techniques (Pierce 2006). Specific dyes (e.g. Rhodamine phalloidin) are an alternative to GFP-marked cell lines and were also used in this study.

Mielichhoferia elongata **and** ***Pohlia drummondii*** both belong to the family of Bryaceae. Both mosses are also protonema mosses and develop chloronema and caulonema cells. These two mosses were used as controls in the labelling experiments.

> *P. drummondii* has leaflets which are lanceolate or egg-shaped, without a leaf margin, they have a leaf vein and the leaflet cells are hexagonal to linear. In the

wild it grows mostly on earth (Frahm et al. 2004). The habitats of *P. drummondii* (www.swissbryophytes.ch) are pioneer corridors on forest roads, snowfields, alpine pastures and also crevices. They can be found from the montane to the nival altitudes and occur mainly in sunny locations. This moss can develop on various substrates, like sandy, stony, loamy soil and silicate sand, rock detritus and debris. *P. drummondii* is a green moss and under dry conditions it is moderately to clearly shining, due to oily droplets in the leaflet cells. Under natural conditions it forms loose to dense lawns, cushions or has scattered individual plants.

M. elongata (www.swissbryophytes.ch) is forming very dense, blue-green to yellowish-green cushions, which grow usually up to 5 cm high. Its natural habitats are shady rock formations containing heavy metals from the montane to the lower alpine level and they need mostly strongly acidic moist rocks. The leaflets are ovate, and they have a flat leaf margin getting dentate to the tip.

1. 2 Subcellular structures

The plant cell contains organelles like the nucleus, chloroplasts and mitochondria but needs also subcellular structures like the endoplasmic reticulum for transport of proteins, protein ripening in compartments and a cytoskeleton. Some of these structures are described in the following.

The **Endoplasmic reticulum (ER)** is spanning from the outer nuclear envelope through the whole cell (Heß 2004). The ER is a network of membrane enclosed channels and its lumen is separated only by a single membrane from the cytosol. The ER is divided in two domains: the smooth ER and the rough ER with associated ribosomes. The smooth ER is responsible for storage and release of calcium ions. In comparison, the rough ER is producing the proteins, which are necessary for the cell to survive (Bolsover 2004). The ER is responsible for the production, the processing, and the transport of proteins and lipids in the cell. It is not only necessary for transport of information within the cell, but also for the connectivity between plant cells. An overexpression of ER-protein is also able to affect mitochondrial shape (Mueller and Reski 2015). The ER is moved through the help of microtubules in animal (Waterman-Storer and Salmon 1998) and plant cells (Hamada et al. 2014).

Reticulon is a protein of the ER, it is responsible for the membrane curvature (Goyal and Blackstone 2013), and also for the formation of ER tubules (Tolley et al. 2010). All of the reticulons have a RTN homology domain and are present in all eukaryotes (Oertle and Schwab 2003). The hydrophobic regions are more conserved than the others (Nziengui and Schoefs 2009). Reticulon has the function of forming the curvature of the ER membrane and anchoring of enzymes in the membrane (Nziengui and Schoefs 2009). An overexpression of Reticulon leads to constrictions and so to more ER tubules (Tolley et al. 2008). This can also be induced, which was shown in yeast (Hu et al. 2008). In humans Reticulon protein can also induce programmed cell death through an increase of calcium in the ER (Di Sano et al. 2007).

Calnexin is a protein of the ER and a lectin. It has the function of a chaperon and is responsible for folding proteins, especially glycoproteins (Leach MR and Williams D. B. 2000 - 2013). In *A. thaliana*, two Calnexins among other chaperons were found, Calnexin 1 and Calnexin 2 (Wang et al. 2005). Calnexins are expressed along the whole development through the whole plant tissues, with some differences in reproductive organs. In the leaf cells of *A. thaliana,* they showed a network of tubules, which looked like the ER. Even in the plasmodesmata a signal was seen, but the Calnexin was not specifically bound there, rather the proteins went through the cell wall (Liu et al. 2017). A study provides some evidence that besides another proteins Calreticulin-2 and Calnexin help to maintain the structure of the ER, when there is an infection with a virus (Niehl et al. 2012). The Calnexin in *Pisum sativum* showed a calcium binding domain and even the phosphorylation of Calnexin was proven (Ehtesham et al. 1999).

1. 3 Cytoskeleton

Cells not only contain organelles, like the chloroplasts, furthermore they need cytoskeletal elements like microtubules and actin microfilaments, which give the cell its structure and form. They also allow the organelles to move within the cytosol and are essential for cell division.

Microtubules are build out of tubulin, a globular protein, alpha and beta tubulin build a heterodimer and polymerize to protofilaments, 13 of these filaments build the wall of a microtubule and form a ring structure (Plattner and Hentschel 2017). Alpha and beta tubulin have different genes in *A. thaliana* (Hashimoto 2015). Microtubules maintain the cell form, function as tracks for vesicles during endo and exocytosis, are responsible for positioning of organelles and they form centrioles, basal bodies, the spindle apparatus, flagella and cilia. The Golgi apparatus has the tendency to be at the minus pole of the microtubule and the ER lies between the plus and minus pole (Plattner and Hentschel 2017). Microtubules have various functions in cellular processes, including cell division and mitosis. They are important for correct cell plate assembly, when forming a new cell wall (Chen et al. 2018). They work as tracks for the organelles, especially for the ER (Hamada et al. 2014). These authors also described that microtubules are also involved in tubule formation of the ER and organization of the ER, the ER tubules extend bidirectional to the minus and plus end of the microtubules. In contrast another study showed that actin-myosin is responsible for the movement of ER in plants (Sparkes et al. 2011). Cell movement is stopped when cells were treated with actin drugs but not with microtubule-drugs (Lang-Pauluzzi and Gunning 2000). Microtubules change their form during plasmolysis, as becoming wavier and forming thick bundles, this was shown in hypocotyl cells of *A. thaliana* (Lang et al. 2014).

Microfilaments are made of actin. Actin is a globular protein and exists as G-actin in the cell and is phylogenetically very conserved. It can polymerize to filamentous structures and is then bound as F-actin. Actin filaments are two entwined filaments. Microfilaments are responsible for contraction of part of the cells and also the whole cell, for the movement of cells, the structure of the cell and local structuring of the cell (Plattner and Hentschel 2017). The actin filaments not only give the shape to the cell, they are also responsible for the movement of components like vesicles in the cytosol (Thomas *et al*, 2014). Locally

myosin and actin can interact, so that the microfilaments contract. The F-actin interacts with myosin to transport organelles at high velocity (Deeks and Hussey 2001).

The Life-Act GFP cell line showed that actin is essential for tip growth, not only in pollen tubes from *Lilium formosanum* and *Nicotiana tabacum*, but also in the protonemata of *P. patens*. The fixed protonema shows a tip localized collar or an aggregation of filaments along with a cortical mesh-work of actin and a network around chloroplasts. Also, an apical patch of actin filaments in chloronema cells and a focal point of F-actin in caulonema cells were seen. Apical networks were seen in in pollen tubes from *Lilium formosanum* and *Nicotiana tabacum*, in the protonemata of *P. patens* and they showed an intense change during growth (Vidali et al. 2009).

F-actin plays a role in mitosis in plants and therefore in cell division, it establishes and maintains the division site (Cleary 2001), the actin serves as a cable for Myosin VIII (Wu and Bezanilla 2014). Actin is involved in guard cell movement, shown in *Nicotiana tabacum*. During the closure of the stomata, the actin is polymerized and uniformly distributed. After plasmolysis the actin filaments form short and thick fragments. Some thick bundles remained near the detached plasma membrane and are responsible for the remain of the connection to the cell wall (Yu et al. 2018). In *A. thaliana* hypocotyl cells it was shown that actin reacted to plasmolysis and adjusted to the new protoplast size, actin followed the shape of the plasma membrane (Lang et al. 2014).

Myosin is a motor protein, which is highly conserved. Myosin, together with actin, is found in the muscle cells of animals and is responsible for movement of the muscle (Nabi 2011). They can be defined in at least 17 Myosin classes, probably some with single head and some with double head molecular structure (Hodge and Cope 2000). Myosin V has two heads and can carry vesicles and organelles along actin filaments by using ATP. Myosin II is necessary for cell division (Bolsover 2004).

Myosin has evolved uniquely in plants (Bezanilla et al. 2003). As they have two classes of Myosin VIII and XI. In comparison Myosin XI is responsible for cytoplasmic streaming and for tip growth in *P. patens*. Only two genes are responsible for coding Myosin XI in *P. patens*, which are redundant in their function (Vidali et al. 2009). **Myosin VIII** is necessary for proper branch formation of the protonema cells (Wu and Bezanilla 2014), a malfunction leads to a protonemal pattering defect (curved protonema cells), it controls the rate of development, and furthermore it is responsible for proper growth and pattering in low-nutrient conditions (Wu et al. 2011). Myosin VIII also has an important role in cytokinesis, where it localizes at the spindle apparatus and forms a ring at the phragmoplast and a second outer ring. When the phragmoplast expands, the inner ring reaches the outer one. This is an insurance that the phragmoplast expands to right position (Wu and Bezanilla 2014).

1. 4 Plasmolytic solutions

Plant cells can respond to osmotic changes in their environment. The plasmalemma and the tonoplast are both bio membranes which are semipermeable. This means that water and some soluble substances can enter the cell through the membranes. Osmosis is the diffusion of water through a semipermeable membrane. If the outer medium is hypotonic in comparison to the inner medium, the concentration inside is higher than the outside, water enters the cell in response to the osmotic value of the vacuole. When the outer

medium is hypertonic in comparison to the inner medium, the concentration on the outside is higher and water leaves the cell in plasmolysis. Plasmolysis is the detachment of the protoplast from the cell wall in a hypertonic medium. At the beginning of plasmolysis, the turgor pressure is zero and the protoplast detaches only from the edges of the cell wall. When the plant is put in a hypotonic medium the water enters the cells again and the cells are deplasmolysing (Heß 2004). There are many different forms of plasmolysis like concave, convex, band and cap plasmolysis (Oparka 1994). A change in the ER during plasmolysis was shown by the study of Cheng et al (2017), where the cisternalization increased. Even a decrease in streaming and less mobility of the ER in the Hechtian strands and reticulum was shown (Cheng et al. 2017). It was suggested that the fibrils, which connect the cell wall with the plasma membrane, the Hechtian strands (Hecht K. 1912), are made of cellulose and are stabilized by pectins (Lang et al. 2004). They act as anchors for the plasma membrane and hold the tension between them (Lang et al. 2004)(Lang et al. 2004). The Hechtian reticulum is the anchor area of the Hechtian strands and forms a `sandwich´ structure (Cheng et al. 2017). Hechtian strands are under tension, but they react not all the same. Some break due to much tension, but cells of cold hardened plants tend to break less often (Buer et al. 2000). In Hechtian strands, microtubules and actin filaments are found (Lang-Pauluzzi and Gunning 2000), but cytoskeletal elements seem not to be involved in the construction of Hechtian strands (Lang-Pauluzzi 2000). In a study on *Tradescantia virginiana* leaf epidermal cells, cell to cell connections persist during plasmolysis and the cortical apical patch works as an attachment for the plasma membrane. Malformed spindles and phragmoplasts develop when the cells are plasmolysed during mitosis (Cleary 2001).

1. 5 Aims of the study

- The aim of this study is to control the ER, Life-act, GFP-Tub lines, Myosin VIII, Reticulon and Calnexin cell line to find out if they show the expected structures. It was expected that the ER cell line shows the network of the ER, the Life-act cell line the microfilaments and the GFP-Tub cell line the microtubules. Furthermore, the Myosin VIII was expected in newly build chloronema cells near the cell wall, the Reticulon and Calnexin cell lines, when correct expressed and linked to the GFP show the tubules of the ER. It would be interesting to find out where the similarities and differences in subcellular structures of the known structures and organelles from vascular plants are. *M. elongata* (Bryales) and *P. drummondii* (Bryales) were also examined to find out, if there are differences between different mosses species. We wanted to see if the subcellular structures in the protonema and leaflet cells behaved differently in the GFP modified cell lines.
- Some cell lines showed a higher increase in biomass then the others, even within the GFP cell lines, so this was also included in the research.
- The subcellular structures should be shown with specific dyes, which are known from literature and vascular plants like *A. thaliana*. The results are then compared with the GFP-cell lines, which are more specific than the dyes.
- Furthermore, we wanted to test if the dyes are able to penetrate the moss cells/cell walls or if they need some sort of permeabilization.
- Because of the cortical location of the subcellular structures, we wanted to test their response to osmotic stress. We also wanted to find out which subcellular structures can be found in the Hechtian strands and if there is a difference between the different cell types.

2 Material and Methods

2. 1 Plant material

We used *P. patens* (Funariaceae) wild type for labelling experiments (Control). For the other experiments *P. patens* cell lines marked with GFP were used. These cell lines are “Wt ER me-GFP” (ER), “Wt Life-Act me-GFP” (Life-act), “Myosin VIII 3GFP” (Myosin VIII), “Wt Tub me-GFP” (GFP-Tub), “Wt Calnexin -4 mRubyz” (Calnexin) and “Wt Reticulon -3 mRubyz” (Reticulon). The GFP marked cell lines, which were cloned via a vector, were generated by Dr. Magdalena Bezanilla.

Furthermore, we used other mosses for control of the labelling with the fluorescence dyes. These mosses were *M. elongata* (Bryaceae) and *P. drummondii* (Bryaceae). Because there was a problem with labelling of the actin in the mosses with the dye Rhodamine Phalloidin*,* we used *Allium cepa* for control of the labelling.

2. 2 Propagation of the moss material

To have enough material to investigate the mosses, the plant material has to be multiplied. This has been done under sterile conditions with cell cultures. In the sterile bench (Ehret, Aura-V), tiny parts of the mosses were inserted in plates containing a growth medium for *P. patens* ($PpNH_4$). The mosses were kept in a growth chamber (Conviron) with 20 °C with a day/night rhythm of 14/10.

The culture medium was PpNH4. Recipe for 1 litre of media: The beaker was filled with distilled water to half (0,5 l). Then, 2 ml $MgSO_4x7H_2O$ (500x stock solution, Sigma Aldrich), 2ml KH_2PO_4 (500x stock solution, Merck), 2 ml $CaNO_3x4H_20$ (500x stock solution, Merck), 0.0013 g $FeSO_4x7H2O$ (this was outweighed with fine balance, Merck), 1 ml microelements (1000x stock solution) and 2 ml Di-ammonium Tartrate (500x stock solution, Fluke) were added. The microelements contain H_3BO_3 614 mg (Sigma/Roth), $CuSO_4x5H_20$ 55 mg (Merck), $MnCl_2x4H_2O$ 389 mg (Roth), $CoCl_2x4H_2O$ 55 mg (Alfa Aesar), $ZnSo_4x7H_2O$ 55 mg (Merck), Kl 28 mg (Riedel-de Haën) and $Na_2MoO_4+2H_2O$ 25 mg (Merck). Then the volume was brought up to the final volume of 1 litre. After that, the medium was ensured to be resolved. Then the media was transferred into 5x 250 ml Erlenmeyer flasks each filled with 200 ml and 1,4g of Agar Agar (Roth). After that, the opening was closed with cotton wool and enclosed with aluminium foil. At the end, the flasks were autoclaved. The autoclaved PpNH4 was then filled in petri dishes, where the mosses were planted when the agar was hard.

2. 3 Growth experiment and area calculations

Petri dishes with cell lines of *P. patens* (Control), GFP-marked lines of *P. patens* and two other moss species *M. elongata* and *P. drummondii* have grown for 22 days under the same conditions, but with different closure of the petri dishes. One petri dish of each cell line was closed with two layers of Parafilm (Bemis) and another one with three layers of 3M tape (Micropore TM). Within the petri dishes, nine areas with parts of the mosses of the respective cell lines were inserted. At the beginning of the experiment and every second or third day a picture was taken. This was done to ensure a more or less regular

growth and to ensure that the mosses still were in good condition, so there was no infection with a fungus or a bacterium. For statistical measurements only the values of the areas of the beginning of the experiment and of the day 22 were taken. The mean and median area ratios of the nine areas were calculated and the difference of the areas between the beginning and the 22nd day, also the standard deviation was calculated. Also, the percentage of growth of the areas and their difference was calculated. The starting area was taken as 100% and then the percentage of the area of the 22nd day was calculated. Furthermore, also the multiplication factor was calculated. The area was measured with ImageJ, so the values are in pixel per pixel and only represent the area ratio. 245 pixel measure 1 cm, this means the mean value of area ratio of the control 7779,222 pixel^2, measures 31,75 cm^2. In the appendix (supplementary data 2: table 3 to 5) all calculated values are shown. A student's T-Test comparing the control cell line with the other cell lines and a correlation between day 0 and day 22 were done.

2. 4 Light and confocal microscopy

The light microscope Nikon Eclipse Ni with interference contrast and dark field mode, was used to get a first impression of the moss and determine if the cells are still intact. Conventional fluorescence microscopy was used to ensure that the GFP marked cell lines still showed the fluorescence of the GFP, therefore the microscopes Nikon Eclipse Ni and Nikon Labophot were used. Because mosses leaflets and the protonema only have one cell layer, the mosses were not especially prepared nor sectioned.

The confocal laser scanning microscope (CLSM) was used in this study to analyse some subcellular structures of *P. patens*. In order to investigate the subcellular structures in the confocal microscope they either have to be genetically altered (GFP) or fluorescence dyes are needed. Only the chloroplasts and the cell wall show auto-fluorescence in mosses. The conventional fluorescence was used to localize the actual fluorescence of the specimen. The transmission mode was used to show outlines of the cells (cell wall) and their interior structures (chloroplasts).

With the confocal microscope, serial scans are possible and the out of focus light and blurry effects are diminished, also z-scan and 3D reconstructions are possible. The out of focus light is blocked by the pinhole and cannot be detected by detectors. Even the signal-to-noise ratio can be decreased by a slower scanning time or by a higher frame/line average (http://www.univie.ac.at/cius/microscopy).

Final pictures were taken with a CLSM Leica TCS SP5 DM-6000 CS and a Leica DFC 450C camera. The objective was always 63x water field immersion, the higher magnification was made using confocal magnification or computer-generated magnification. The line average was set at three and the frame average at one for taking pictures, but for time lapse movies of the ER, the line average was set only on one, because the ER moves so quickly and would blur the picture.

The excitation was produced with the Argon laser 488 nm for the GFP-lines and for both of the styryl dyes, for Rhodamine Phalloidin the excitation was 540 nm and was therefore produced with the white light laser. The white light laser was set to emit 540 nm with 30% and the range of the photomultiplier was chosen around the range of 565 nm. The emission settings for the GFP were 500- 550 nm, for the chloroplasts 650 -750 nm and for the styryl dyes 570 – 650 nm.

The pictures in the result part show always the GFP-channel in green, the chloroplast channel in red, the styryl dyes were in blue, the Rhodamine phalloidin in *P. patens* in yellow and in *A. cepa* in red and the Transmission channel in black/white. A description of the picture compilation is shown in table 1. Most of the time an overlay channel is described.

GFP (green)	Various dyes (blue/yellow/red)
Chloroplast autofluorescence (red)	Transmission (black/white)
Overlay	

Table 1: Description of the picture compilations in the result part

Also, maximum and average projections were made. For some cell lines (ER, Actin and Tubulin) fluorescence quantifications were made. Movies of 3D reconstructions of maximum projections and average projections were generated in LAS AF (software by Leica). Pictures of the maximum projections of plasmolysing cells were used for making time lapse movies (in Movie Edit Touch, MAGIX Software GmbH). All movies can be found on the attached DVD and a description is provided in the appendix.

2. 5 Labelling

The **styryl dye FM 4-64 and FM1-43** stain the plasma membranes; they label first the plasma membrane near the cell wall and then the other membranes in the cell through endo- and exocytosis of vesicles.

- The **styryl dye FM 4-64** (FM™ 4-64 Dye (*N*-(3-Triethylammoniumpropyl)-4-(6-(4-(Diethylamino) Phenyl) Hexatrienyl) Pyridinium Dibromide)) is lipophilic and has been reported to selectively stain yeast vacuolar membranes with red fluorescence (excitation/emission maxima ~515/640 nm according to www.thermofisher.com). The excitation and emission were set differently for moss cells (excitation at 488nm and emission between 570 and 650 nm). The styryl dye FM 4-64 stains the plasma membranes and it also visualizes the vacuolar organelle morphology and its dynamics. The dye was applied in the concentration of 8 µM and 36 µM for 30 minutes and then washed out with distilled water. The examination of the labelled object was right after washing out the cells or 30/60 minutes later.

- The **styryl dye FM1-43** (FM™ 1-43 Dye (*N*-(3-Triethylammoniumpropyl)-4-(4-(Dibutylamino) Styryl) Pyridinium Dibromide)) labels the plasma membrane (www.thermofisher.com), so it can also dye endocytosis vesicles. It is often used to track vesicle trafficking and to examine exocytosis and endocytosis. This dye was excited with the same wavelength as the FM4-64. After an application with a concentration of 8 µm of the dye for 30 minutes, it was washed out with distilled water. The examination of the labelled object was right after washing out the cells or 30/60 minutes later.

The **Rhodamine Phalloidin** (Rhph) dye labels the F-actin and shows the actin filaments. The phalloidin is derived from a mushroom and toxic. Rhodamine is fluorescenting and more resistant to photobleaching and therefore used often in studies for permeabilized and fixed cells, like shown in the protocol from Chazotte (Chazotte 2010). It is recommended to fix the cells before staining with formaldehyde and not glutaraldehyde,

because it would interfere with the fluorescence (Chazotte 2010). We wanted to try these label on living, but permeabilized cells.

- Rhodamine Phalloidin (Rhph) (www.thermofisher.com) very specifically dyes the actin filaments in the cells; it only labels the actin. It normally stains selectively the F-actin and should be superior to antibody staining. The concentration was 300 units. It is optimal for fixed and permeabilized samples. The buffers were used for permeabilization and stabilization of the cells (TRAAS a permeabilization buffer, PBS and PM5E see below). The Nonident P40 Substitute (www.sigmaaldrich.com) solubilizes the membrane proteins during an isolation of membrane-protein complexes and allows the dye to enter the cell. Rhodamine phalloidin has to be excited at 540 nm and its emission is at 565 nm. The dye was applied for 15 and 30 minutes and then washed out with the respective buffer.
  TRAAS buffer: 1 % Mannitol (4 % stock: 250 µl, Mannit (Roth)), 50 mM PIPES (200 mM stock: 250 µl, Sigma), 5 mM EGTA (500 mM stock: 10 µl, Sigma), 2 mM $MgSO_4$ (20 mM stock: 100 µl, Sigma), 0,01 % NP-40 (10 % stock: 1 µl, Sigma), 5 % DMSO (100 % stock: 50 µl, Merck), in 439 µl H_20 distilled. For dilution of Rhph put 4 µl Rhph in 236 µl TRAAS buffer.

2. 6 Plasmolytic solutions

We wanted to show how the different cell lines reacts to lower and higher concentrations of Mannitol. Therefore, we used concentrations of 0,4 M Mannitol to see the beginning of plasmolysis and 0,8 M to see increased plasmolysis, and concentrations of 0,5 M and 0,6 M to see average plasmolysis. The mosses were either in a “flow chamber”, which facilitates substitution of the medium directly under the microscope or were put directly in the plasmolyticum after preparation and the slide was enclosed with Vaseline. The mannitol solutions were as fotloos Mannit (Roth) has the molecular weight of 182,28 g per Mol. One Mol correspond to 182,28 g per litre and so 0,6 Mol correspond to 182,18 g multiplied with 0,6 Mol, which results in 109,308 g per litre. For 100 ml 10,93 g must be weighed and for 10 ml 1,093 g, respectively. The volume was then filled up with distilled water. The final concentrations of the Mannitol were measured with the advanced Micro-Osmometer 3MO plus (Drott). Some divergence of the concentration of the mannitol and its higher measured osmolarity can be a result of the opening of the tubes and the transpiration of the water during use for experiments. Every measurement in the osmometer was repeated at least three times and the mean values can be seen in the table 2.

Calculated concentration of Mannitol (Mol)	Mean osmotically measured values (mOsm)
0,4	414
0,5	529,67
0,6	646,67
0,8	856

Table 2: Measured mean values of the osmolarity of the four final Mannitol solutions

2. 7 Statistics

During plasmolysis a change in the ER was recognized, it seemed that the cisternae were changing, because of that statistical measurements were made. The pictures of cisternae of the ER cell line, from the beginning of the plasmolysis and after 15 or 32 minutes were first blackened (in GIMP 2), so they could be measured with the ImageJ. Only assemblages of more than 15 pixels were seen as cisternae. In the first picture of the ER, six cells were measured before plasmolysis and after 15 minutes. The values in figs. show the pixel values: in 20 µm 98 pixel are resolved. Another six cells were measured in the second picture, this time before plasmolysis and after 32 minutes: in 20 µm 43 pixel are resolved. In Excell (MS office), the number of the cisternae and the sum of the area of the cisternae were used for creating graphs. In the appendix (supplementary data 3: table 6 to 9) the calculated values are shown. A student's T-test was applied for significance of the beginning and the end values.

3 Results

3. 1 Growth experiment

Seven cell lines of *P. patens* and two other mosses, *M. elongata* and *P. drummondii*, were planted on solid medium in petri dishes enclosed with either 3M tape or Parafilm. For a period of 22 days the mosses were held in a growing chamber and afterward their increase in biomass was measured.

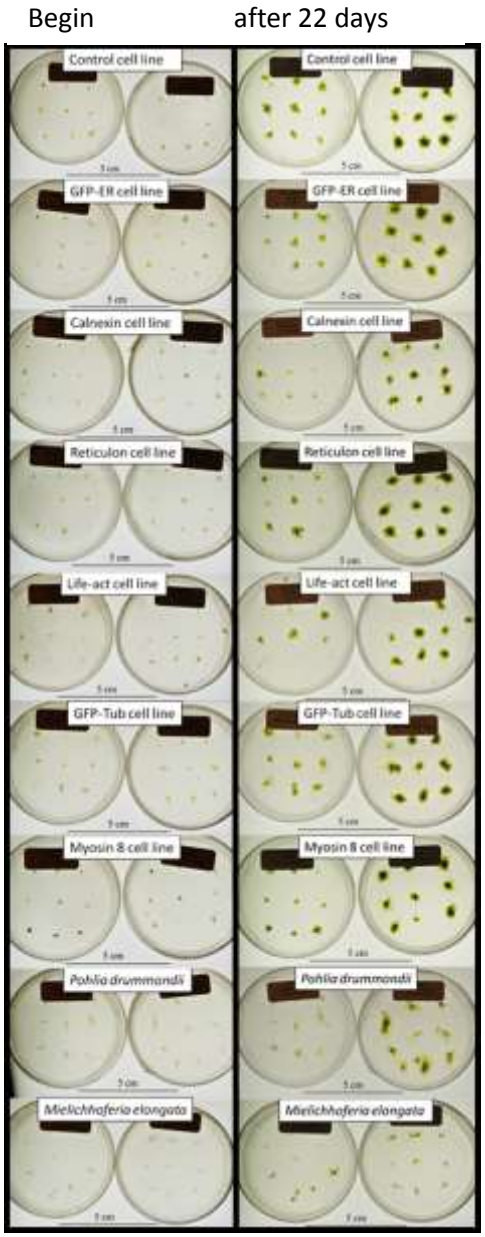

The moss area has increased in all the petri dishes (fig. 1). In the petri dishes enclosed with 3M tape growth was much more than in the ones enclosed with Parafilm. Even within the GFP marked cell lines a difference can be distinguished. This can also be seen in fig. 2, were there is a remarkable difference between the petri dishes.

In the mean area ratio the mosses show a higher value in the 3M tape dishes (fig. 2), the Calnexin cell line had the highest growth and *M. elongata* the lowest growth.

Within the values of the Parafilm dishes, the GFP-Tub cell line had the highest growth (fig. 3), but that was also due to its higher area ratio (cell content) at the beginning.

Fig. 4 (mean area ratio) and 5 (mean area ratio difference) show comparisons of 3M tape and Parafilm covered petri dishes, where the cell lines always grown more in the 3M tape covered dishes.

In the mean difference of the percentage (fig. 6) it is shown that GFP-Tub still grew more than most of the other mosses, but the Reticulon and Calnexin cell line have the highest value.

The lowest differences in the percentage (fig. 6) have the cell lines Myosin VIII and Life-act, the mean difference of percentage shows similar results (fig. 7).

Overall the cell lines covered in 3M tape multiplied their area the most (fig. 8).

Fig. 1: Macroscopic pictures of petri dishes of the GFP cell lines of *P. patens*, the control of *P. patens*, *M. elongata* and *P. drummondii*, at begin of the experiment (left block) and after 22 days (right block), closed with 3M tape (right column within each block) and Parafilm (left column within each block).

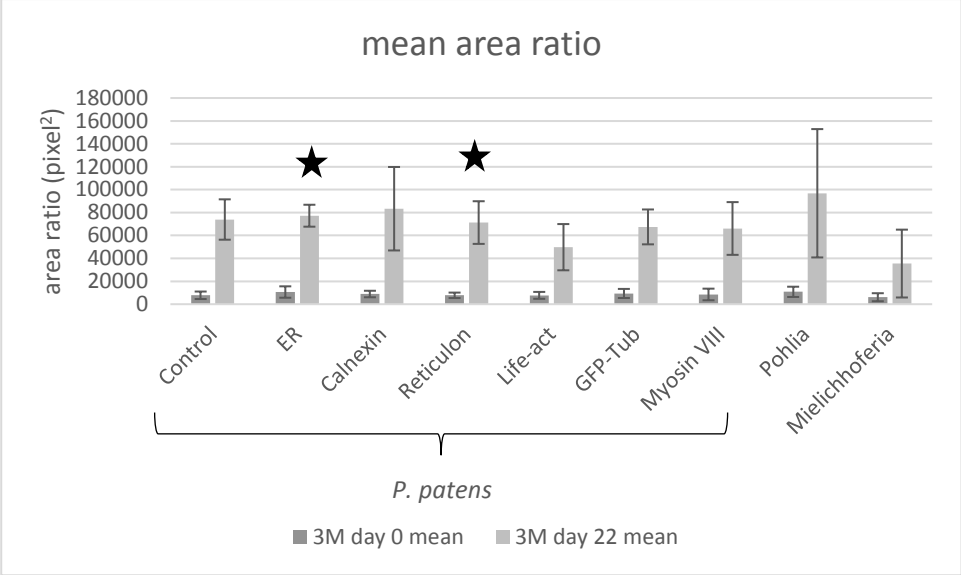

Fig. 2: Mean area ratios of cell lines held in petri dishes closed with 3M tape cultivated for 22 days, error bar indicates standard deviation, significance indicated by a star

In fig. 2 clearly an increase in area can be seen for all of the cell lines. Most of the GFP cell lines show less growth then the control *P. patens*, only Calnexin and ER have a higher growth than the control. In the mean area ratio *P. drummondii* grows the fastest and *M. elongata* the slowest. Significance was shown for ER and Reticulon in comparison to the control. Statistical significance with a T-test for comparing the values of the day 22 of the control with the other cell lines showed for the 3M tape enclosed mosses, that ER and Reticulon cell line had a high significance (fig. 2).

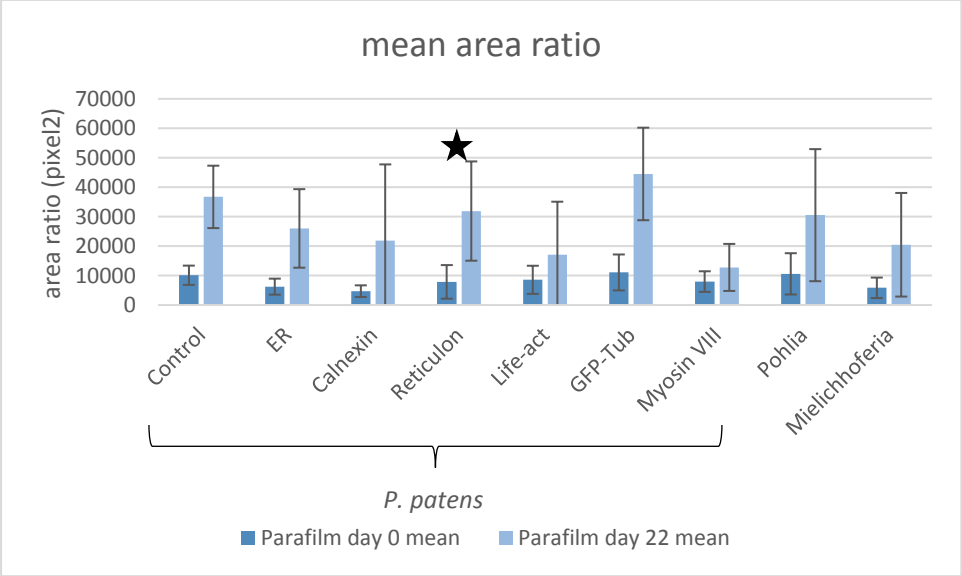

Fig. 3: Mean area ratios of cell lines held in petri dishes closed with Parafilm cultivated for 22 days, error bar indicates standard deviation, significance indicated by a star

The increase in area (fig. 3) for the mosses in petri dishes covered with Parafilm is less than in covered petri dishes with 3M tape. Most of the GFP cell lines show less growth then the control *P. patens*, only GFP-Tub has a higher growth than the control. The GFP-Tub cell line had the highest growth within this group, but that was probably because of its higher area ratio (cell content) at the beginning. In the mean area ratio *P.* and GFP-Tub grow the fastest and GFP cell line Myosin VIII the slowest. This can also be seen in the tables (Appendix; supplementary data 2: table 3 to 5). Significance was shown for Reticulon in comparison to the control. For the Parafilm enclosed one's significance for the Reticulon cell line was given.

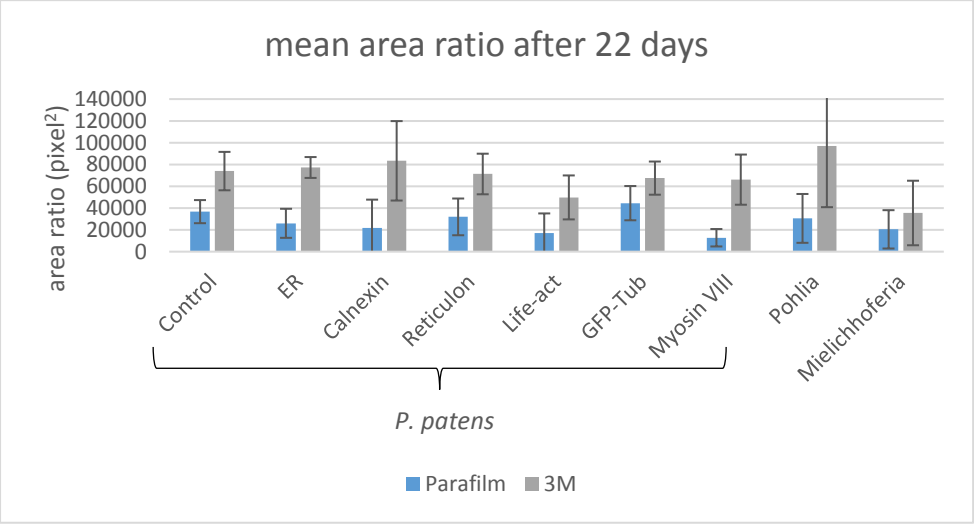

Fig. 4: Comparison of mean values of growth of 3M and Parafilm covered petri dishes after 22 days, error bar indicates standard deviation

The graph in fig. 4 shows good evidence that the mosses have grown more in the 3M tape dishes. The Calnexin cell line had the highest growth within the *P. patens* cell lines. *P. drummondii* had the highest growth and *M. elongata* the lowest growth in the 3M tape dishes. *M. elongata* always grows slow and *P. drummondii* grows a little bit faster. Some minor differences between the GFP cell lines can be seen. In comparison to Parafilm covered petri dishes the 3M tape covered petri dishes showed that at the end of the experiment the GFP cell lines Calnexin, ER, GFP-Tub and Myosin VIII had higher values compared to the control cell line. And had a lower area in Reticulon and Life-act in comparison to the control cell line. The cell lines with a lower area ratio in Parafilm showed higher values in the 3M tape in petri dishes.

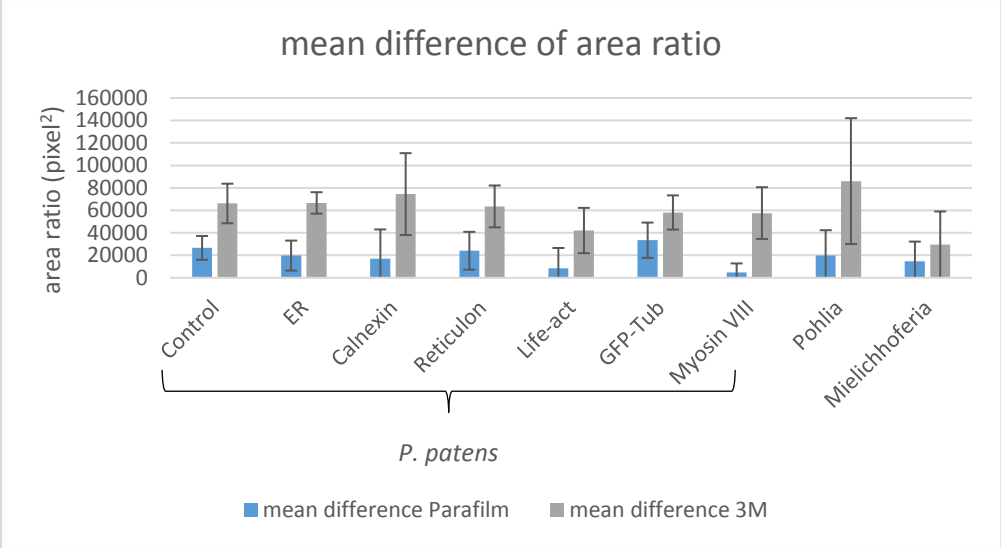

Fig. 5: Difference of growth mean values: how many they have grown after 22 days, error bar indicates standard deviation

Fig. 5 shows the difference of the area ratio. It stands for the increase in biomass in the petri dishes. The 3M tape covered petri dishes have, like in the other tables, the higher values. *P. drummondii* had the highest growth and *M. elongata* the lowest growth in the 3M tape dishes, but far less values in the petri dishes covered with Parafilm. Nearly all of the GFP cell lines, except GFP-Tub, have in the Parafilm covered petri dishes a lower growth than the control.

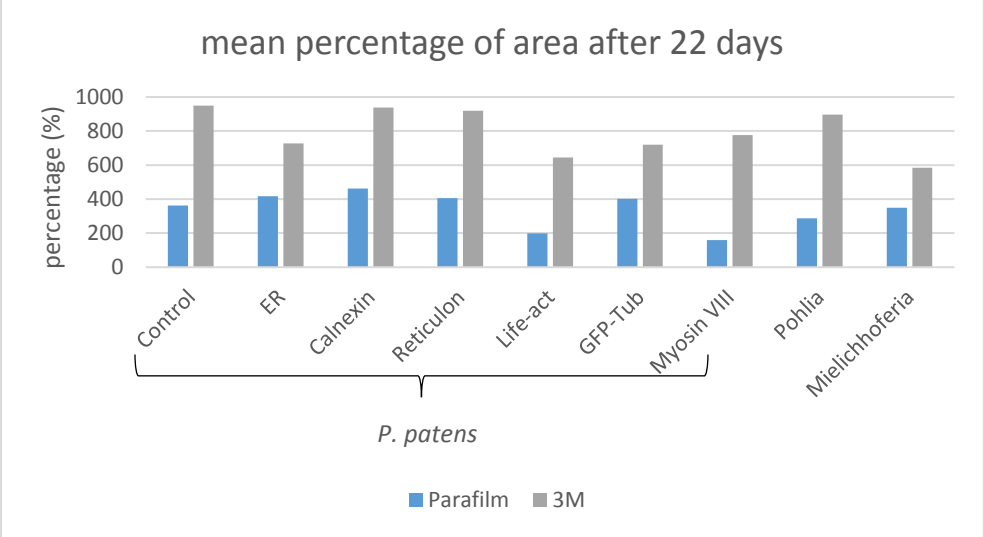

Fig. 6: Comparison of mean percentages values of 3M and Parafilm covered petri dishes begin and end of growth (after 22 days), error bar indicates standard deviation

In the comparison of 3M and Parafilm of mean percentage values of the area ratios (fig. 6) a higher percentage of area can be seen for control cell line and the GFP cell lines Calnexin and Reticulon. In the 3M tape these cell lines seem not to be as affected as the other GFP cell lines. When covered with Parafilm only the Life-act and Myosin VIII cell line show lower values than the control. *P. drummondii and M. elongata* show in both treatments lower values than the control of *P. patens*.

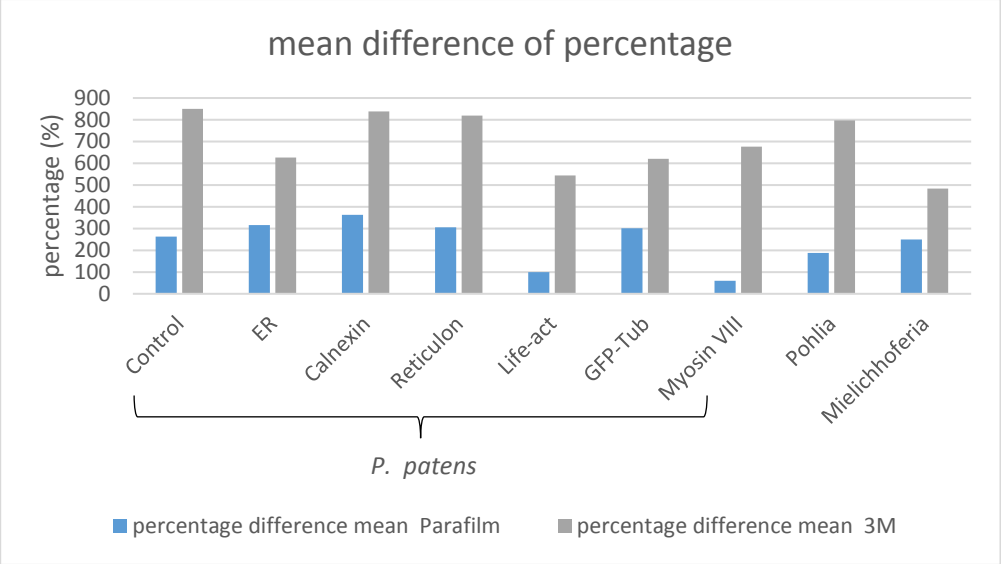

Fig. 7: Comparison of mean differences of percentage of 3M and Parafilm covered petri dishes begin and end of growth (after 22 days), error bar indicates standard deviation

The mean difference of the percentage between the day 0 and day 22 (fig. 7) shows for Parafilm for Life-act and Myosin VIII cell line the lowest and for ER and Calnexin cell line higher values than the control cell line. *P. drummondii* has a lower percentage difference than the control cell line and *M. elongata* in Parafilm covered dishes. The Myosin VIII, Calnexin and Reticulon cell line have an higher value of median percentage difference in the 3M tape variant, with an high difference between the values.

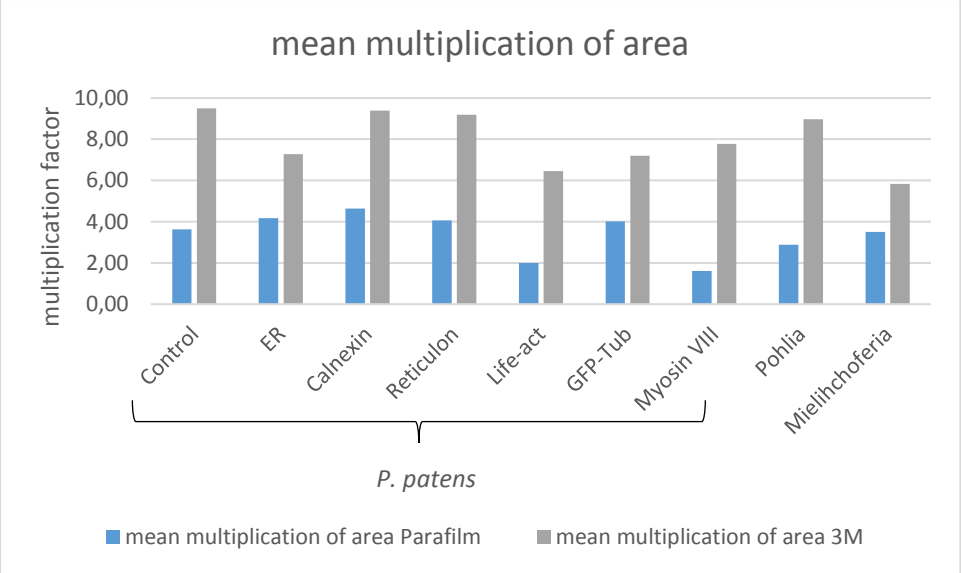

Fig. 8: Comparison of mean multiplication factors of 3M and Parafilm begin and end of growth (after 22 days), error bar indicates standard deviation

The mean area of ER and Calnexin cell line have multiplied the most and Life-act and Myosin VIII cell line the least in Parafilm treatment (fig 8). In the 3M treatment Calnexin and Reticulon cell line have multiplied the most among the GFP cell lines.

3. 2 Morphology: Bright field, dark field and Interference contrast

At first, we wanted to get an overview of *P. patens* and the other two mosses, which were needed for the labelling experiment, *M. elongata* and *P. drummondii*. Therefore, the mosses were investigated under the light microscope, also the interference contrast and dark field were used to get an impression of the mosses. The light microscope was able to show structural differences between the chloronema and caulonema and the leaflet cells.

P. patens

The leaflet cells contain more chloroplasts and depending on their position in the leaflet, their forms change a bit. Fully developed chloronema cells have more chloroplasts than caulonema cells and have a perpendicular cell wall. Whereas the caulonema cells have less chloroplasts and a diagonal cell wall.

In fig. 9, the habitus of *P. patens* with its green stem and leaflets can be seen. The rhizoids are not shown.

Fig. 9: Bright field image of stem with leaflets of *P. patens* (scale bar 500 µm)

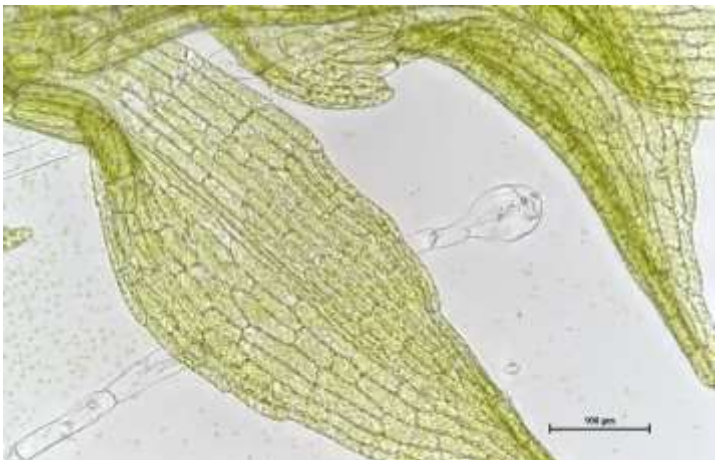

In fig. 10, the lanceolate leaflet of *P. patens* with its leaf vein is shown. The leaflet cells are more or less 100 µm long and 15 µm wide. The leaflet itself can be up to 757 µm long. The margin of the leaf is dentate.

Fig. 10: Bright field image of a leaflet of *P. patens* (scale bar 500 µm)

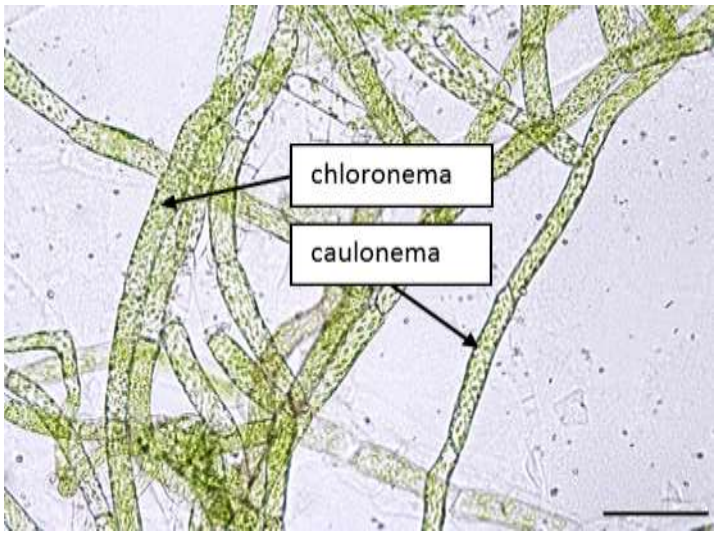

The protonema of *P. patens* is shown in fig. 11 (chloronema and caulonema indicated by an arrow). The cells of chloronema and caulonema are more or less 100 µm long and 20 µm wide. Sometimes cells between these two forms can be found in the protonema.

Fig. 11: Bright field image of a protonema cells of *P. patens* chloronema and caulonema; arrows: chloronema and caulonema cell (scale bar 100 µm)

In fig. 12, a newly formed leafy bud can be seen, which grows out of the upper part of the stem of the moss (indicated by an arrow). This leafy bud contains also many chloroplasts.

Fig. 12: Bright field image of an upper stem part with a bud of *P. patens* (scale bar 100 µm)

Fig. 13: Bright field image of protonema cells of *P. patens* Myosin VIII GFP cell lines; arrow: bulb cell (scale bar 100 µm)

The Myosin VIII cell line formed more bulbs (indicated by an arrow in fig. 13) than the other GFP cell lines, this is illustrated in fig. 13. Sometimes the protonema cells form these round structures; it is likely that they are formed under stress conditions.

P. drummondii

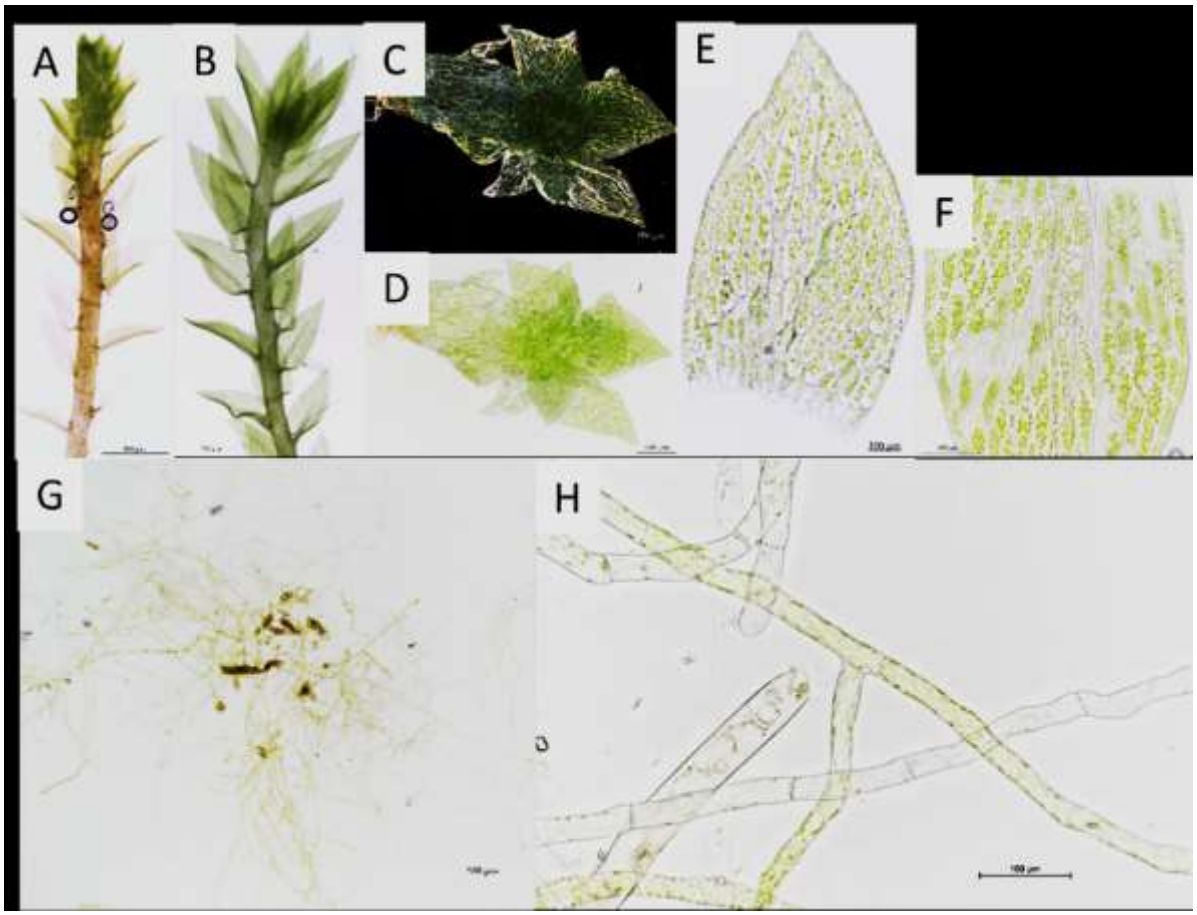

Fig. 14: Habitus of *P. drummondii* A and B) Bright field images of stem with leaflets (scale bar 500 µm). C) dark field picture of gametophyte (scale bar 100 µm) D) Bright field image of gametophyte (scale bar 100 µm). E) Bright field image of leaflet (scale bar 100 µm). F) Bright field image of leaflet cells (scale bar 100 µm). G) Bright field image of protonema (scale bar 500 µm). H) Bright field image of chloronema cells (scale bar 100 µm).

The stems of *P. drummondii* are mostly red, relatively stiff and unbranched, this can be seen in fig. 14 A. Leaflets are stiff, even, loose, when dry and under moist conditions upright. The leaflets are oval to lanceolate, (fig. 14 E), the leaflets are around 700 µm long. Its rib ends just before the tip (fig. 14 E). Leaflet cells are elongate and rhombic, (fig. 14 F). The leaflet margin is flat and at its base inverted. In fig. 14 C and D, a newly formed gametophytic plant is shown, at the base it's a little bit lighter green, with less chloroplasts. Protonemata with chloronema and caulonema cells can be seen in fig. 14 G and H. They look like the protonemata of *P. patens* and also measure about the same size.

M. elongata

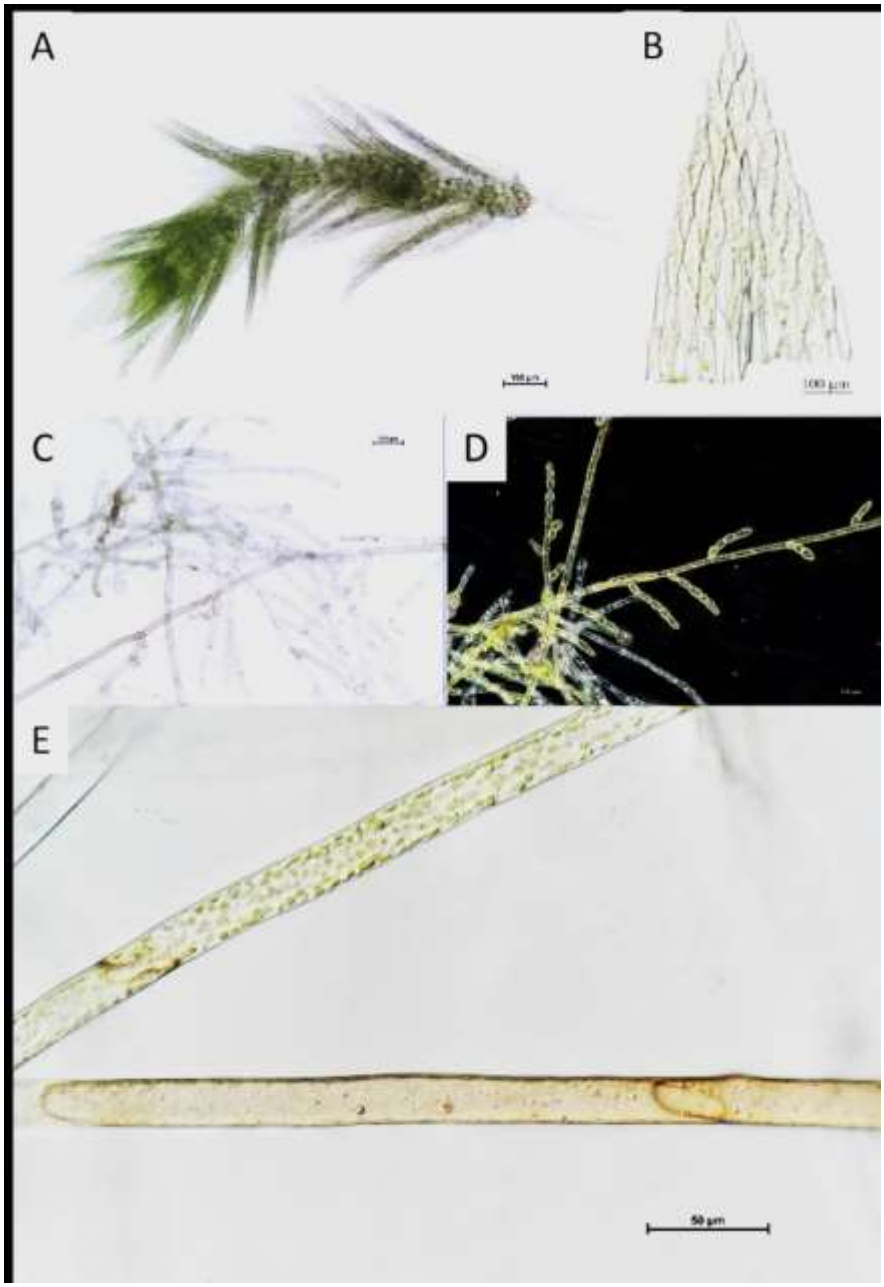

Fig. 15: Habitus of *M. elongata* A) Bright field image of stem with leaflets (scale bar 100 µm). B) Interference contrast picture of leaflet (scale bar 100 µm). C) Bright field image of protonema (scale bar 100 µm). D) dark field picture of protonema (scale bar 100 µm). E) Interference contrast picture of caulonema cell and rhizoid cell below (scale bar 50 µm).

The leaflets of *M. elongata* are standing dense (fig. 15 A), when dry they are fitting and under moist conditions they are upright protruding. Their form is ovate and 370 µm long. The leaflet margin is flat, but dentate against the tip. Its rib is ending in front of the leaf tip, this is also shown in fig. 15 B. Leaflet cells are in the middle of the leaflet rhombic. Like the other two mosses also *M. elongata* derives protonemata (fig. 15 C and D), with the same size, the rhizoid cell looks like caulonema cells but are without chloroplasts (fig. 15 E).

3. 3 Conventional fluorescence of GFP cell lines

The conventional fluorescence is a good way to get a first impression of the different cell lines. The conventional fluorescence also gives a good indication where the excitation and emission of the fluorescence material are and if GFP is present, but it has a wider range and it cannot be as precise as confocal microscopy.

GFP-ER cell line

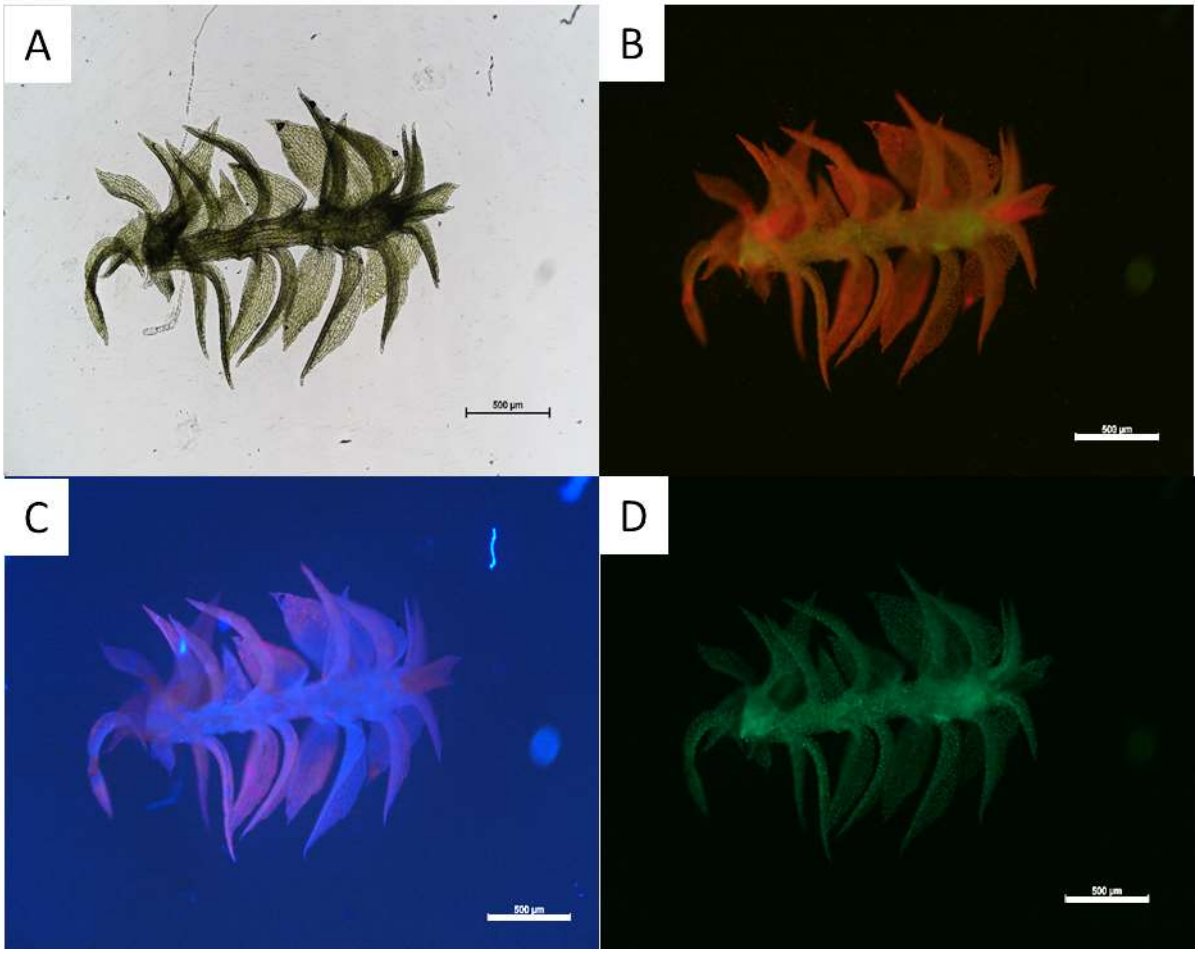

Fig. 16: *P. patens* ER cell line picture of stem with leaflets (scale bar 500 µm). A) Bright field image B) Excitation with filter of 450 – 490 nm. C9 Excitation with UV light. D) Excitation with FITC filter

Fig. 16 A shows the *P. patens* ER cell line in the light microscope. Fig. 16 B to D show the fluorescence of the moss under different excitation wavelengths this allows the comparison of the different filters. The excitation filter with 450 – 490 nm, shows the chloroplasts in red and the GFP in green (fig. 16 B). The UV light filter shows the fluorescence of the cell wall in blue and the chloroplasts in red (fig. 16 C). In the last picture (fig. 16 D), when using the FITC filter, only the fluorescence of the GFP in green can be seen. The GFP is distributed evenly in the whole moss, but at this magnification no subcellular structures can be seen. An aggregation of chloroplasts in the leaflets in comparison to the stem can be seen (fig. 16 B).

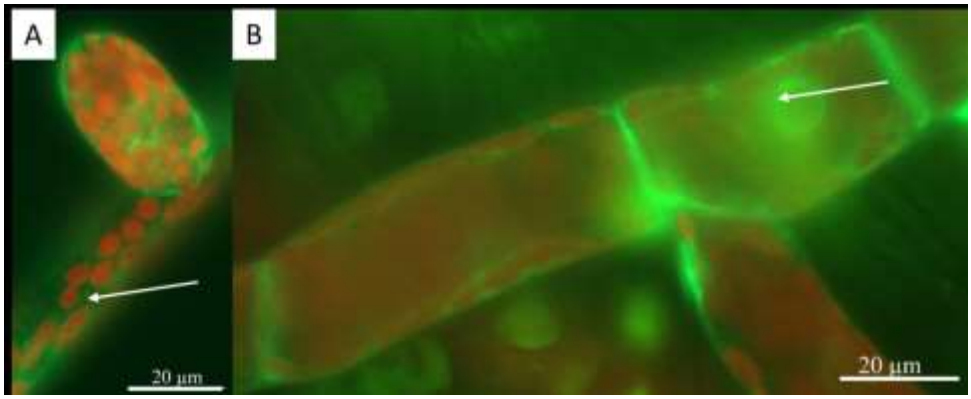

Fig. 17: *P. patens* ER cell line picture of chloronema cells excitation with filter of 450 – 490 nm; arrow cortical ER A) chloronema cell with newly formed cell. B) Chloronema cells at a branching point; arrow: ER around nucleus (scale bar 20 µm)

Fig. 17 shows the high fluorescence intensity of the GFP, which shows not only the ER near the cell wall, but also the ER around the nucleus (fig. 17 B, indicated by an arrow), and the cortical ER (fig. 17 A, indicated by an arrow). The netlike structure of the ER can already be hinted at in fig. 17 A.

Life-act cell line

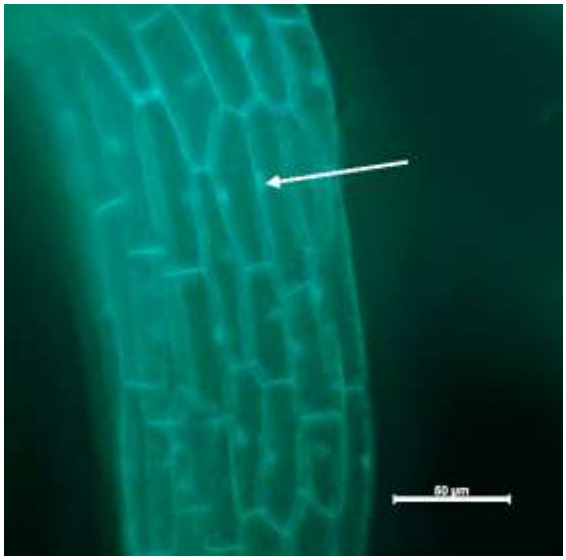

In fig. 18 the leaflet cells are shown with the fluorescence of GFP actin. The GFP-actin is seen in close vicinity to the plasma membrane and the nucleus (indicated by an arrow) and some structure within the cell, but no clear distinguishable form can be seen in conventional fluorescence.

Fig. 18: *P. patens* Life-act cell line picture of leaflet cells Excitation with FITC filter; arrow: actin near nucleus (scale bar 50 µm)

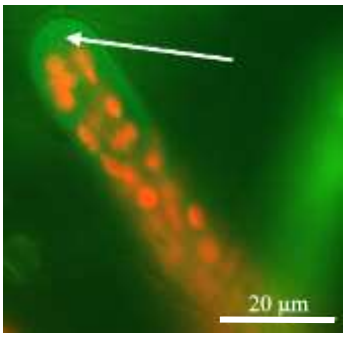

In fig. 19 an accumulation of actin at the tip of the cell is indicated by an arrow. The GFP fluorescence is mostly seen around the cell wall.

Fig. 19: *P. patens* Life-act cell line picture of a chloronema cell Excitation with filter of 450 – 490 nm; arrow: accumulation of actin (scale bar 20 µm)

GFP-tubulin cell line

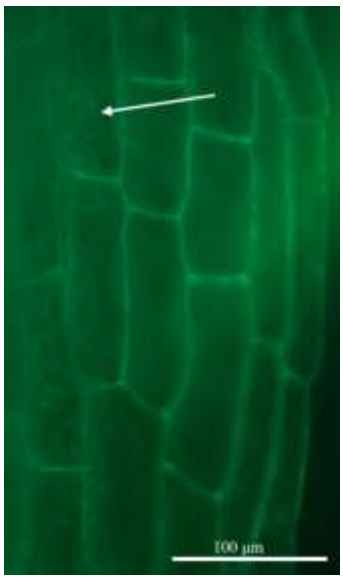

In the leaflet cell of the GFP tubulin cell line (fig. 20), the tubulary structure of tubulin (indicated by an arrow) can be seen very clearly. In this layer of the cell no nucleus can be seen, but also the plasma membrane near the cell wall show fluorescence, indicating tubulin in the cell cortex.

Fig. 20: *P. patens* GFP-Tubulin cell line picture of leaflet cells excitation with FITC filter; arrow: microtubules (scale bar 100 µm)

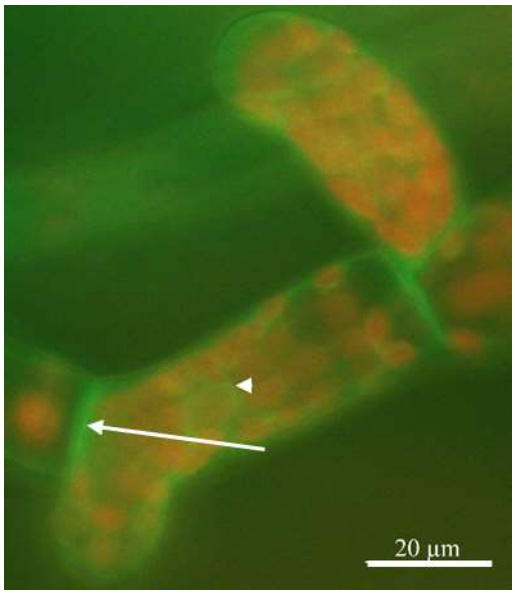

In fig. 21 the GFP-Tubulin shows fluorescence at the “cortical” part of cell (indicated by an arrow) and between the chloroplasts (indicated by an arrowhead). No subcellular structures can be distinguished in this conventional fluorescence mode as a lot of out of focus light blurs the vision.

Fig. 21: *P. patens* GFP-Tubulin cell line picture of a chloronema cells excitation with filter of 450 – 490 nm; arrow: connecting cell wall; arrowhead: tubulin between chloroplasts (scale bar 20 µm)

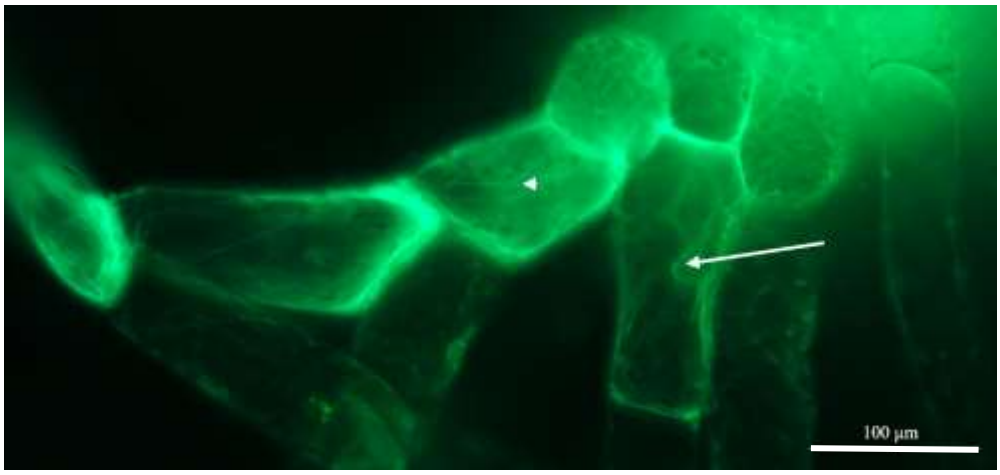

Fig. 22: *P. patens* GFP-Tubulin cell line picture of a chloronema cells excitation with FITC filter; arrow: microtubules around nucleus; arrowhead: tubulary structures (scale bar 100 µm)

The fluorescence of the GFP-tubulin in the protonema (fig. 22) shows the GFP-tub near the cell wall and close to the nucleus (indicted by an arrow) and some tubulary structure within the cell (marked with an arrowhead).

Myosin VIII cell line

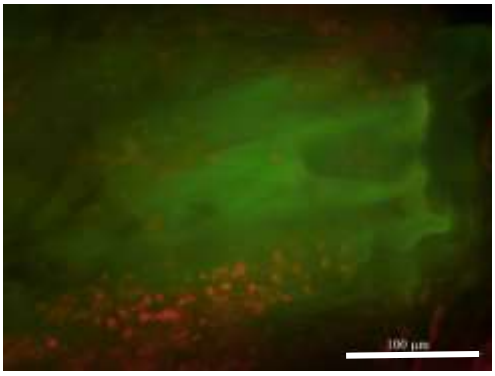

The Myosin VIII cell line shows a fluorescence of dead cell walls in an excitation of 450 – 490 nm, the chloroplasts show fluorescence in red (fig. 23). The GFP was only seen in “empty” cells, these dead cells did not degrade the GFP anymore and prove that GFP was present in the cell.

Fig. 23: *P. patens* Myosin VIII cell line picture of leaflet cells excitation with filter of 450 – 490 nm (scale bar 100 µm)

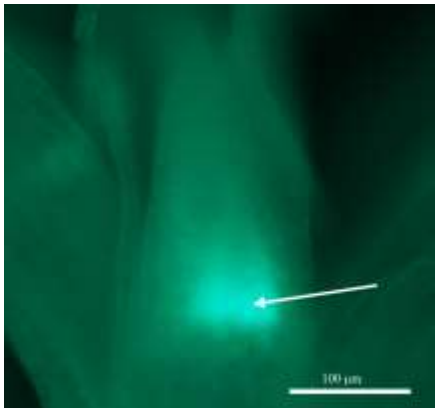

In the upper part of the stem there is an accumulation of GFP (fig. 24, indicated by an arrow). In the confocal microscope, this accumulation was not seen.

Fig. 24: *P. patens* Myosin VIII cell line picture of upper part of gametophyte excitation with FITC filter; arrow: accumulation of GFP (scale bar 100 µm)

Reticulon cell line

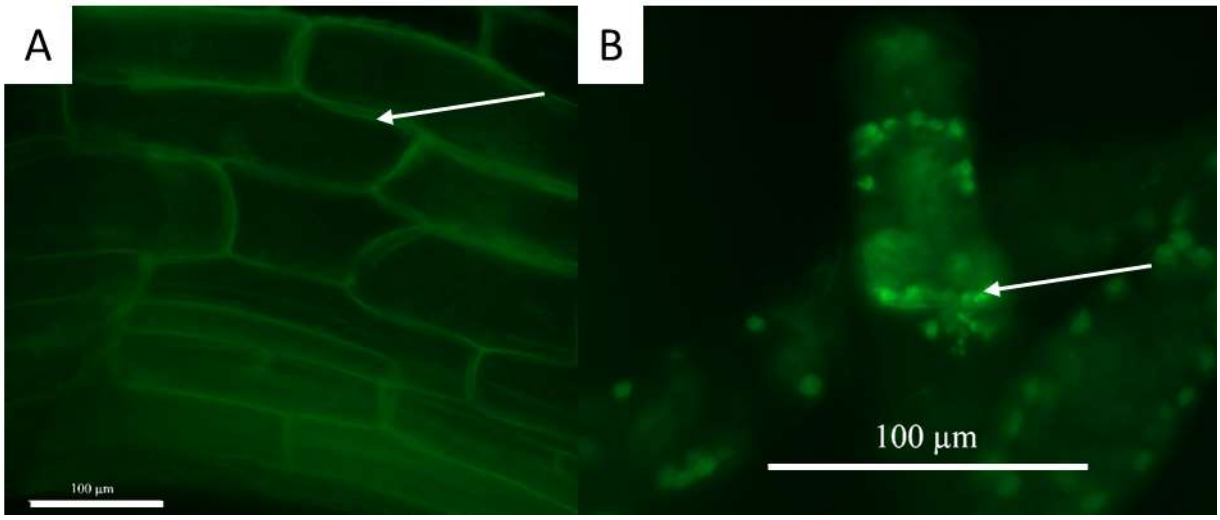

Fig. 25: *P. patens* Reticulon cell line excitation with FITC filter (scale bar 100 µm) A) leaflet cells; arrow: GFP close to the plasma membrane B) Chloronema cell; arrow: chloroplasts

In this excitation the GFP of the Reticulon cell line, the GFP in the cell cortex is seen (fig. 25 A, indicated by an arrow) and fluorescence of the chloroplasts. The chloroplasts arranged in a star like structure at the tip of one of the protonema cells (fig. 25 B, indicated by an arrow).

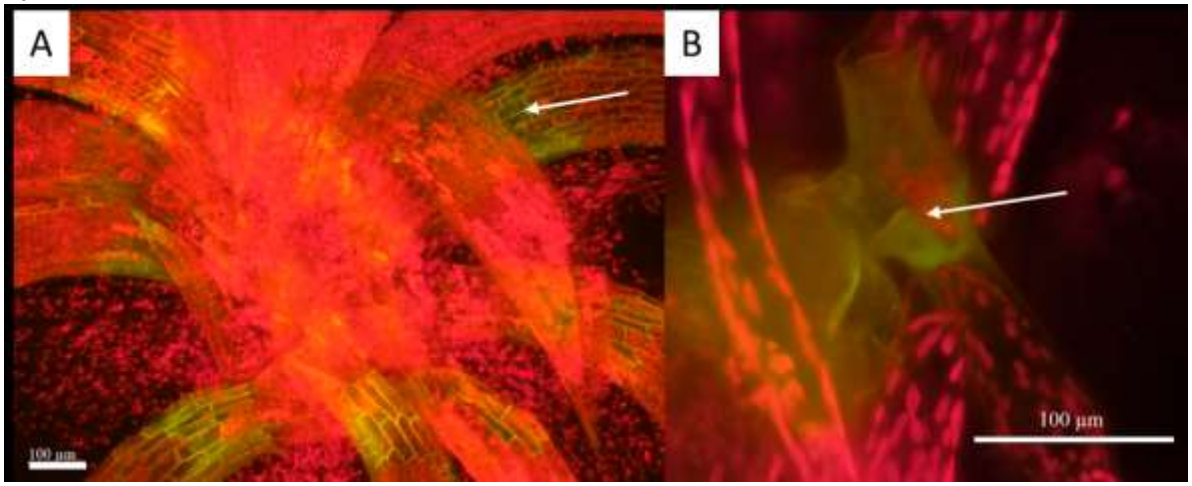

Fig. 26: *P. patens* Reticulon cell line excitation with filter of 450 – 490 nm (scale bar 100 µm) A) leaflet cells; arrow: GFP near plasma membrane B) Chloronema cell at a branching point; arrow: GFP in dead cell

Another excitation shows not only the GFP (fig. 26 A and B), but also the fluorescence of the chloroplasts. The fluorescence of the GFP near the plasma membrane in the leaflet cells is marked with an arrow in fig. 26 A, this is only seen in some of the cells. Furthermore, the GFP in a protonema cell can be seen in fig. 26 B marked with an arrow, this cell is already dead, because it does not contain chloroplasts and has no cell content anymore. The GFP is not expressed in living cells or is not bound to the Reticulon and therefore cannot show any structures. The not degraded unbound GFP can be seen in the dead cells and shows unspecific labelling.

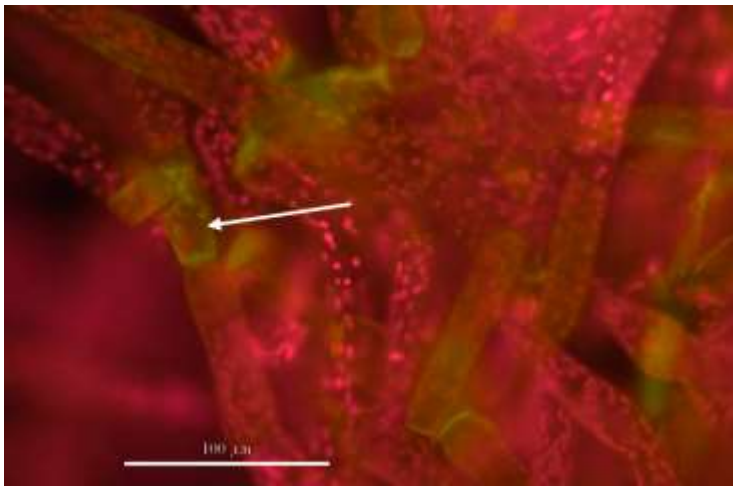

In fig. 27 mostly the fluorescence of the chloroplasts can be seen, but also the fluorescence of GFP around the plasma membrane of a protonema cell (indicated by an arrow). It also seems like the plasma contains the fluorescenting GFP.

Fig. 27: *P. patens* Reticulon cell line protonema cells excitation with filter of 450 – 490 nm; arrow: plasma membrane (scale bar 100 µm)

Calnexin cell line

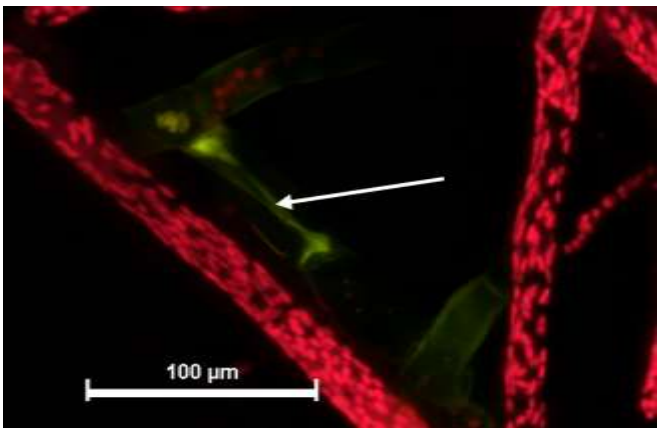

A dead cell, with no more chloroplasts in it, shows unspecific labelling of GFP in the cytosol (fig. 28, indicated by an arrow), it looks like a string through the cell. Around this dead cell living cells, with many chloroplasts can be seen.

Fig. 28: *P. patens* Calnexin cell line protonema cells excitation with filter of 450 – 490 nm; arrow: coagulated plasma (scale bar 100 µm)

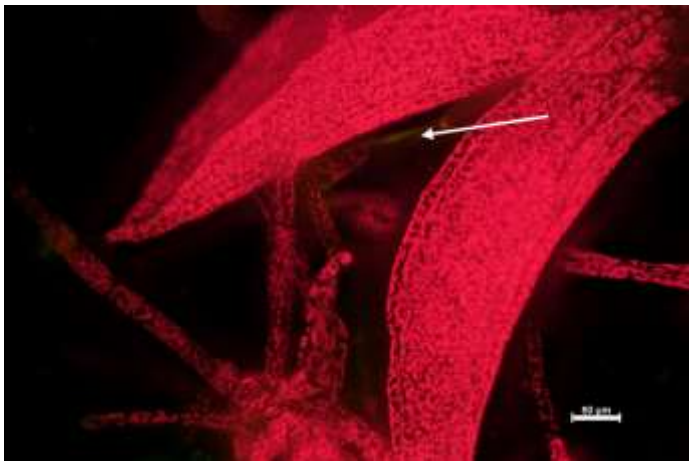

Fig. 29 shows like fig. 28 that the GFP only is seen, when the cells are dead, like the arrow indicating the coagulated plasma in the protonema cell. The leaflet cells do not show any fluorescence of the GFP, because the GFP is not expressed, just fluorescence of the chloroplasts is present.

Fig. 29: *P. patens* Calnexin cell line leaflet and protonema excitation with filter of 450 – 490 nm; arrow: coagulated plasma (scale bar 100 µm)

Conclusion:

The conventional fluorescence is not able to show specific structures of the GFP labelled proteins, for this better resolution and elimination of the out of focus light is needed. This can be provided by the CLSM.

3. 4 Confocal laser scanning microscopy (CLSM): fluorescence of GFP cell lines

The confocal laser scanning microscope allows a better look at the different subcellular structures of the GFP cell lines of *P. patens*. However, this was not always the case. In the GFP-ER cell line the ER stretches through the cell like a net and encloses the nucleus and chloroplasts. Even the movement of the ER can be seen and the constantly changes between tubules and cisternae. The ER was also found near the plasma membrane. The actin in the Life-act cell line was not so much aggregated around the chloroplasts and more at the outer edges of the cell. The tubulin in the GFP-Tubulin cell line formed tube-like structures, which were encircling the chloroplasts. The microtubules are just in the outer parts of the cell, this was shown in a 3D reconstruction. The other three cell lines, Myosin VIII, Calnexin and Reticulon showed the GFP in parts of the chloroplasts, but they did not show the Myosin VIII near the cell wall in young chloronema cells and the Calnexin and Reticulon as tubules in the cell, they all showed unspecific labelling of GFP.

GFP-ER cell line

The ER forms a netlike structure in all the different cell types, it is always found around the nucleus and the chloroplasts. Even the ER in the cell cortex, near the cell wall and the plasma membrane, can be shown with the GFP-ER cell line. The ER forms cisternae and tubules, which are always changing and forming new formations.

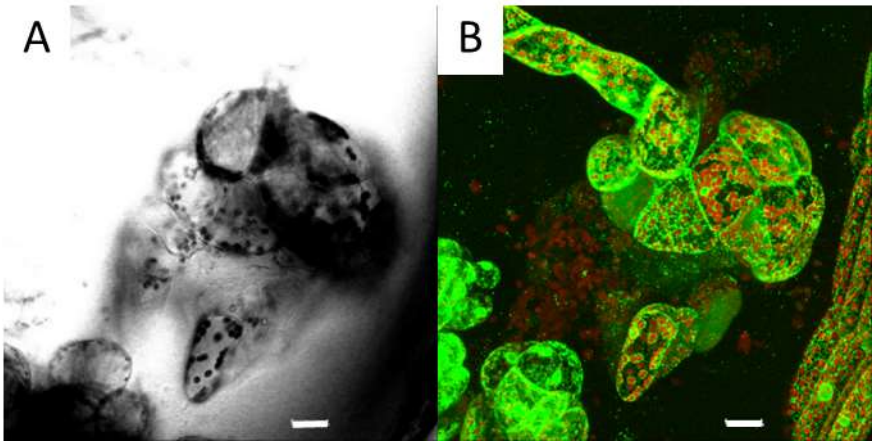

Fig. 30: *P. patens* ER cell line bud cell A) Transmission channel B) Maximum projection overlay of GFP and chloroplast channel (scale bar 20 µm)

Fig. 30 shows a leafy bud in the transmission mode. In the leafy bud many chloroplasts are present and they are fluorescenting in red. The ER is seen around the chloroplasts and nucleus, and in close contact to the plasma membrane. In movie 1, the 3D reconstruction of the bud can be seen from different angles and the 3D appearance of the ER.

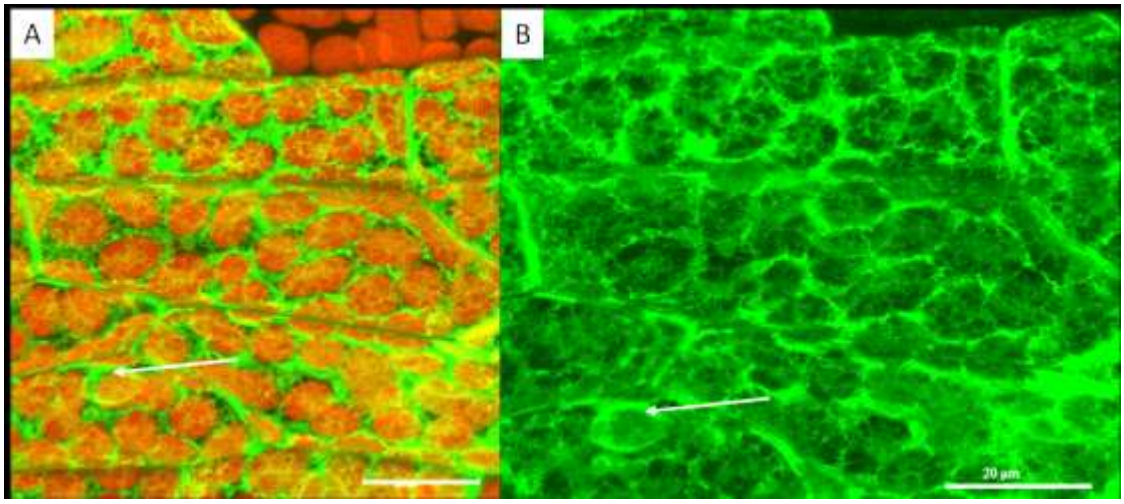

Fig. 31: *P. patens* ER cell line leaflet cells, Maximum projection A) overlay of GFP and chloroplast channel; arrow: nucleus; arrowhead: ER around chloroplasts B) only GFP channel; arrow: nucleus; arrowhead: ER around chloroplasts (scale bar 20 µm)

In the leaflet cell the structure of the ER is good to distinguish (fig. 31). The ER varies between cisternae and tubules between the chloroplasts. The ER accumulates around the chloroplasts (indicated by the arrowhead) and forms a sort of sheet around them. They encircle them with tubules, maybe for better transport of vesicles and protein transport. The ER is aggregating around the nucleus (indicated by the arrow) and has connections to the tubules and cisternae.

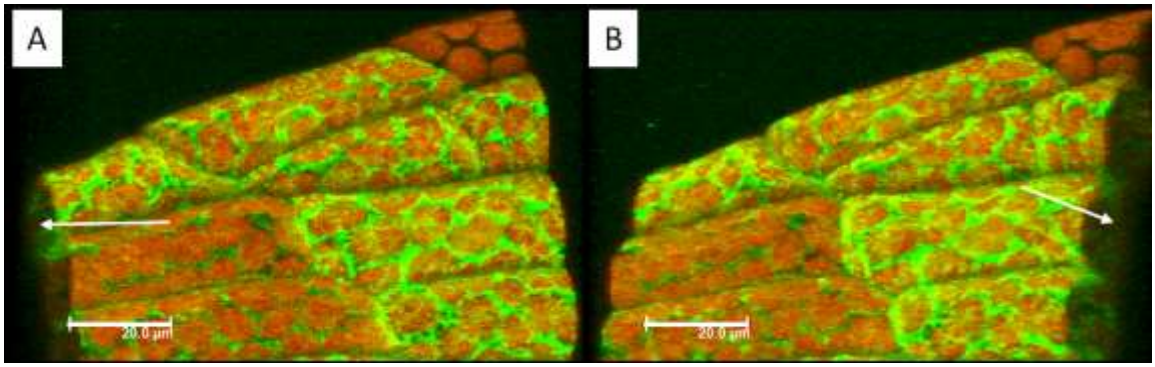

Fig. 32: *P. patens* ER cell line leaflet cells, 3D Reconstruction of Maximum projection overlay of GFP and chloroplast channel A) left angle B) right angle, arrows: interior of the cell (scale bar 20 µm)

In fig. 32, a 3D reconstruction (movie 2) shows that the ER is mostly cortically located at the cell wall, but is also spanning the whole cytosol and forms cytoplasmic strands through the vacuole (indicated by an arrow). Some cells show more ER than others, especially around the chloroplasts, due to different expression levels.

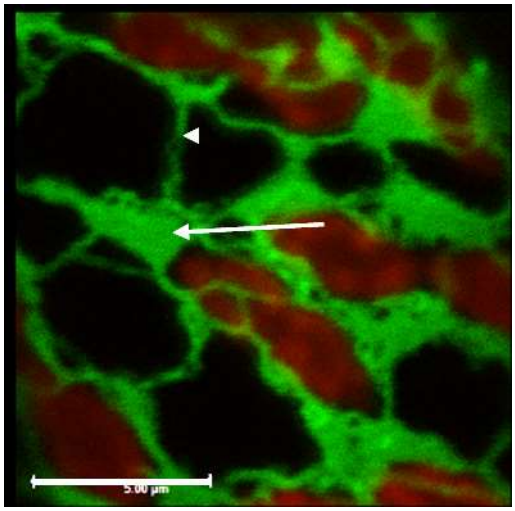

In a higher magnification the movement of the ER is easier to distinguish (fig. 33), this is even demonstrated in a short time lapse movie (movie 3). The cisternae (indicated by an arrow) are not plain sheets, but also have holes and are changing in a few seconds in size and form. The tubules of the ER (indicated by arrowhead) are between these cisternae and are around the chloroplasts.

Fig. 33: *P. patens* ER cell line leaflet cell with tubes and cisternae of ER, Maximum projection overlay of GFP and chloroplast channel; arrow: ER cisternae; arrowhead: ER tubule (scale bar 5 µm)

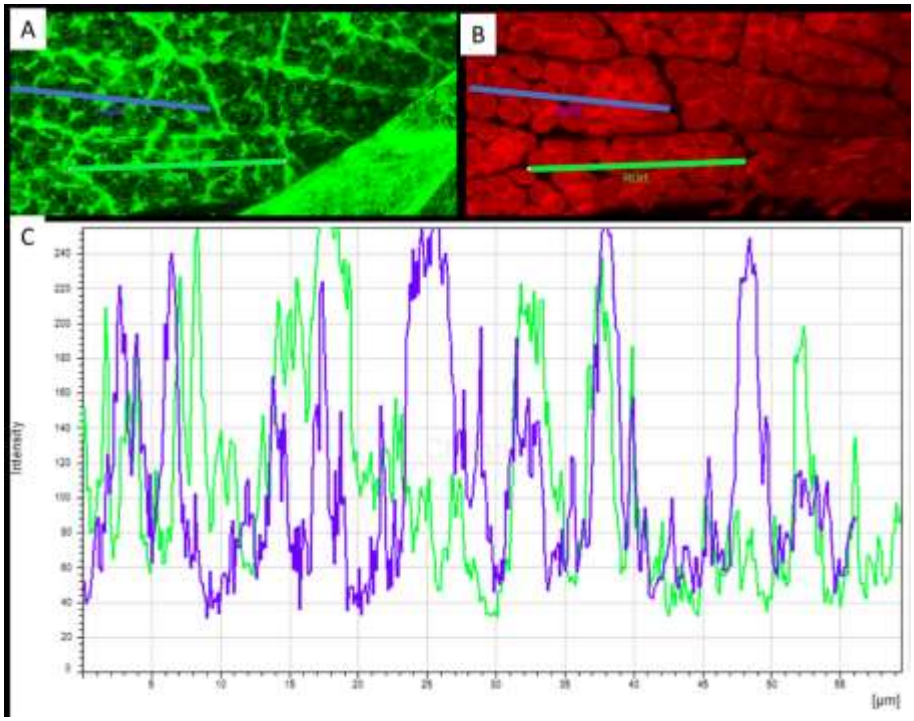

Fig. 34: *P. patens* ER cell line leaflet cells, Maximum projection fluorescence measurement, line of region of interest one in green and two in blue at a random cell length, A) GFP channel B) chloroplast channel C) Graph of measured intensity of fluorescence of GFP (scale bar 20 µm)

Measurements of the fluorescence intensity of ER-GFP in leaflets (fig. 34) showed that there is no pattern in the leaflets cells and when the line crosses a cisternae there is an higher peak. The network of ER seems not to have a special direction in spreading through the cell.

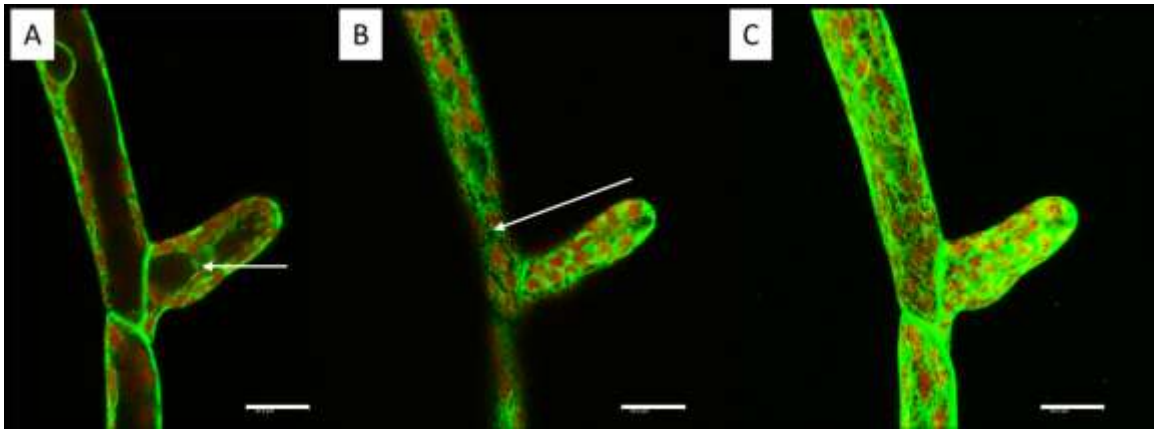

Fig. 35: *P. patens* ER cell line chloronema cell at branching point, overlay of GFP and chloroplast channel A) at the middle of the cell; arrow: ER around nucleus B) at the upper part of the cell; arrow: ER tubules C) maximum projection (scale bar 20 µm)

Fig. 35 shows the GFP-ER in chloronema cells at a branching point. The ER is around the whole nucleus as indicated by an arrow (35 A). The ER is detected near the cell wall. Some tublary structures can be spotted between the chloroplasts (indicated by an arrow in fig. 35 B). In the maximum projection (fig. 35 C) it can be perceived that there are not so many cisternae formed in chloronema cells, than in caulonema cells or leaflet cells.

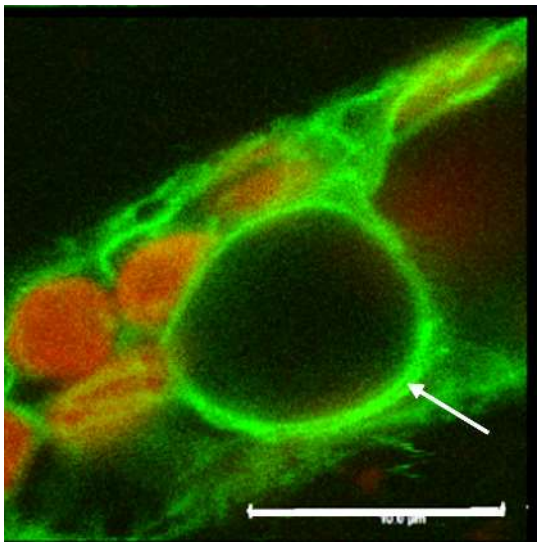

The ER is surrounding the nucleus and in fig. 36 there are two layers of ER seen, also indicated by an arrow. The cortical ER is forming tubules which are connected to the ER around the nucleus and to the chloroplasts or ER cisternae in the cytoplasm.

Fig. 36: *P. patens* ER cell line nucleus of chloronema cell, Maximum projection overlay of GFP and chloroplast channel; arrow: two layers of ER around nucleus (scale bar 10 µm)

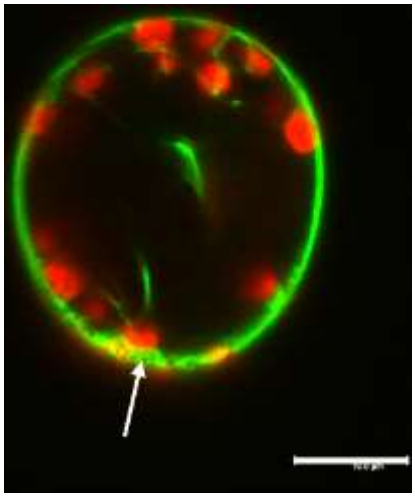

One cell was oriented vertically, so it was possible to see the top of the cell and the ER was like a sheath on top of the cell, this can be viewed in the movie 4 of an average projection. The movie 5 shows a scan through the cell layers. In fig. 37, the ER is at the plasma membrane near the cell wall. Even some circles of ER are revealed (indicated by an arrow). In the middle of the cell less ER and chloroplasts are seen.

Fig. 37: *P. patens* ER cell line vertical chloronema cell in cross section, overlay of GFP and chloroplast channel; arrow: circles of ER (scale bar 10 µm)

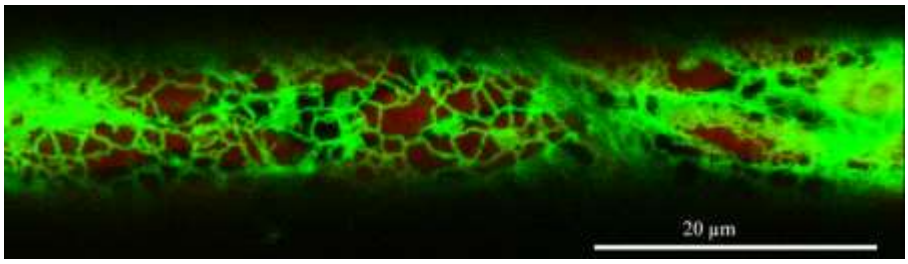

Fig. 38: *P. patens* ER cell line caulonema cell overlay of GFP and chloroplast channel (scale bar 20 µm)

The ER in the protonema, the chloronema and caulonema, also surrounds the nucleus. More cisternae can be found in the caulonema cells (fig. 38 and movie 6). The ER forms also near the cell wall and at the connection between two cells.

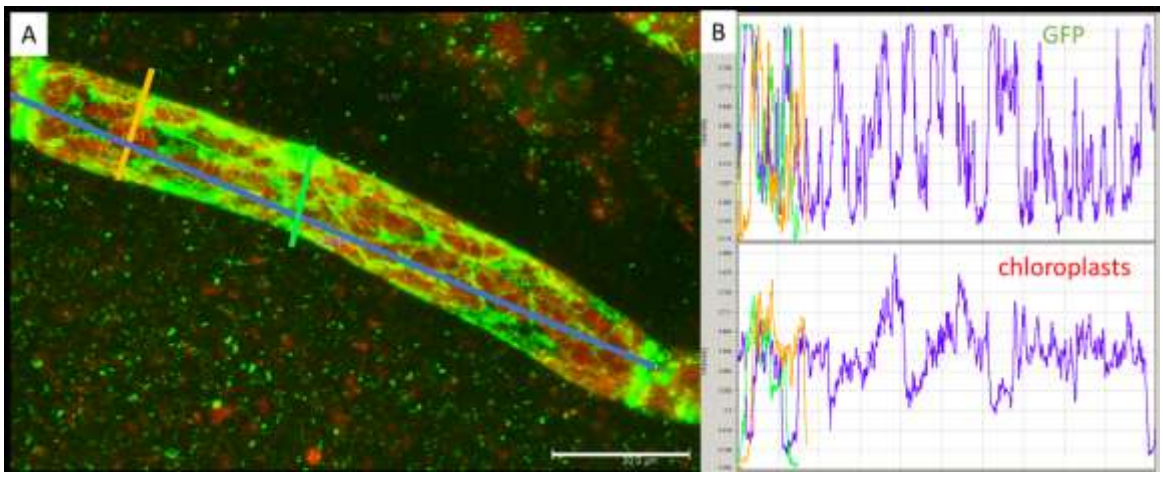

Fig. 39: *P. patens* ER cell line chloronema cell, Maximum projection fluorescence measurement, line of region of interest one in green, two in blue and three in orange A) overlay of GFP and chloroplast channel B) Graph of measured intensity of fluorescence of the two channels (upper Graph GFP channel, lower Graph chloroplast channel) (scale bar 20 µm)

When measuring the GFP-ER of a chloronema cell (fig. 39), similar results like in the leaflet cells are given, when the line of region of interest crosses one cisternae the peak is higher. And there is also a high peak at the cell wall and when measuring the nucleus (as shown by the green line), this is due to the fact that there is an accumulation of ER. Of course,

the measurement of the chloroplast channel presented only a peak, when a chloroplast is beneath the line.

GFP Life-act cell line

The actin filaments do not form single lines in one direction; it appears more like a netlike structure, which is not directed in a special direction. The actin can be found in the cortex near the cell wall, around the nucleus and as a netlike structure through the whole cell.

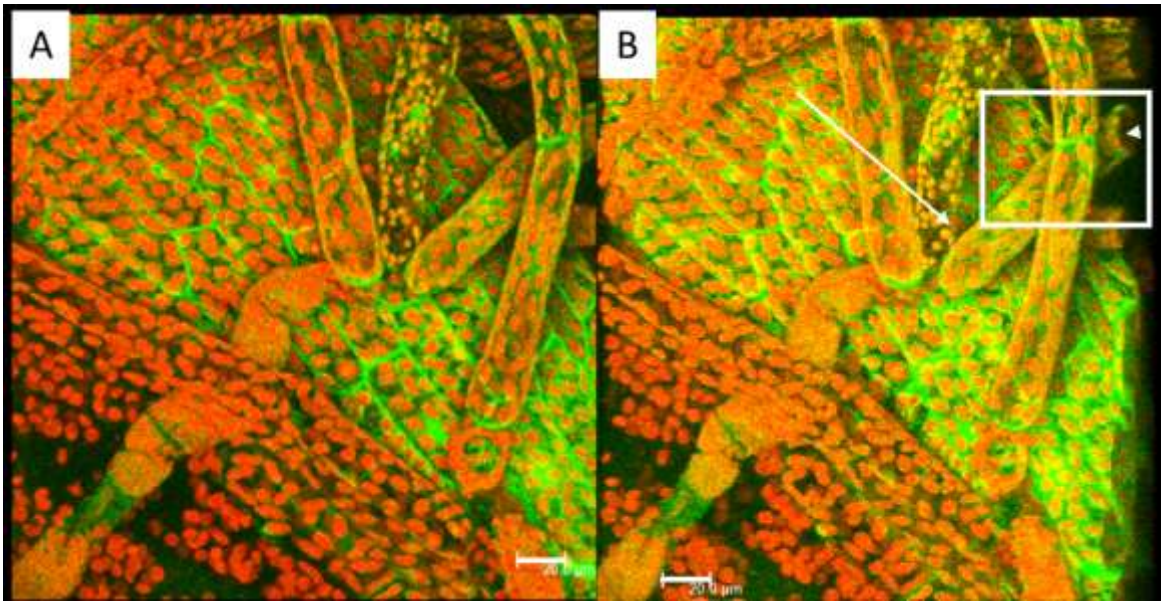

Fig. 40: *P. patens* Life-act cell line leaflet cells with outgrowing protonema cells, A) Maximum projection overlay of GFP and chloroplast channel B) 3D Reconstruction maximum projection overlay of GFP and chloroplast channel; arrow: interior of leaflet cell; arrowhead: interior of chloronema cell (scale bar 20 µm)

In the leaflet sometimes protonema cells can establish (fig. 40), the chloronema cells grow out of the leaflet cells. Here also the fluorescence of the Life-actin can be seen around the nucleus, the cell wall and like a net through the cell in both cell types. In the leaflet cells the fluorescence seems to be much higher. The lower part of the picture also reveals some cells which do not show the GFP fluorescence, this can be, because they degraded the GFP and are about to die. In the 3D Reconstruction of a maximum projection (fig. 40 B) the actin is more in the vicinity of the cell wall (shown in movie 7) and not so much in the middle of the cell. In a higher magnification of fig. 40 B (fig.41) this can be seen better for a chloronema cell (indicated by an arrowhead).

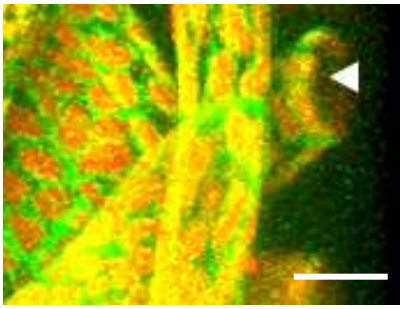

Fig. 41: *P. patens* Life-act cell line leaflet cells with outgrowing protonema cells, 3D Reconstruction maximum projection overlay of GFP and chloroplast channel, higher magnification of the rectangle indicated part of 48B; arrowhead: interior of chloronema cell (scale bar 20 µm)

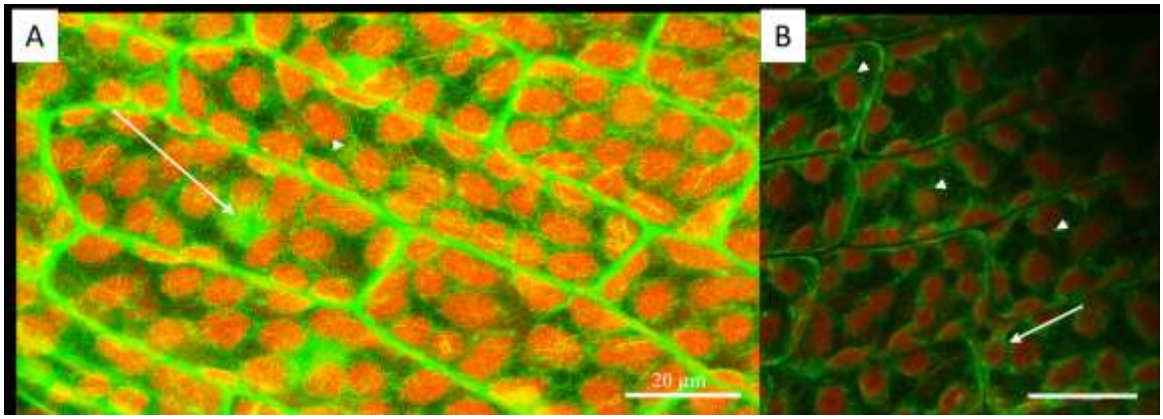

Fig. 42: *P. patens* Life-act cell line leaflet cells, Maximum projection overlay of GFP and chloroplast channel; A) leaflet cells near leaf vein; arrow: actin around nucleus; arrowhead: netlike structure of actin B) leaflet cells near the leaf margin; arrow: actin filaments stretching through cell from chloroplast; arrowheads: G-Actin (scale bar 20 µm)

The leaflet cells show an accumulation of actin around the nucleus (indicated by an arrow) and a netlike structure within the cell (indicated by arrowhead in fig. 42 A). A 3D reconstruction movie was also created (movie 8). The actin is not like the ER accumulated around the chloroplast, it is rather between the chloroplast (arrow in fig. 42 B shows the filaments stretching from a chloroplast). This may help the chloroplast to stay at the same position, these filaments are sometimes filling up the cell. Seldomly some tiny structures, like dots, can be seen (indicated by arrowheads in fig. 42 B). This may be the globulary actin. This was more seen in plasmolysed cells, more information to this is shown in the plasmolysis part later. The actin filaments have no special direction in the cell and form a netlike structure. Furthermore, the cell cortex at the plasma membrane near the cell wall is containing a high amount of actin. In a 3D reconstruction of a maximum projection the actin filaments are more abundant at the outer parts of the cell so near the cell wall and less in the middle of the cell.

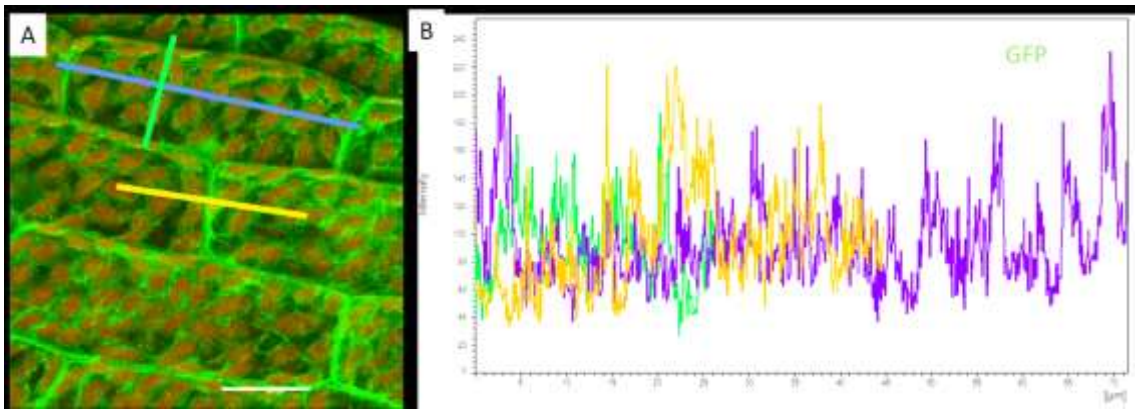

Fig. 43: *P. patens* Life-act cell line leaflet cells, Maximum projection fluorescence measurement, line of region of interest one in green, two in blue and three in orange A) overlay of GFP and chloroplast channel B) Graph of measured intensity of fluorescence of GFP channel (scale bar 20 µm)

When measuring the intensity of the Life-act (GFP) in leaflet cells, there is no distinguishable pattern of direction of the network detected (fig. 43). Near the cell wall, where the plasma membrane is, higher peaks of fluorescence intensity are displayed. Through the cell the peaks remain quite the same.

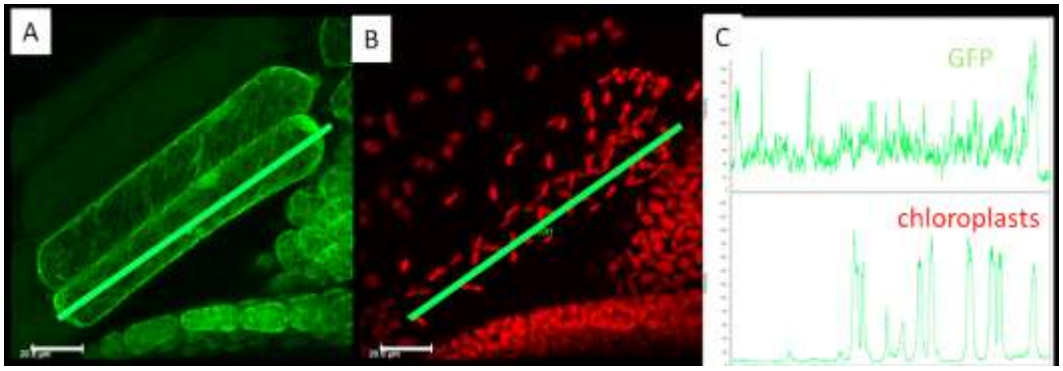

Fig. 44: *P. patens* Life-act cell line chloronema cells lying above a leaflet, Maximum projection fluorescence measurement, line of region of interest one in green A) GFP channel B) chloroplast channel C) Graph of measured intensity of fluorescence of the two channels (upper Graph GFP channel, lower Graph chloroplast channel) (scale bar 20 µm)

In the measurement of the fluorescence of GFP in one chloronema cell above a leaflet (fig. 44), actin is showing a regular appearance, an accumulation at the end of the cell is always present.

In chloronema cells the actin forms also a network around the chloroplasts, it looks like the strands of actin expand from the chloroplasts (indicated by an arrow in fig. 45). It furthermore shows the actin near the plasma membrane and the cell wall (fig. 45, indicated by arrowhead). The fluorescence is not so high in comparison to leaflet cells. The actin can be spotted as tiny actin filaments through the cell. When measuring the fluorescence intensity of GFP in the same cells (fig. 46), higher peaks of intensity are only seen, when the line of region of interests is drawn above a cell wall, otherwise actin is not aggregated in the cell. The chloroplasts are showing kind of a regular pattern in their distribution in the cell.

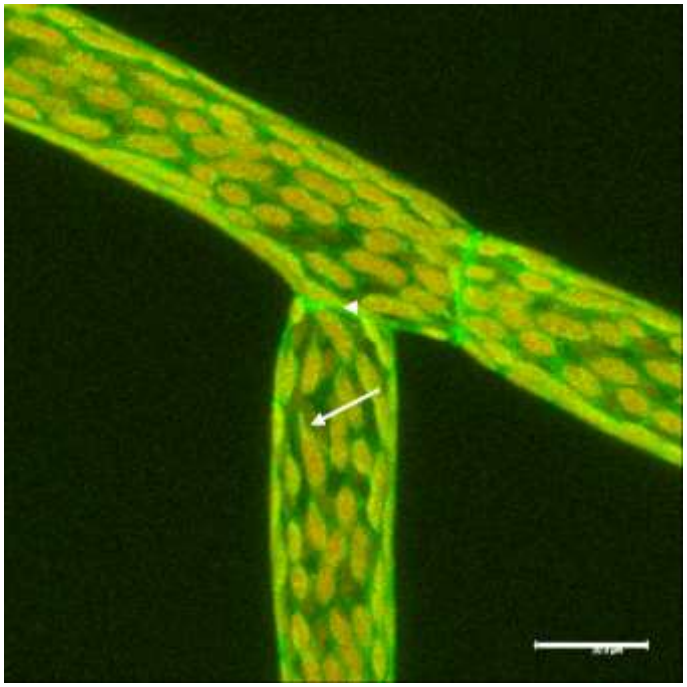

Fig. 45: *P. patens* Life-act cell line chloronema cells at a branching point, Maximum projection overlay of GFP and chloroplast channel; arrow: actin strand near chloroplast; arrowhead: actin near plasma membrane (scale bar 20 µm)

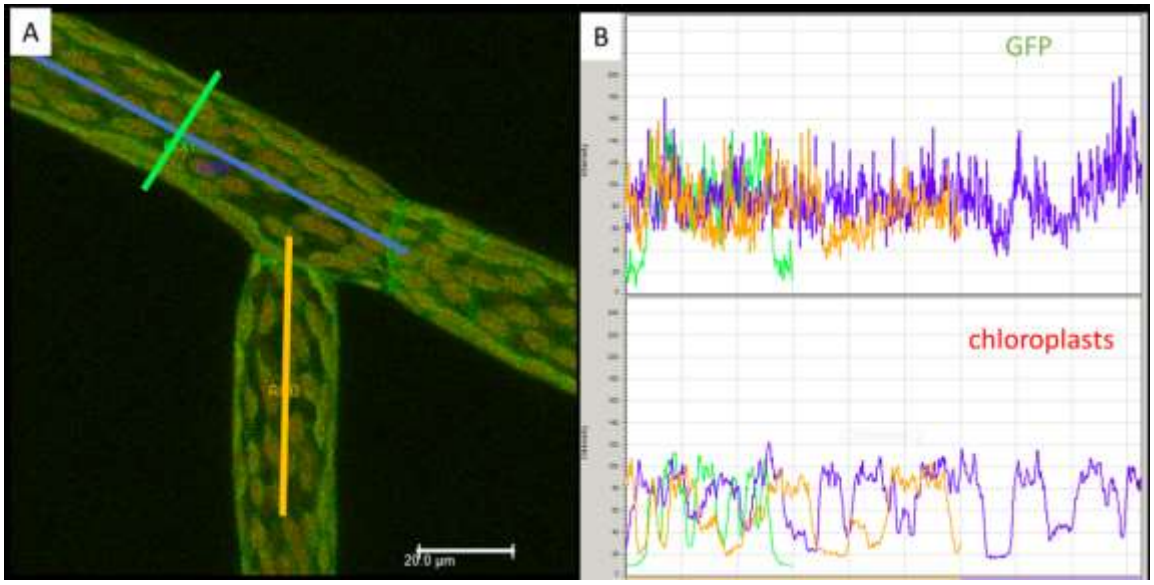

Fig. 46: *P. patens* Life-act cell line chloronema cell at branching point, Maximum projection fluorescence measurement, line of region of interest one in green, two in blue and three in orange A) overlay of GFP and chloroplast channel B) Graph of measured intensity of fluorescence of the two channels (upper Graph GFP channel, lower Graph chloroplast channel) (scale bar 20 µm)

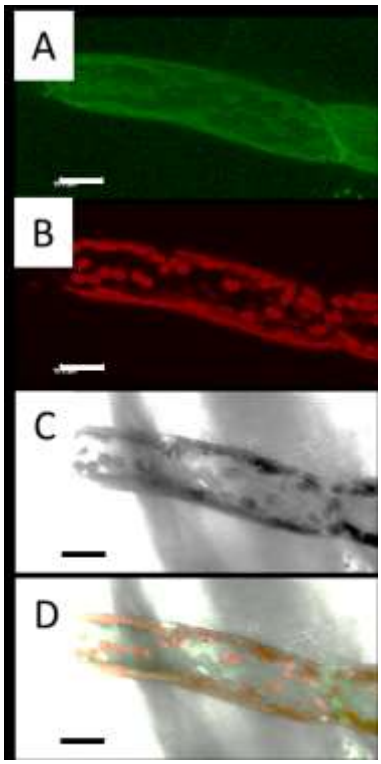

The caulonema cells also show actin cortical near the cell membrane and the chloroplasts and some bundles of actin between the chloroplasts (fig. 47 A). The GFP-actin was best to witness in the leaflet cells, the protonema cells tended to show less.

Fig. 47: *P. patens* Life-act cell line caulonema cell, Maximum projection A) GFP channel B) chloroplast channel C) Transmission channels D) Overlay of all channels (scale bar 20 µm)

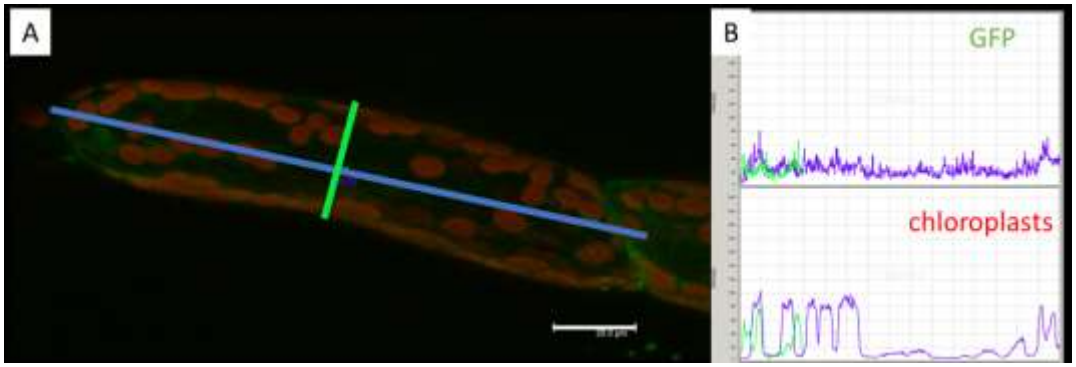

Fig. 48: *P. patens* Life-act cell line caulonema cell, fluorescence measurement, line of region of interest one in green and two in blue, A) overlay of GFP and chloroplast channel B) Graph of measured intensity of fluorescence of the two channels (upper Graph GFP channel, lower Graph chloroplast channel) (scale bar 20 µm)

In the caulonema cell the measurement of the GFP of actin showed similar patterns to chloronema cells (fig. 48), but the intensity was much lower, the Life-act cell line seemed to be finer spread in the caulonema. This cell did not contain many chloroplasts and therefore showed less peaks than the measured cells before.

GFP-Tubulin cell line

The GFP-tubulin was shown around the nucleus. The chloroplasts were seemingly enclosed between the microtubules. Like the other two cell lines before (ER, Life-act) tubulin was also shown in the vicinity of the plasma membrane. In the leaflet even, microtubules in cross section were perceived.

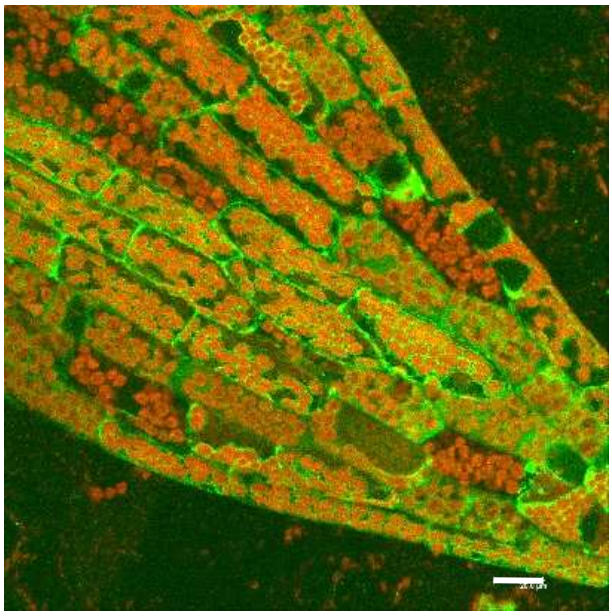

The GFP-Tub shows the tubulin near the plasma membrane and some microtubules around the chloroplasts (fig. 49). In the middle of the leaflet there are still healthy cells, but the outer cells display coagulated plasma and degenerated chloroplasts. In the dead cells the GFP shows unspecific labelling and can be seen at the edges of the cells.

Fig. 49: *P. patens* GFP-Tub cell line leaflet cells, Maximum projection overlay of GFP and chloroplast channel (scale bar 20 µm)

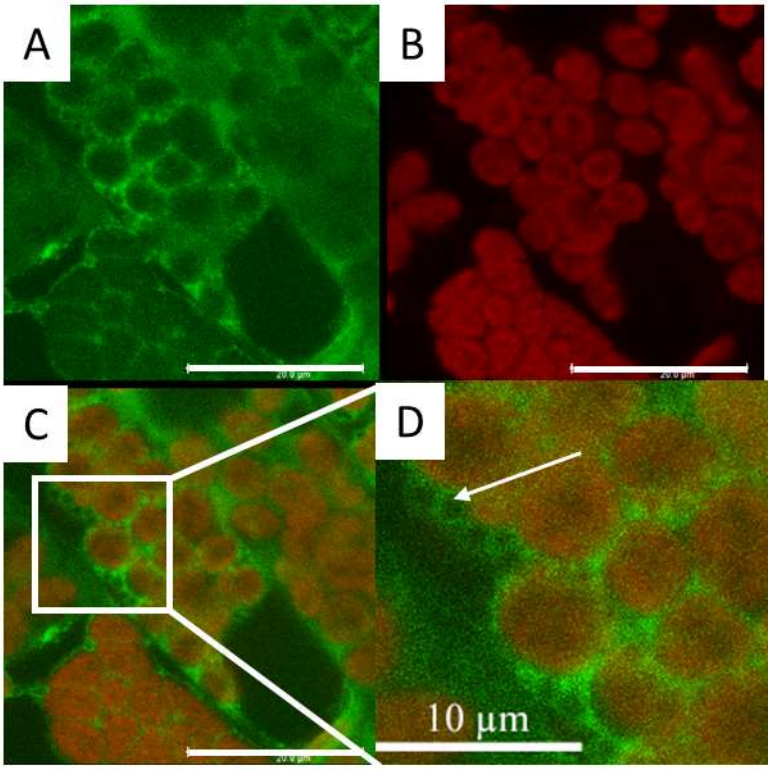

In the leaflet cell some roundish circular structures are distinguishable. In higher magnification they are better too recognize (fig. 50 D, indicated by an arrow). These microtubules are formed around the chloroplasts, maybe they help to keep the chloroplast in place or are needed for the movement of the chloroplast from the top to the bottom of the cell.

Fig. 50: *P. patens* GFP-Tub cell line leaflet cells, Maximum projection A) GFP channel B) chloroplast channel C) overlay of GFP and chloroplast channel (scale bar 20 µm) D) higher magnification of the rectangle indicated part of C; arrow: roundish circular structure of tubulin (scale bar 10 µm)

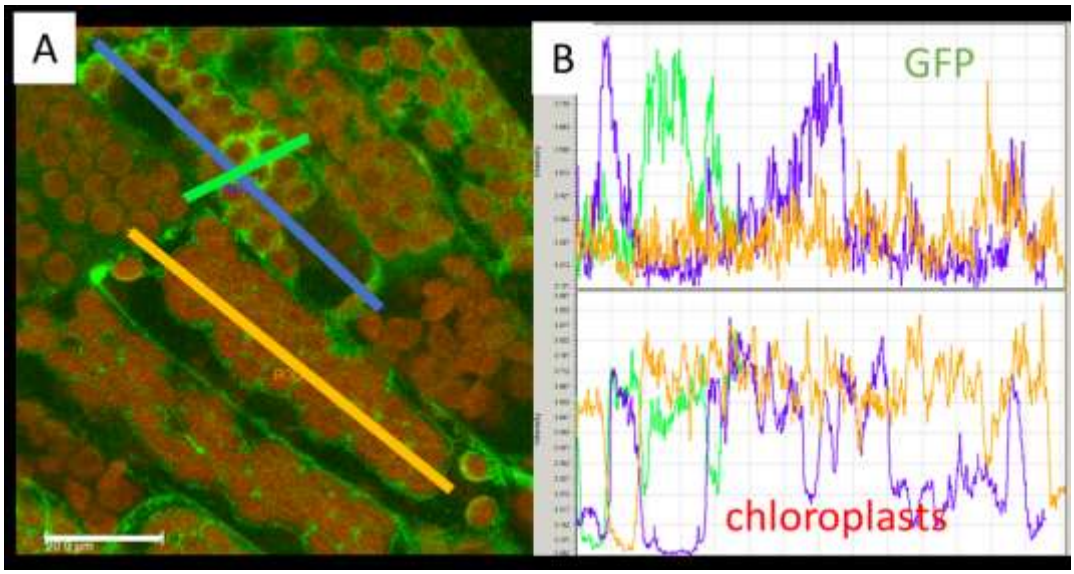

Fig. 51: *P. patens* GFP-Tub cell line leaflet cells, fluorescence measurement, line of region of interest one in green, two in blue and three in orange, A) overlay of GFP and chloroplast channel B) Graph of measured intensity of fluorescence of the two channels (upper Graph GFP channel, lower Graph chloroplast channel) (scale bar 20 µm)

The leaflet cells show no pattern for the GFP of tubulin but demonstrate some higher intensity at the region of interest in green (fig. 51). The blue line of the region of interest shows at the cortex of the cell a higher intensity. The orange line detects just a blurry intensity.

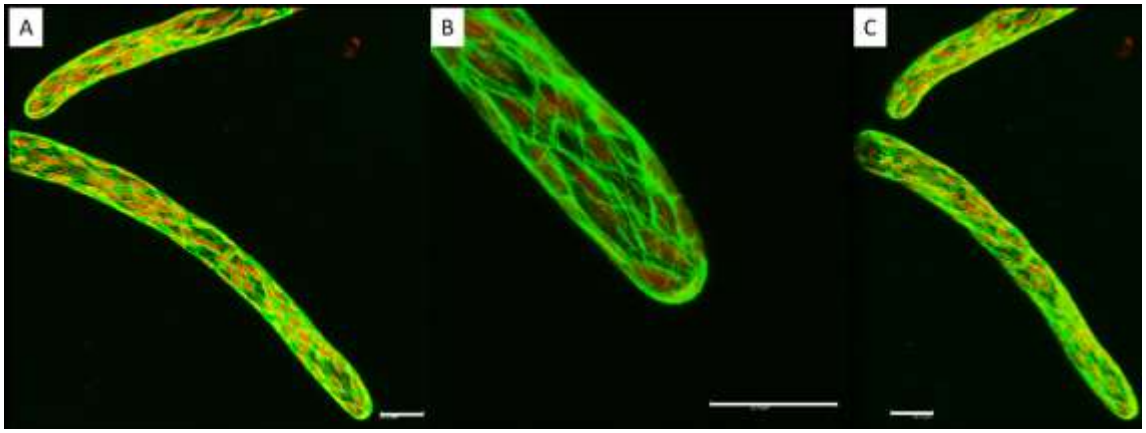

Fig. 52: *P. patens* GFP-Tub cell line chloronema cells, Maximum projection overlay of GFP channel and chloroplast channel A) overlay of GFP and chloroplast channel B) only tip of chloronema cell C) picture of 3D Maximum projection of a movie at a turned angle (scale bar 20 µm)

The tubulin forms tube-like structure through the whole cell, enclosing the chloroplasts between them, they also enclose the whole cell itself (fig. 52 and movie 9). They can be found in close vicinity to the plasma membrane and at the tip of the cell they are also present. In fig. 52 C the tubules seem to be just at the outer part of the cell and not going through the whole cell.

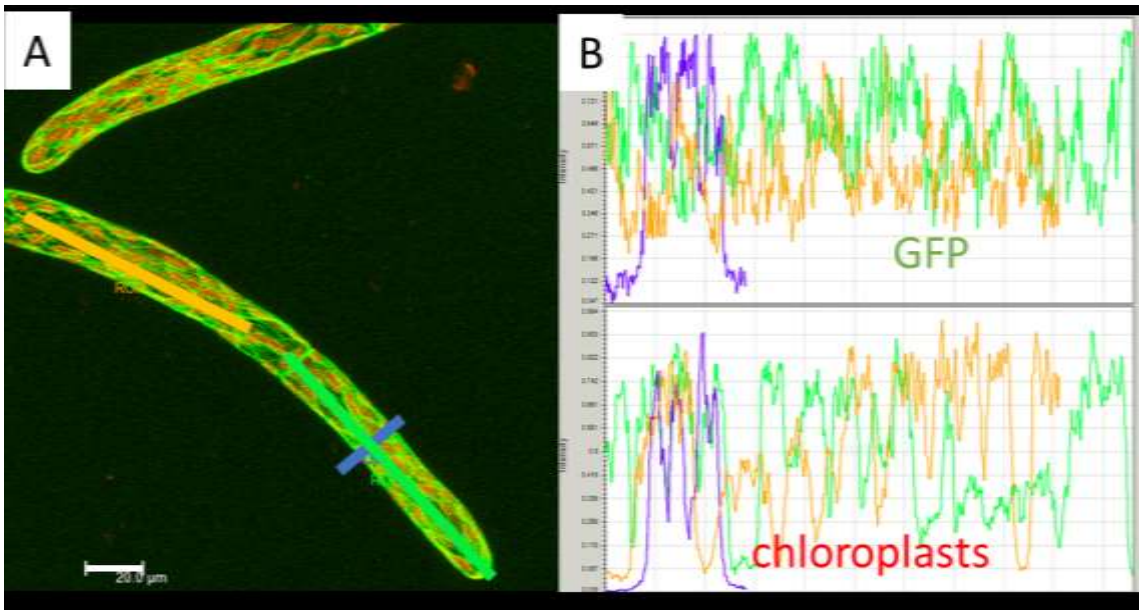

Fig. 53: *P. patens* GFP-Tub cell line chloronema cells, fluorescence measurement, line of region of interest one in green, two in blue and three in orange, A) overlay of GFP and chloroplast channel B) Graph of measured intensity of fluorescence of the two channels (upper Graph GFP channel, lower Graph chloroplast channel) (scale bar 20

In the measurement of intensity of fluorescence of a chloronema cell (fig. 53) the GFP did not really have a regular pattern, but more than the ER, this is visible in the lines of regions of interest green and blue. In the green line of region of interest it is revealed that whenever the chloroplasts have a peak, the peak of GFP tubulin is lower and vice versa.

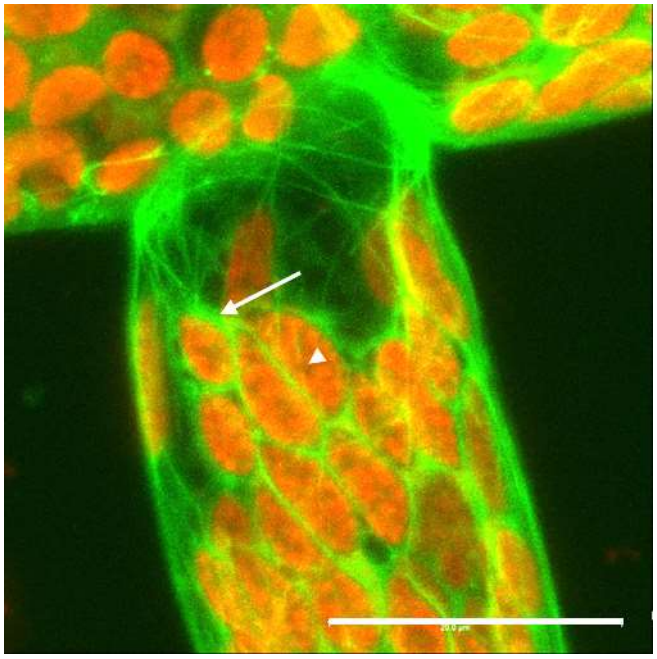

In this chloronema cell (fig. 54) the tubulin is found between the chloroplasts (marked with an arrow) and establishes some finer and thicker bundles of microtubules (seen in 3D reconstruction movie 10). Sometimes it seems like the tubulin goes through the chloroplast (indicated by an arrowhead), this can also be caused when two chloroplasts are closely attached to each other.

Fig. 54: *P. patens* GFP-Tub cell line chloronema cells at a branching point, Maximum projection overlay of GFP channel and chloroplast channel; arrow: thicker bundles of microtubules; arrowhead: micortubule within chloroplasts (scale bar 20 µm)

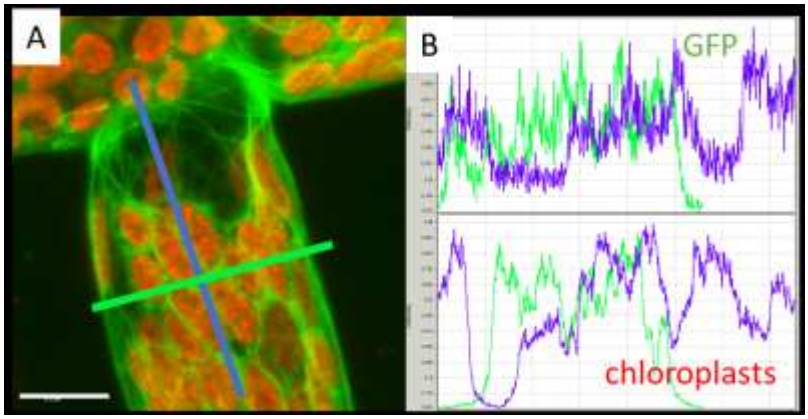

When measuring a chloronema cell at a branching point (fig. 55) the GFP did not show any pattern of occurrence of the tubulin. Between the measurements of intensity of GFP and the chloroplast channel there was no connection distinguishable.

Fig. 55: *P. patens* GFP-Tub cell line chloronema cells at a branching point, fluorescence measurement, line of region of interest one in green and two in blue, A) overlay of GFP and chloroplast channel B) Graph of measured intensity of fluorescence of the two channels (upper Graph GFP channel, lower Graph chloroplast channel) (scale bar 20 µm)

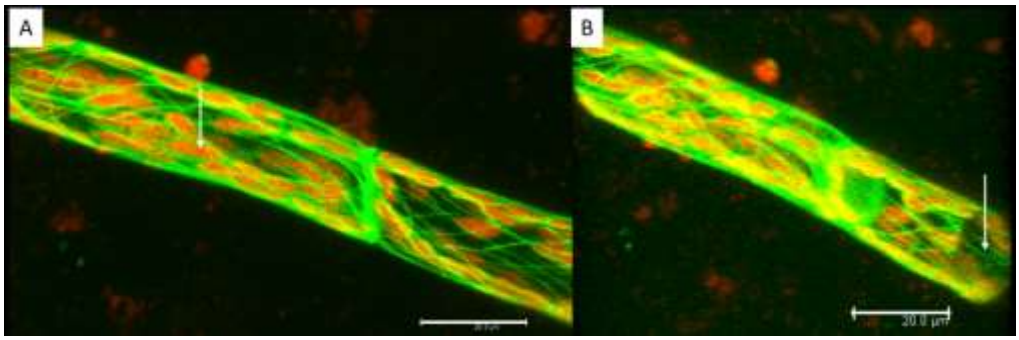

Fig. 56: *P. patens* GFP-Tub cell line caulonema cells, Maximum projection overlay of GFP channel and chloroplast channel A) overlay of GFP and chloroplast channel; arrow: with tubules enclosed chloroplast B) picture of 3D Reconstruction of Maximum projection of a movie at a turned angle; arrow: interior of cell (scale bar 20 µm)

The caulonema cells display the same structures as the chloronema cells. The chloroplasts are enclosed by the microtubules, this is indicated by an arrow for one chloroplast, where it can be seen very clearly (fig. 56 A). In the 3D reconstruction the microtubules seem only to form at the outer part of the cell (indicated by an arrow in fig. 56 B) and accumulate in the cell wall between to neighbouring cells to form a plate.

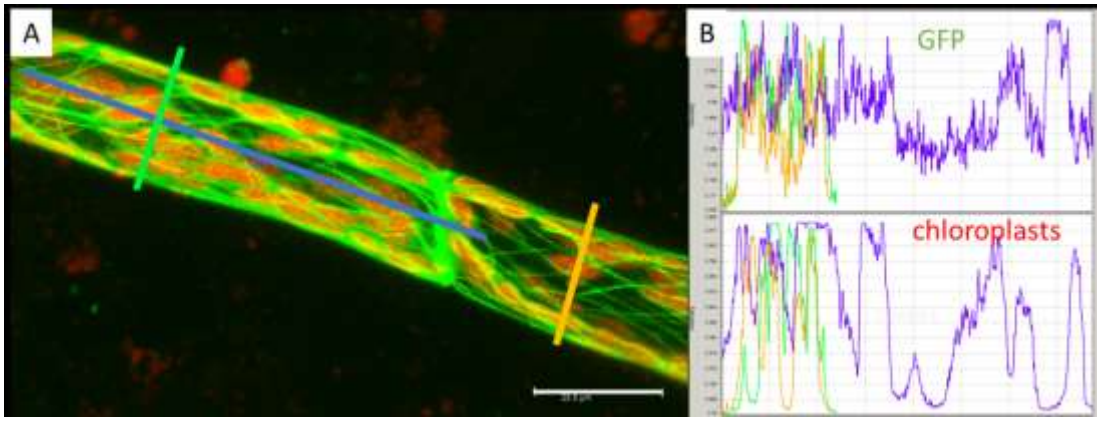

Fig. 57: *P. patens* GFP-Tub cell line caulonema cell, fluorescence measurement, line of region of interest one in green, two in blue and three in orange, A) overlay of GFP and chloroplast channel B) Graph of measured intensity of fluorescence of the two channels (upper Graph GFP channel, lower Graph chloroplast channel) (scale bar 20 µm)

Because of the tiny structures of the tubules no high peaks are seen in the middle of the cell (fig. 57), when measuring the fluorescence intensity of GFP. Higher peaks are shown at the cell wall, where the tubulin accumulates, this is seen in the line of region of interest in blue.

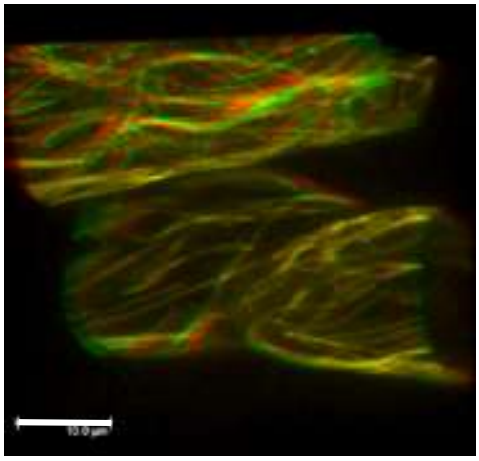

This 3D Reconstruction with 3D effect in fig. 58 demonstrating the three-dimensional structure of the microtubules. This reveals that the tubules are more at the edges of the cells and seem to form a cage around the inner parts of the cell.

Fig. 58: *P. patens* GFP-Tub cell line caulonema cells at a cell to cell connection, 3D reconstruction of Maximum projection with 3D effect only of GFP channel (scale bar 20 µm)

Myosin VIII cell line

The Myosin VIII was detected in the cell membrane near the cell wall, in the cytosol and sometimes in parts of the chloroplasts. But unfortunately, this cell line did not show what was expected. Normally the Myosin VIII would be found near the cell wall at newly formed cells.

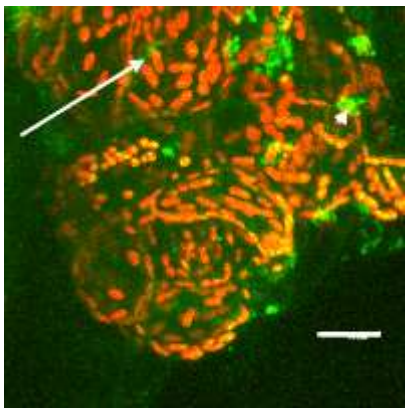

In fig. 59 the GFP of Myosin VIII accumulated (marked with an arrowhead) only in some parts of the cell but did not show any structures. At the cell wall, the GFP showed unspecific labelling (indicated by an arrow).

Fig. 59: *P. patens* Myosin VIII cell line budding cells, Maximum projection overlay of GFP channel and chloroplast channel; arrow: unspecific labelling of GFP near plasma membrane; arrowhead: accumulated GFP (scale bar 20 µm)

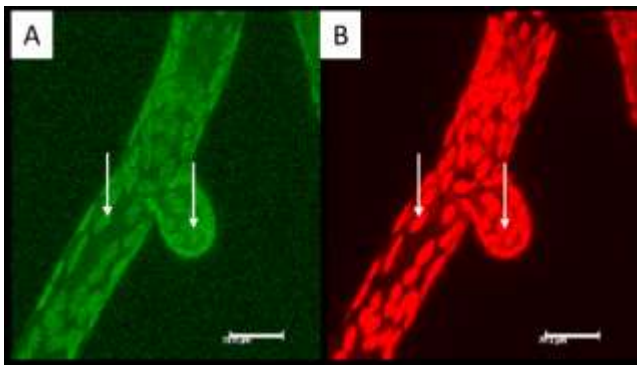

Sometimes Myosin VIII showed the fluorescence like the chloroplasts, this is indicated by arrows in fig. 60.

Fig. 60: *P. patens* Myosin VIII cell line chloronema cells with a newly formed cell, Maximum projection A) GFP channel B) chloroplast channel; arrows: chloroplasts (scale bar 20 µm)

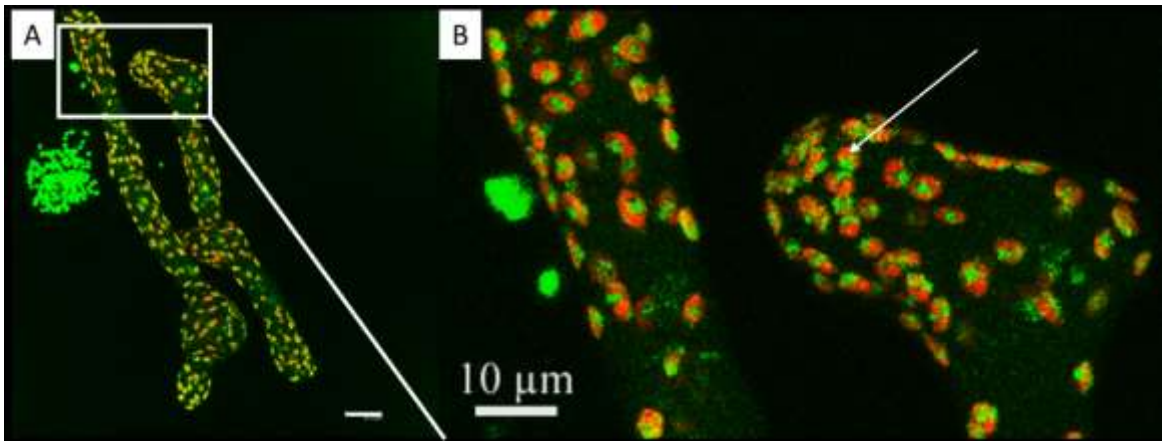

Fig. 61: *P. patens* Myosin VIII cell line chloronema cells, A) Maximum projection overlay of GFP channel and chloroplast channel (scale bar 20 µm) B) higher magnification of the rectangle indicated part of A; arrow: GFP in chloroplast (scale bar 10 µm)

In fig. 61 A the chloroplasts show also the GFP fluorescence, but no more structures can be seen. In the higher magnification of the cell in fig. 61 B it can be perceived, that just some parts of the chloroplasts showed a fluorescence of the GFP and not the whole chloroplast showed the GFP (indicated by an arrow).

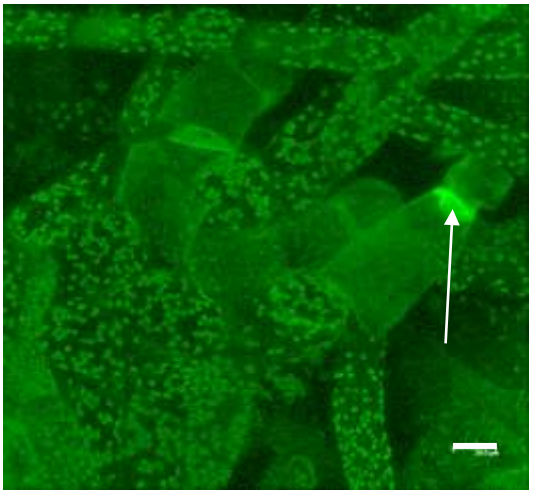

In the conventional fluorescence the fluorescence of the GFP was seen in the cytosol and in the plasma membrane near the cell wall between some cells (marked by an arrow in fig. 62), only when the Gain was very high, and the offset was very low, then this was also seen in the confocal laser scanning microscope, but it was not anymore a true confocal picture.

Fig. 62: *P. patens* Myosin VIII cell line chloronema cells near the stem, Maximum projection GFP channel; circle: plasma membrane (scale bar 20 µm)

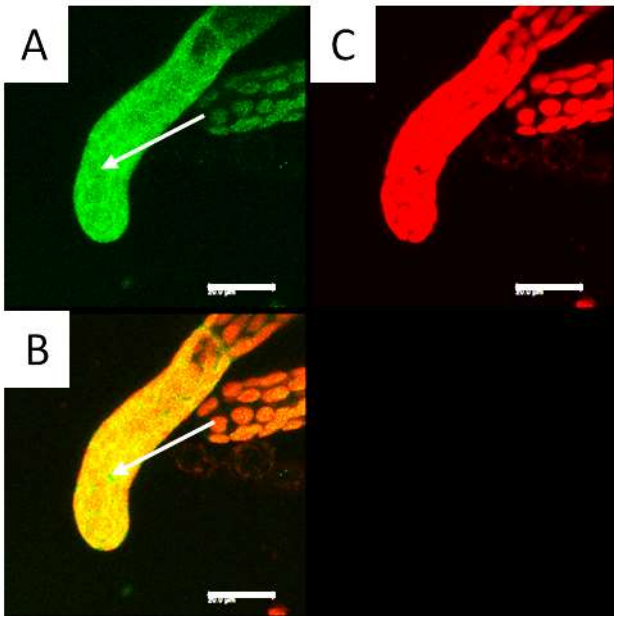

Fig. 63 shows a structure between the chloroplasts, this is indicated by an arrow (fig. 63 C) and it can be seen in the movie 11. This was only seen when the brightness and contrast are very high, but just in this young chloronema cell and in no other cell. In the GFP channel (fig. 63 A) there is a tubulary structure of the GFP shown and not just an accumulation.

Fig. 63: *P. patens* Myosin VIII cell line chloronema cell Maximum projection A) GFP channel; arrow: tubulary structure of GFP B) chloroplast channel C) overlay of GFP and chloroplast channel; arrow: GFP between chloroplasts (scale bar 20 µm)

Reticulon GFP-cell line

The GFP-Reticulon protein was not good to recognize, it was seen in cytosol as a destructed protein. Sometimes only in parts in the chloroplasts the GFP was present. Because of that, it seemed like the Reticulon is associated with the chloroplasts. But this was likely only unspecific labelling.

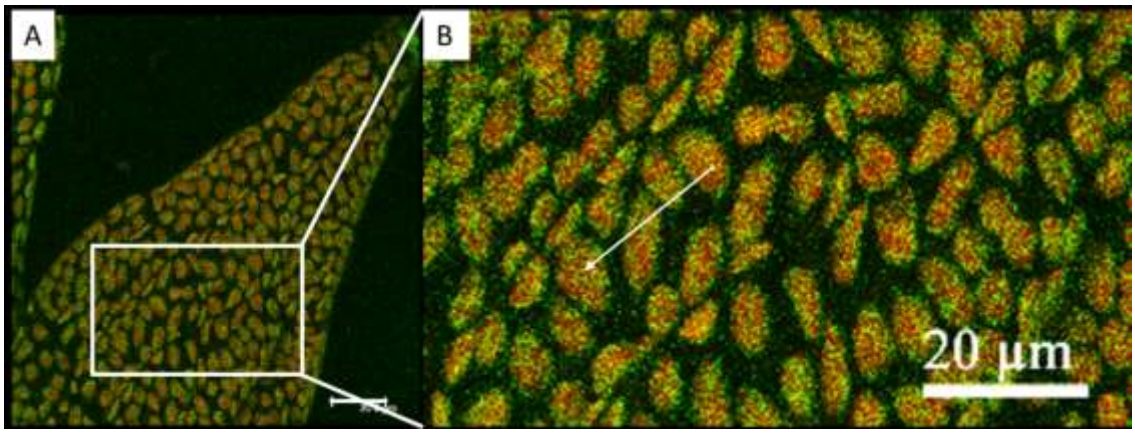

Fig. 64: *P. patens* Reticulon cell line leaflet cells, A) Maximum projection overlay of GFP channel and chloroplast channel (scale bar 20 µm) B) higher magnification of the rectangle indicated part of A; arrow: GFP within chloroplast (scale bar 20 µm)

In some parts of chloroplasts of leaflet cells the GFP of Reticulon was seen, this is indicated by an arrow in fig. 64 B. Only in higher magnification a structure within the chloroplasts can be distinguished. Maybe it showed the ER around the chloroplasts.

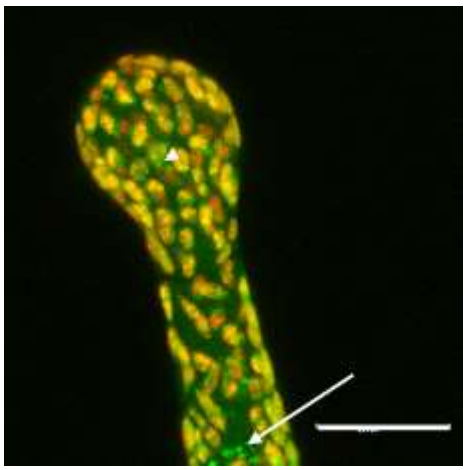

In fig. 65 the Reticulon can be seen in the chloroplasts. Just some parts of the chloroplasts seem to contain the GFP, and GFP in the cytosol (indicated by an arrow), it seems the cell did not express the Reticulon properly. In the middle of the tip cell an accumulation of GFP is present (indicated by an arrowhead), this could be the nucleus or just a random accumulation in the cytosol.

Fig. 65: *P. patens* Reticulon cell line chloronema end cell Maximum projection overlay of GFP channel and chloroplast channel; arrow: GFP in cytosol; arrowhead: accumulation of GFP (nucleus) (scale bar 20 µm)

Calnexin GFP cell line

Unfortunately, also the Calnexin cell line did not show what was expected. The GFP was not good to distinguish in the cells and showed unspecific labelling. The fluorescence of Calnexin was spotted in close vicinity to the plasma membrane, in the cytosol and the chloroplasts.

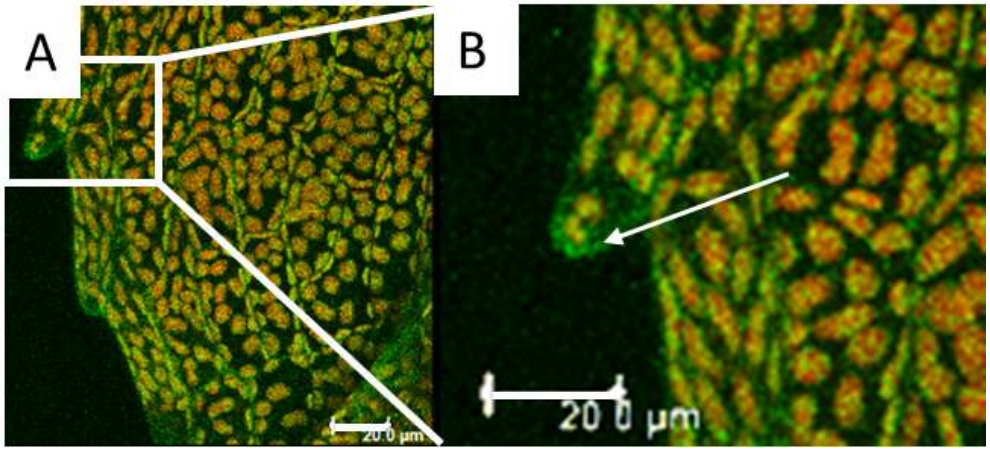

Fig. 66: *P. patens* Calnexin cell line leaflet cells, A) Maximum projection overlay of GFP channel and chloroplast channel (scale bar 20 µm) B) higher magnification of the rectangle indicated part of A; arrow: plasma membrane; arrowhead: GFP in chloroplast (scale bar 20 µm)

In the leaflet cell the Calnexin (fig. 66) shows the GFP near the plasma membrane (indicated by an arrow) and the same fluorescence as the chloroplasts. In higher magnification (fig. 66 B) it is revealed that the GFP was just in some parts of the chloroplasts (indicated by arrowhead).

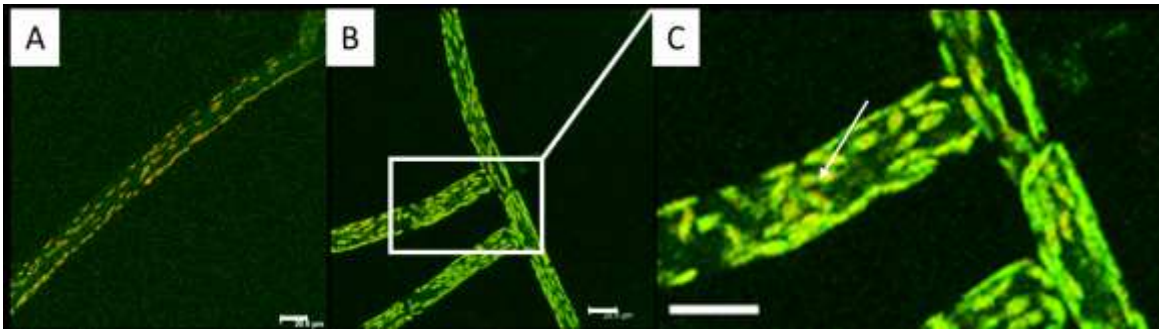

Fig. 67: *P. patens* Calnexin cell line protonema cells, Maximum projection overlay of GFP channel and chloroplast channel A) chloronema cell B) caulonema and chloronema cells at a branching point (scale bar 20 µm) C) higher magnification of the rectangle indicated part of C; arrow: GFP in chloroplast (scale bar 20 µm)

In the protonema cells (fig. 67) it is the same like in the leaflet cells, but the fluorescence near the plasma membrane is not so good to distinguish, in the conventional fluorescence also the cytoplasm showed fluorescence. In higher magnification (fig. 69 C) the GFP is seen in parts of the chloroplasts and around them (indicated by an arrow).

3. 5 Labelling

We wanted to test with specific dyes and if they show the same structures as the GFP-lines. We first started with the labelling of the plasma membranes with the styryl dyes FM4-64 and FM1-43, followed by staining of the actin filaments, with Rhodamine Phalloidin.

styryl dye FM4-64

It was expected that the styryl dye FM4-64 (www.thermofisher.com) labelled the plasma membranes in the different cell types. The dye was mostly seen in the plasma membrane near the cell wall, in all of the different species and sometimes also in vesicles. The typical structure of the ER with its sheets and tubules were only seen in the ER-GFP cell line, as expected.

Control cell line

In the control cell line of *P. patens,* the styryl dye FM4-64 labelled the plasma membrane near the cell wall in all of the different cell types and sometimes vesicles in the cells of the protonema, also the chloroplasts showed sometimes an emission in this range.

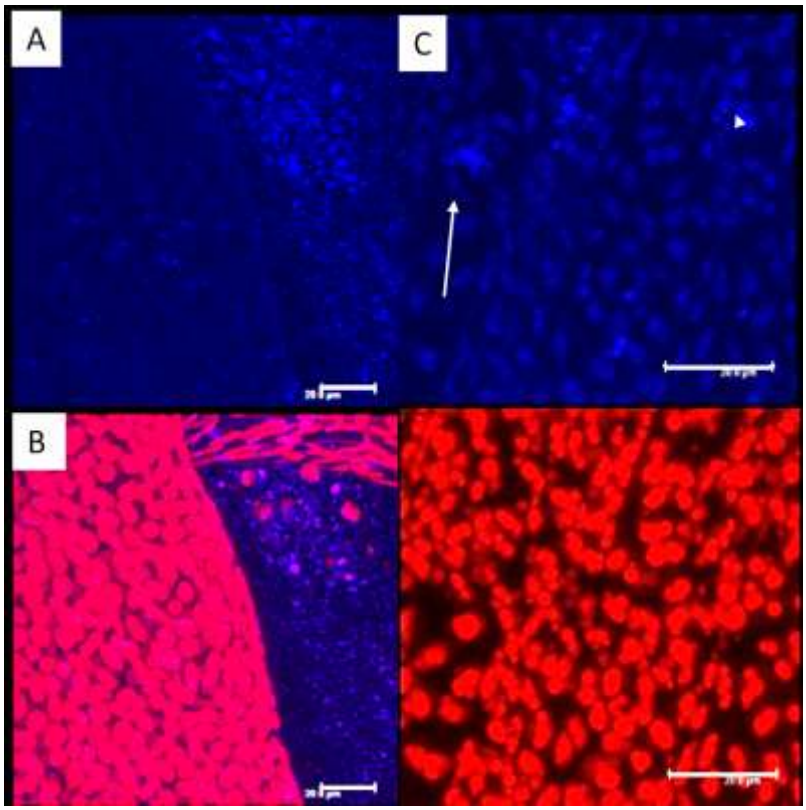

In fig. 68 leaflet cells in different magnification are shown. In fig. 68 A and B the cells were not enough washed out so the plasma membrane is not so easy to distinguish in the FM4-63 channel (indicated by an arrow). Figs. 70 C and D display in the FM4-64 channels the same problem (plasma membrane is indicated by arrow), here also the chloroplasts show the same fluorescence as the FM4-64 dye.

Fig. 68: *P. patens* Control cell line leaflet cells labelled with FM4-64, Maximum projection A) FM4-64 channel; arrow: plasma membrane B) overlay of FM4-64 channel and chloroplast channel; Higher magnification of leaflet cells C) FM4-64 channel; arrow: plasma membrane D) chloroplast channel (scale bar 20 µm)

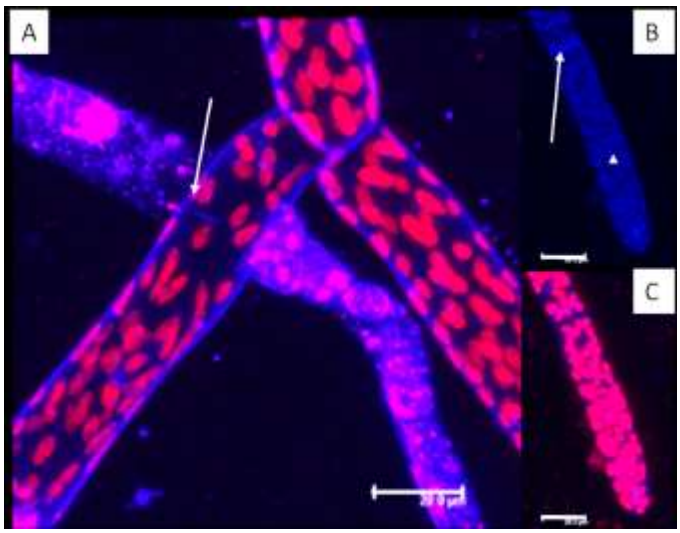

In fig. 69 the plasma membranes in chloronema cells are stained, this is also indicated by an arrow. In fig. 69 B not only the plasma membrane (indicated by an arrow) is stained, even the chloroplast show a fluorescence in this range, this is indicated by an arrowhead.

Fig. 69: *P. patens* Control cell line chloronema cells labelled with FM4-64, Maximum projection A) chloronema cells at a branching point overlay of FM4-64 and chloroplast channel; arrow: plasma membrane B) chloronema cell FM4-64 channel; arrow: plasma membrane; arrowhead: chloroplast C) overlay of FM4-64 and chloroplast channel (scale bar 20 µm)

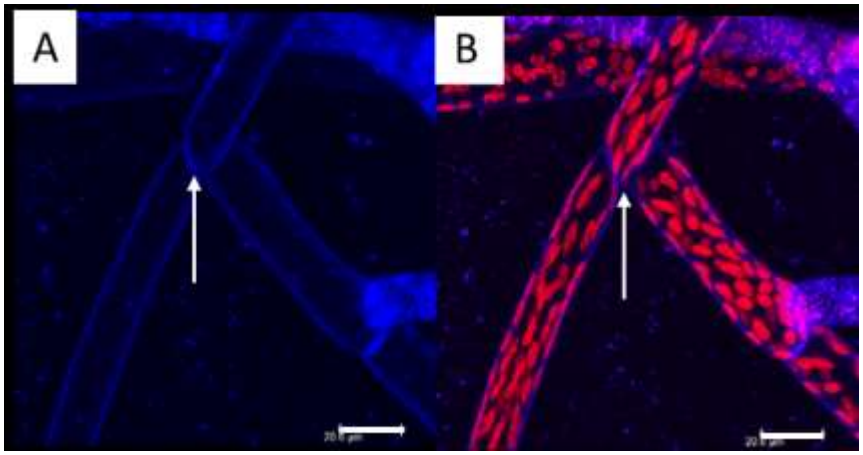

In the caulonema cells the plasma membrane is labelled like expected with the FM4-64 (indicated by arrows in fig. 70 A and B).

Fig. 70: *P. patens* Control cell line caulonema cells labelled with FM4-64, Maximum projection A) FM4-64 channel; arrow: plasma membrane B) overlay of FM4-64 and chloroplast channel; arrow: plasma membrane (scale bar 20 µm)

GFP-ER cell line

In the ER- GFP cell line, the dye FM4-64 showed the plasma membrane near the cell wall and some tiny and bigger vesicles in the chloronema cells. In blue the dye labelled the vesicles between the ER tubules and cisternae; even bigger vesicle can be depicted. Vesicles, the plasma membrane and sometimes the outer membrane of the nucleus were stained by the FM4-64 in the leave cells.

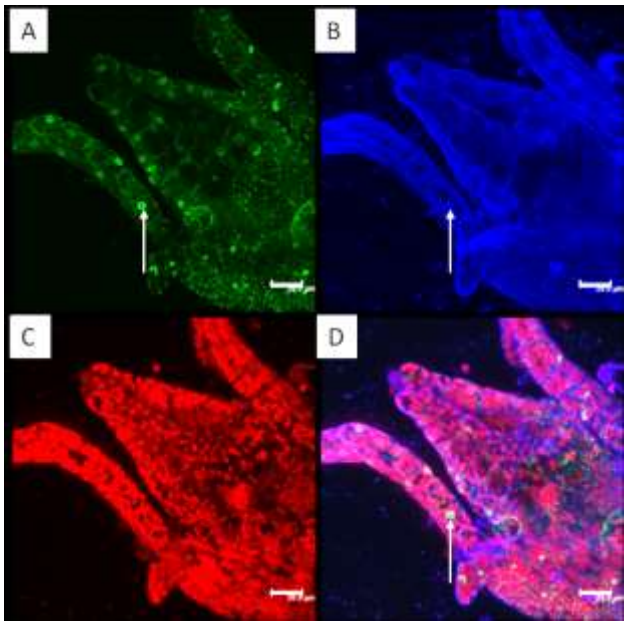

The GFP shows the same structures as the unstained GFP ER cells. The FM4-64 dye labelled the plasma membrane in all the cells also the stem cells (fig. 71). In at least one cell (indicated by arrows in figs. 71 A, B and D) the nucleus was labelled.

Fig. 71: *P. patens* ER cell line upper part of the stem labelled with FM4-64, Maximum projection A) GFP channel; arrow: nucleus B) FM4-64 channel; arrow: nucleus C) chloroplast channel D) overlay of GFP, FM4-64 and chloroplast channel; arrow: nucleus (scale bar 20 µm)

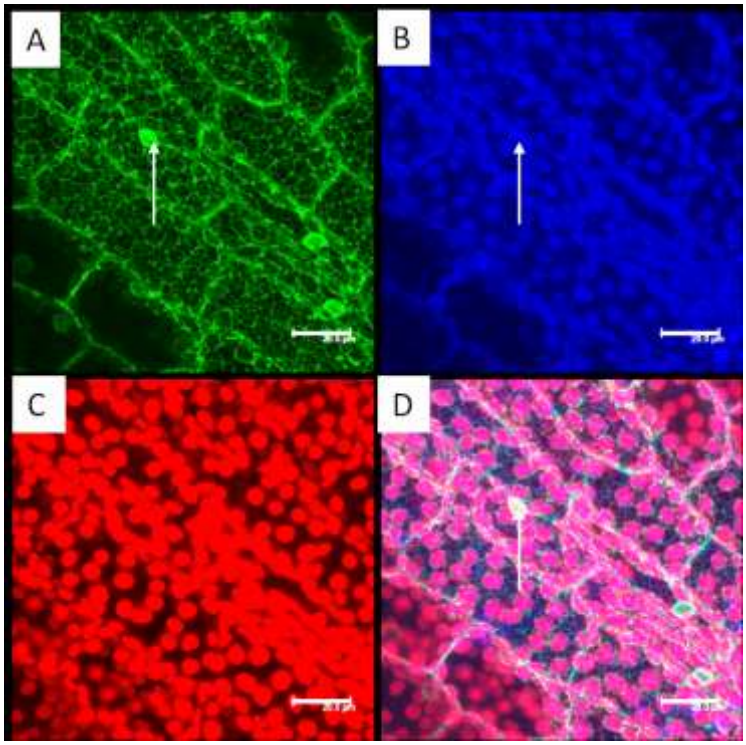

The leaflet cells showed fluorescence for the FM4-64 in the plasma membrane, the same fluorescence for the chloroplasts and sometimes the nucleus (indicated by arrows in fig. 72 A, B and D).

Fig. 72: *P. patens* ER cell line upper part of the stem labelled with FM4-64, Maximum projection A) GFP channel; arrow: nucleus B) FM4-64 channel; arrow: nucleus C) chloroplast channel D) overlay of GFP, FM4-64 and chloroplast channel; arrow: nucleus (scale bar 20 µm)

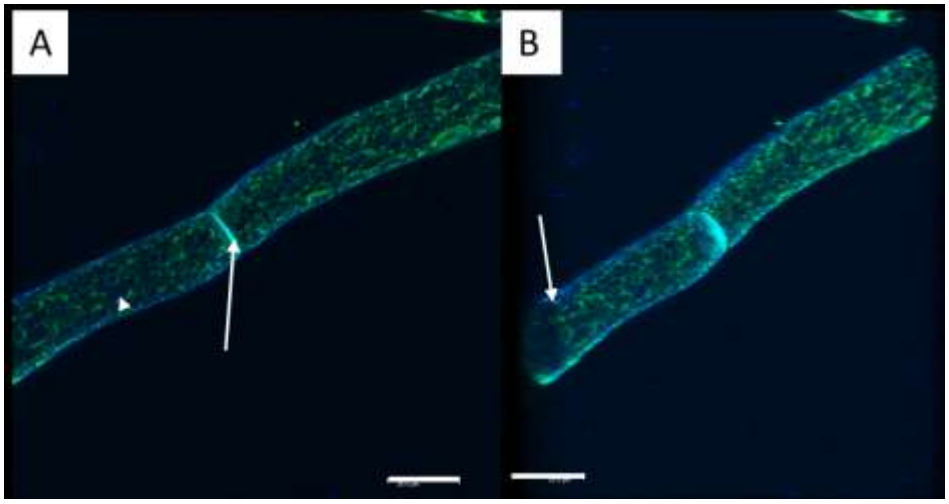

Fig. 73: *P. patens* ER cell line chloronema cell labelled with FM4-64, A) Maximum projection overlay of GFP and FM4-64 channel; arrow: plasma membrane; arrowhead: vesicle B) 3D reconstruction Maximum projection of overlay of GFP and FM4-64 channel; arrow: plasma membrane (scale bar 20 µm)

In the overlay of GFP and FM4-64 channels the plasma membrane between two neighbouring chloronema cells shows fluorescence for both labels (fig. 73 A indicated by an arrow). The GFP channel shows the structure of the ER with its tubules and cisternae and the FM4-64 channel shows the plasma membrane and the endo- exocytosis vesicles (tiny dots in blue within cell, indicated by arrowhead in fig. 73 A). In the 3D reconstruction of the same cell the FM4-64 is mostly seen in the plasma membrane around the whole cell, this is indicated by an arrow in fig. 73 B and shown in the movie 12.

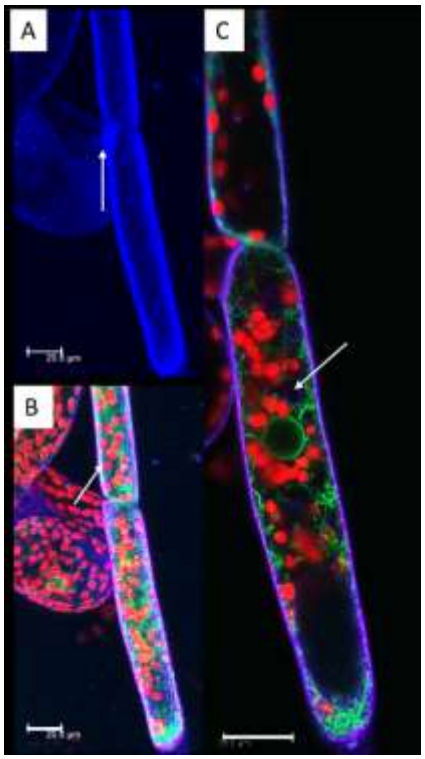

The overlay of the GFP, FM4-64 and chloroplast channels shows the overlap of the GFP and FM4-64 channels at the plasma membrane (fig. 74 B, indicated by arrow). In the 3D reconstruction (movie 13) of the FM4-64 channel of the same cell it is shown that the dye is in the plasma membrane (indicated by an arrow in fig. 74 A). Bigger vesicles stained with FM4-64 between the ER tubules marked with GFP are also detected (indicated by arrow in fig. 74 C).

Fig. 74: *P. patens* ER cell line chloronema cell labelled with FM4-64, A) 3D Reconstruction of Maximum projection of FM4-64 channel; arrow: plasma membrane B) 3D Reconstruction of Maximum projection of overlay of GFP, FM4-64 and chloroplast channel; arrow: plasma membrane C) overlay of GFP, FM4-64 and chloroplast channel; arrow: vesicle (scale bar 20 µm)

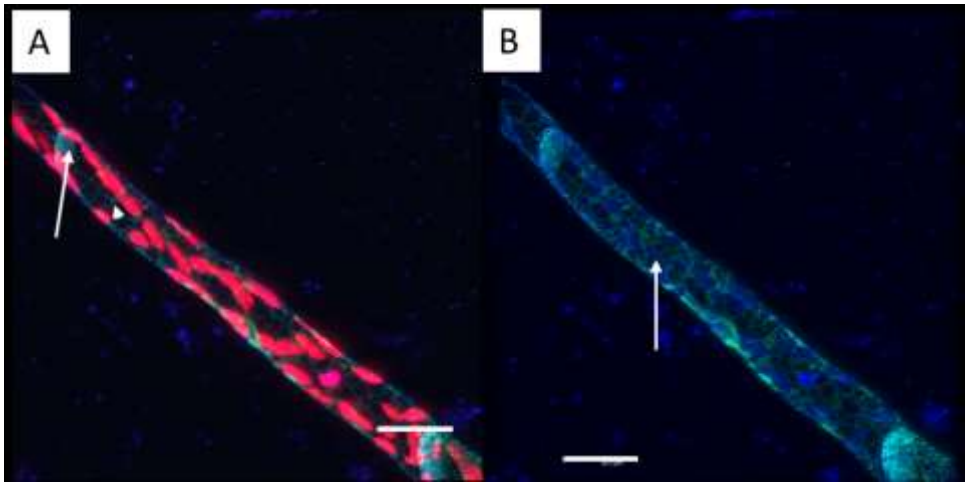

Fig. 75: *P. patens* ER cell line caulonema cell labelled with FM4-64, A) Maximum projection overlay of GFP, FM4-64 and chloroplast channel; arrow: plasma membrane; arrowhead: ER cisternae B) 3D Reconstruction Maximum projection of overlay of GFP and FM4-64 channel; arrow: plasma membrane (scale bar 20 µm)

In caulonema cells it is a similar picture like in the chloronema cells. Here also the plasma membrane between two neighbouring cells with its diagonally cell wall is showing fluorescence for the GFP and FM4-64 channel (indicated by the upper arrow in fig. 75 A). The GFP displays additionally the tubules and cisternae (indicated by the lower arrow in fig. 75 A). In the 3D Reconstruction of the same cell it is revealed that the FM4-64 is at the outer parts (plasma membrane) of the cell, but it seems the cell is not fully covered yet (indicated by an arrow in fig. 75 B).

M. elongata

In the caulonema of *M. elongata* the dye did not only show the plasma membrane, but also some tiny vesicles within the cell. In one fig. some vesicles were shown, but the dye was not washed out so carefully, so this picture is not so reliable. In the leaflet cells mostly, the plasma membrane was stained, but also sometimes the chloroplasts showed the same fluorescence. Only in the caulonema cell, some tubulary structures can be seen, maybe these were fusing vesicles. In the chloronema cells it seemed like the vacuole is dyed, but this are many tiny vesicles. In the tip of a chloronema cell there can be spotted an accumulation of the dye, so it seemed to be an accumulation of exo- and endocytosis vesicles, the exo- and endocytosis was there the highest.

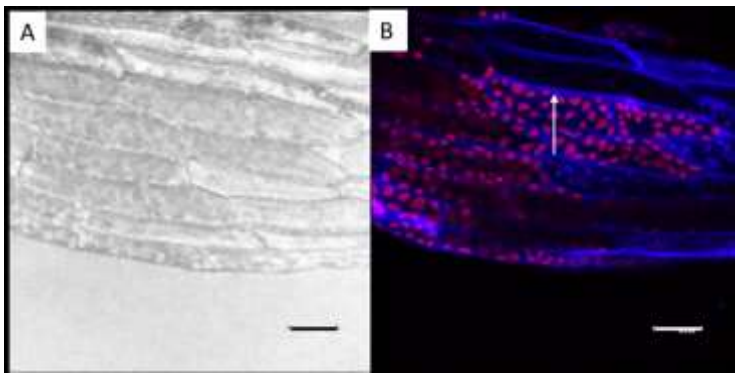

In the leaflets of *M. elongata* the plasma membrane was labelled efficiently, this is also indicated by an arrow in fig. 76 B.

Fig. 76*: M. elongata* cell line leaflet cells labelled with FM4-64, A) Maximum projection of Transmission channel B) FM4-64 and chloroplast channel; arrow: plasma membrane (scale bar 20 µm)

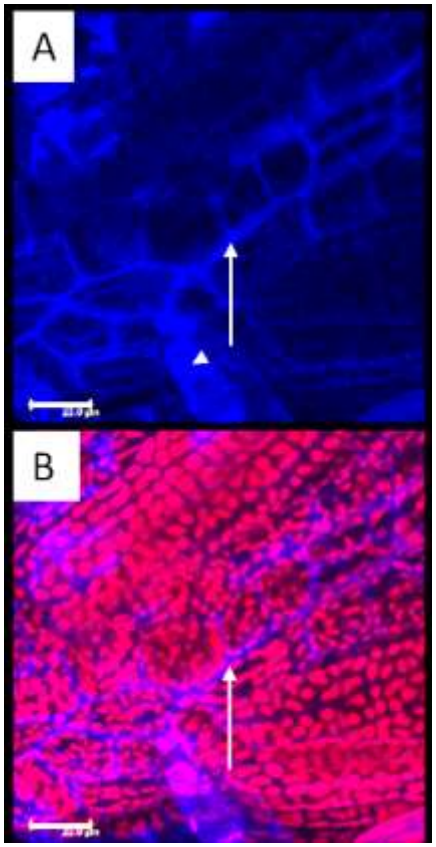

The FM4-64 labelled the plasma membrane in stem cells like in the leaflet cells (indicated by arrows in fig. 77). The chloroplast showed a similar fluorescence like the FM4-64. In dead cells, where the plasma was coagulated the FM4-64 also entered the cell and labelled the whole cell interior (indicated by an arrowhead in fig. 77 A).

Fig. 77*: M. elongata* cell line stem cells labelled with FM4-64, Maximum projection of A) FM4-64 channel; arrow: plasma membrane; arrowhead: stained coagulated plasma B) FM4-64 and chloroplast channel; arrow: plasma membrane (scale bar 20 µm)

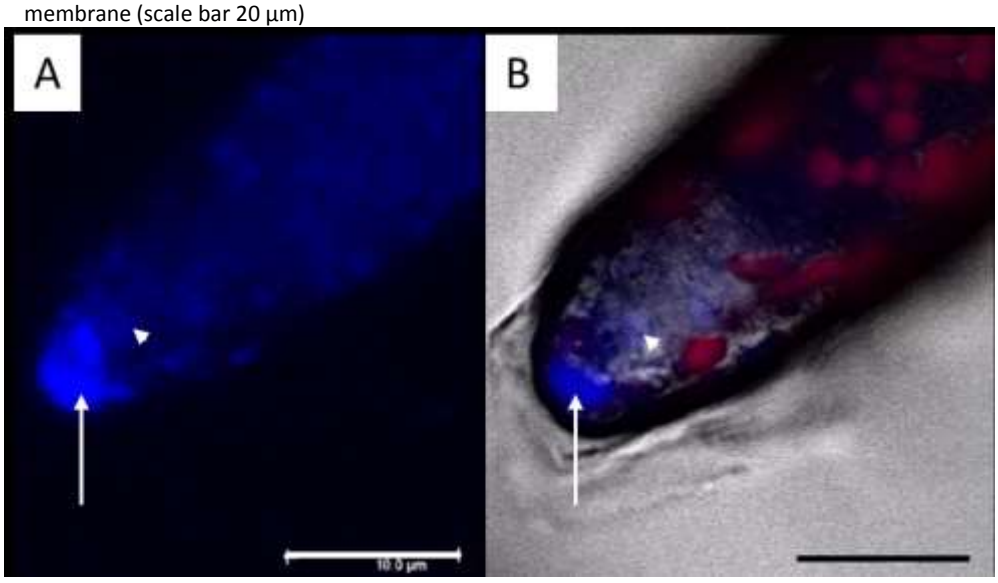

Fig. 78*: M. elongata* cell line chloronema tip cell labelled with FM4-64, Maximum projection of A) FM4-64 channel; arrow: accumulation of FM4-64; arrowhead: vesicle B) FM4-64, chloroplast and Transmission channel; arrow: accumulation of FM4-64; arrowhead: vesicle (scale bar 10 µm)

In fig. 78 the tip of a chloronema cell is shown, where at the tip an accumulation of FM4-64 is indicated by arrows. This accumulation is due to many endo- and exocytosis vesicles, the dye entered here the most and is accumulating through the vesicles there. Behind this accumulation many tiny vesicles are shown (indicated by an arrowhead in fig. 78 A)

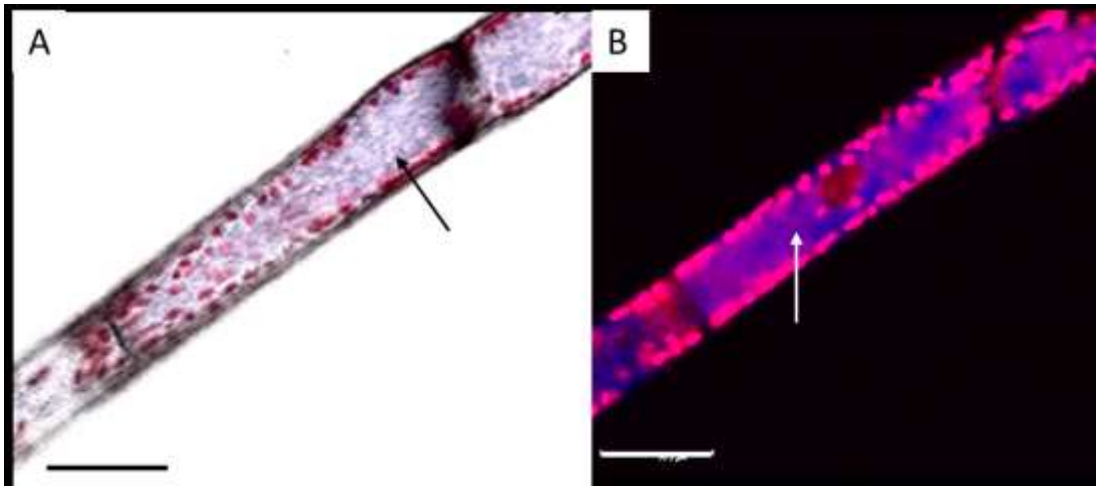

Fig. 79: *M. elongata* cell line chloronema cell labelled with FM4-64 A) overlay of FM4-64, chloroplast and Transmission channel; arrow: vesicles B) overlay of FM4-64 and chloroplast channel; arrow: FM4-64 in vacuole (scale bar 20 µm)

In fig. 779 B it looks like the whole vacuoles of the chloronema cells are labelled (indicated by arrow in fig. 79 B). But in the combination with the Transmission channel and at a different layer of the cell, it is shown that there are many tiny vesicles in the cell (indicated by arrow in fig. 79 A).

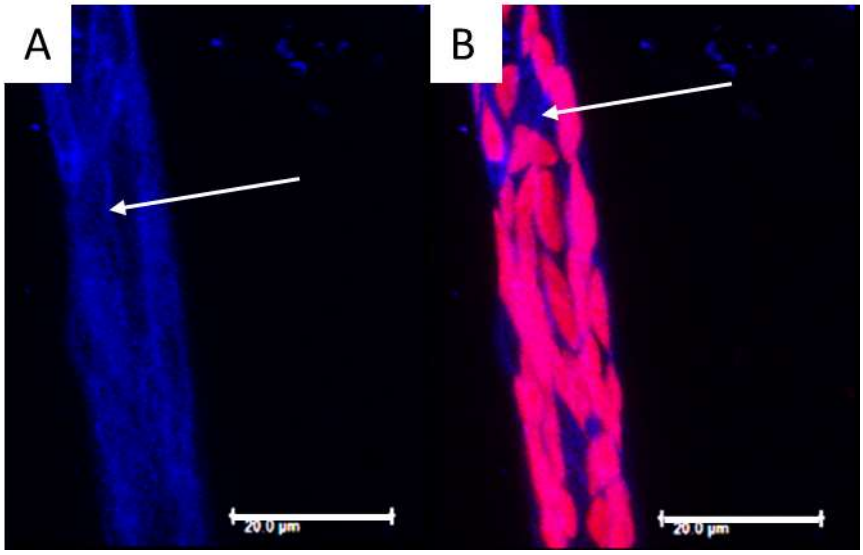

Fig. 80*: M. elongata* cell line caulonema cells labelled with FM4-64 Maximum projection A) FM4-64 channel; arrow: tubulary structures stained by FM4-64 B) overlay of FM4-64 and chloroplast channel; arrow: plasma membrane (scale

The caulonema cells of *M. elongata* showed some tubulary structures, but this are possibly fused vesicles, or the plasma membrane was not fully labelled and showed lines of the dye (indicated by arrow in fig. 80 A). It still labelled the plasma membrane (indicated by an arrow in fig. 80 B).

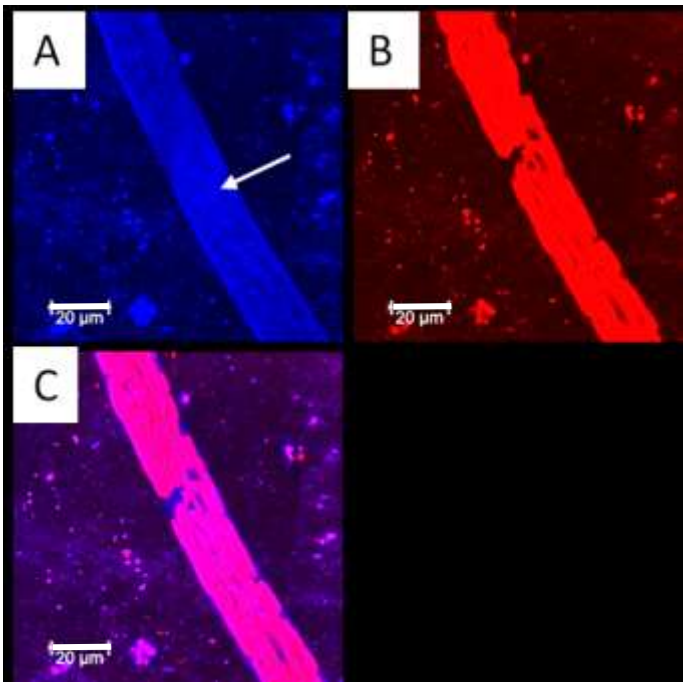

In another caulonema cell, many tiny vesicles can be recognized in the FM4-64 channel indicated by an arrow in fig. 81. In a 3D reconstruction of another caulonema cell (movie 14) also many vesicles can be seen.

Fig. 81*: M. elongata* cell line caulonema cells labelled with FM4-64 Maximum projection A) FM4-64 channel; arrow: vesicles B) chloroplast channel C) overlay of FM4-64 and chloroplast channel (scale bar 20 µm)

P. drummondii

In the leaflet of *P. drummondii* the plasma membrane was labelled like expected and some vesicles can be perceived. In the protonema cells the plasma membranes were stained and some vesicles between the sheets of the ER can be seen, but not like tubulary structures in the caulonema of *M. elongata.* There were also many tiny vesicles in the tip of the chloronema cell. It also seemed to dye the vacuole and accumulate there, but this was due to the maximum projection and was just showing the dye in the plasma membrane of the upper layer. In the tip cell of the chloronema there was an accumulation of the chloroplasts, but also many endo- and exocytosis vesicles can be seen. The caulonema stained with FM4-64 showed cell walls and some vesicles.

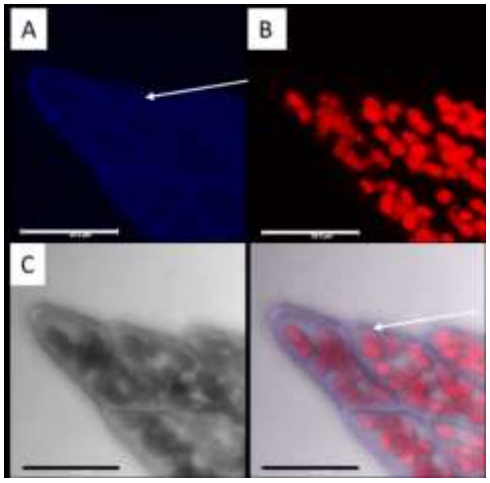

The FM4-64 stained the plasma membrane in the leaflet cells, this can be seen very good in the overlay of the FM4-64 channel with chloroplast and the Transmission channel (indicated by arrows in fig. 82 A and D). Because of the Maximum projection it seems like the whole vacuole is labelled, but in movie 15 of a 3D reconstruction it is revealed that the label is not in the whole cell.

Fig. 82*: P. drummondii* cell line leaflet cells labelled with FM4-64 Maximum projection A) FM4-64 channel; arrow: plasma membrane B) chloroplast channel C) Transmission channel D) overlay of FM4-64, chloroplast channel and Transmission channel; arrow: plasma membrane (scale bar 20 µm)

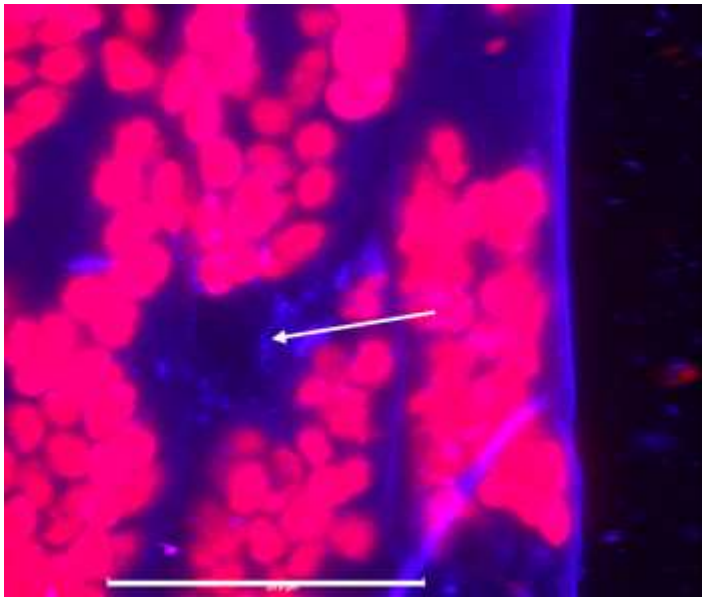

In the leaflet cells at a higher magnification not only the labelled plasma membrane is shown, furthermore some tiny vesicles are labelled (indicated by an arrow in fig. 83).

Fig. 83*: P. drummondii* cell line leaflet cells labelled with FM4-64 Maximum projection overlay of FM4-64 channel and chloroplast channel; arrow: vesicles (scale bar 20 µm)

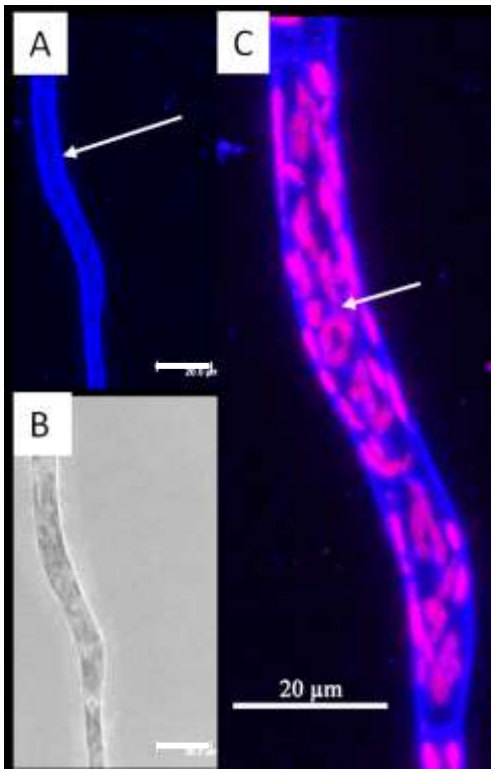

In the chloronema cells from *P. drummondii* the dye FM4-64 labelled the plasma membrane indicated by arrow in fig. 84 A. It also labelled many vesicles through exo- and endocytosis with different sizes (indicated by arrow in fig. 84 C).

Fig. 84*: P. drummondii* cell line chloronema cells labelled with FM4-64 Maximum projection A) FM4-64 channel; arrow: plasma membrane B) Transmission channel C) overlay of FM4-64 and chloroplast channel; arrow: vesicle (scale bar 20 µm)

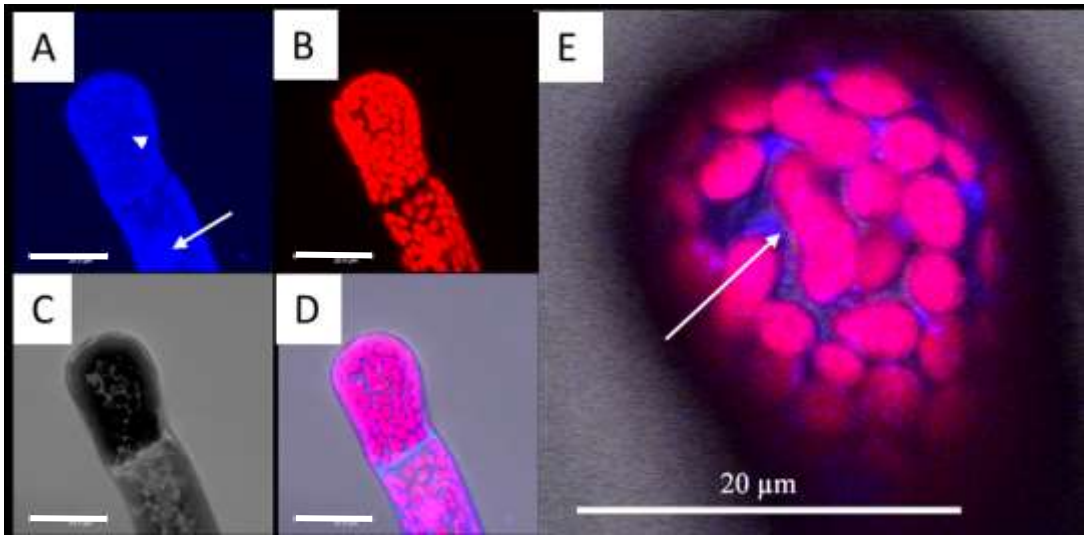

Fig. 85*: P. drummondii* cell line chloronema tip cell labelled with FM4-64 Maximum projection A) FM4-64 channel; arrow: accumulation of FM4-64 (nucleus); arrowhead: vesicle B) chloroplast channel C) Transmission channel D) overlay of FM4-64, chloroplast channel and Transmission channel E) Higher magnification of tip cell at one layer, overlay of FM4-64, chloroplast channel and Transmission channel; arrow: FM4-64 between chloroplasts (vesicles) (scale bar 20 µm)

In a chloronema tip cell not only the plasma membrane, but also many vesicles were labelled by the FM4-64 (indicated by an arrowhead in fig. 85 A). The mass of vesicles can be seen in the movie 15 in the 3D reconstruction of the cell. At a higher magnification and an overlay with the chloroplast channel, it was shown that the bigger vesicles are between the chloroplasts (indicated by an arrow in fig. 85 E). In the cell below, it seems like the nucleus is labelled (marked with an arrow in fig. 85 A), but a part of the fluorescence was also labelled in the chloroplast channel and in the transmission channel no structure like a nucleus is seen.

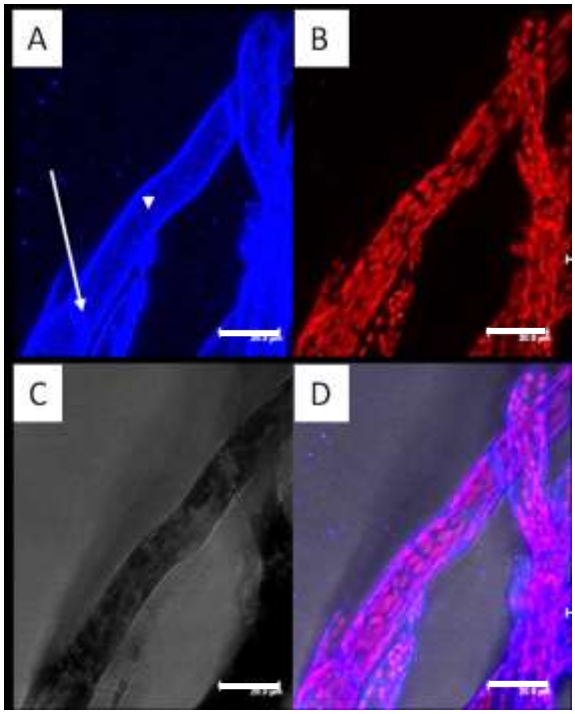

The caulonema cells (fig. 86) presented the same results as the chloronema cells. The plasma membrane was labelled (indicated by an arrow in fig. 86 A) and many vesicles within the cell (indicated by an arrowhead in fig. 86 A).

Fig. 86*: P. drummondii* cell line caulonema cells labelled with FM4-64 Maximum projection A) FM4-64 channel; arrow: plasma membrane; arrowhead: vesicle B) chloroplast channel C) Transmission channel D) overlay of FM4-64, chloroplast channel and Transmission channel (scale bar 20 µm)

FM1-43

The styryl dye FM 1-43 should stain the plasma membranes and is also used for describing vesicle trafficking (www.thermofisher.com). The dye labelled in all species and all the different cell types the plasma membrane like it was expected and most of the time labelled also the vesicles. Many tiny vesicles were stained in the cell of the chloronema in the ER-GFP cell line and in all the protonema cells of *M. elongata*. In the leaflets of the control, the plasma membrane was labelled. In *M. elongata* the FM1-43 stained some netlike structures in the leaflets, this were many vesicles near each other. In the chloronema of *M. elongata* also some tubulary structures can be seen, this looked like some strands of the dye. In *P. drummondii* even a cell wall connection of the caulonema cell was recognizably labelled by the dye, there some open parts can be seen, which are maybe some pores of the cell wall or it just shows vesicles near the cell wall.

Control cell line

In the control of *P. patens* the FM1-43 showed in protonema and in the leaflets the plasma membrane, but no vesicles are present, because they were already recycled, the pictures were taken after an hour of incubation in the dye.

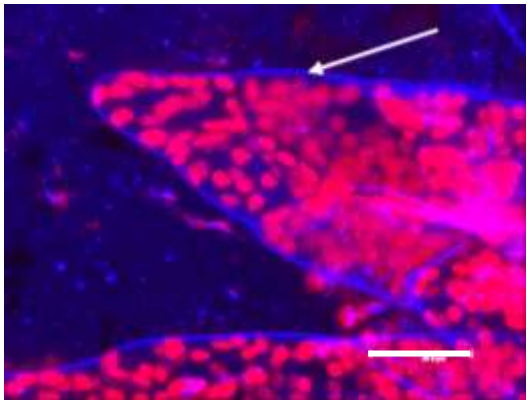

In the leaflet cell of the control cell line only the plasma membrane is labelled by FM1-43 (indicated by an arrow in fig. 87), the other structures are caused by the background. This can be also seen in movie 17.

Fig. 87: *P. patens* Control cell line leaflet cells labelled with FM1-43, Maximum projection of FM1-43 channel and chloroplast channel; arrow: plasma membrane (scale bar 20 µm)

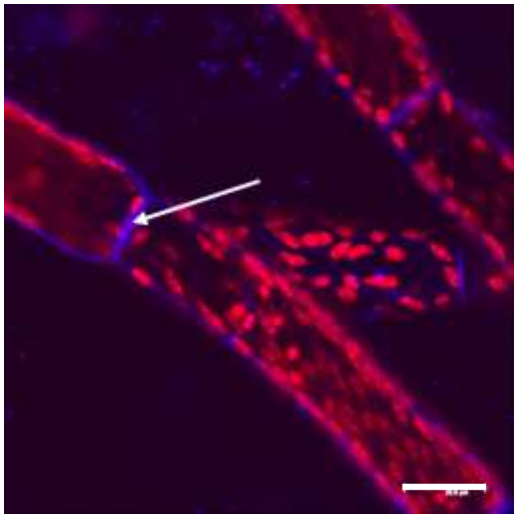

The chloronema and caulonema cells of the control cell line show like the leaflet cells only fluorescence of FM1-43 in the plasma membrane, this is indicated by an arrow for the chloronema cells in fig. 88.

Fig. 88: *P. patens* Control cell line chloronema cells labelled with FM1-43, Maximum projection of FM1-43 channel and chloroplast channel; arrow: plasma membrane (scale bar 20 µm)

GFP-ER cell line

In the ER-GFP cell line the FM1-43 showed the plasma membrane and many tiny vesicles in the cell of the chloronema, most of the vesicles were around the nucleus with some connections to it. The double staining with FM1-43 and GFP proved that the ER is in close vicinity to the plasma membrane and not in the cell wall. In the caulonema the vesicles got less, but the plasma membrane was also stained. In the leaflet only, the plasma membrane showed a clear fluorescence of the dye, other structures were not identified.

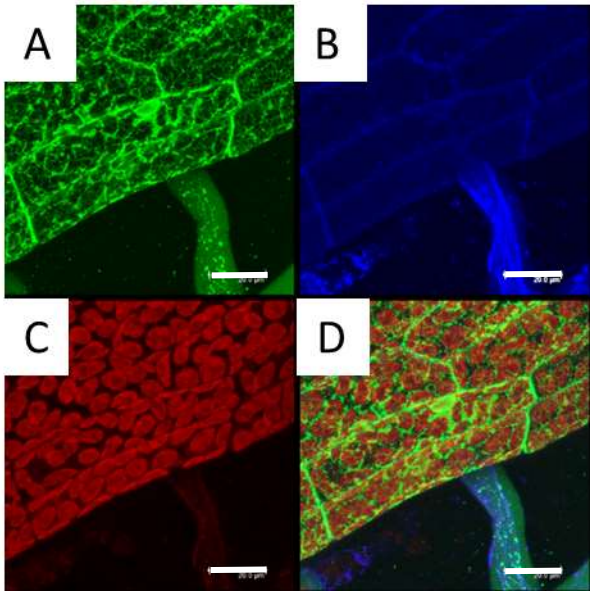

The FM1-43 dye was able to stain the plasma membrane in the leaflet cells of the GFP-ER cell line, this is marked with an arrow in fig. 89. The dye shows the labelling within the cell and in the vicinity of the nucleus, but not so significantly as the plasma membrane.

Fig. 89: *P. patens* ER cell line leaflet cells labelled with FM1-43, Maximum projection of A) GFP channel B) FM1-43 channel; arrow: plasma membrane C) chloroplast channel D) overlay of GFP, FM1-43 and chloroplast channel (scale bar 20 µm)

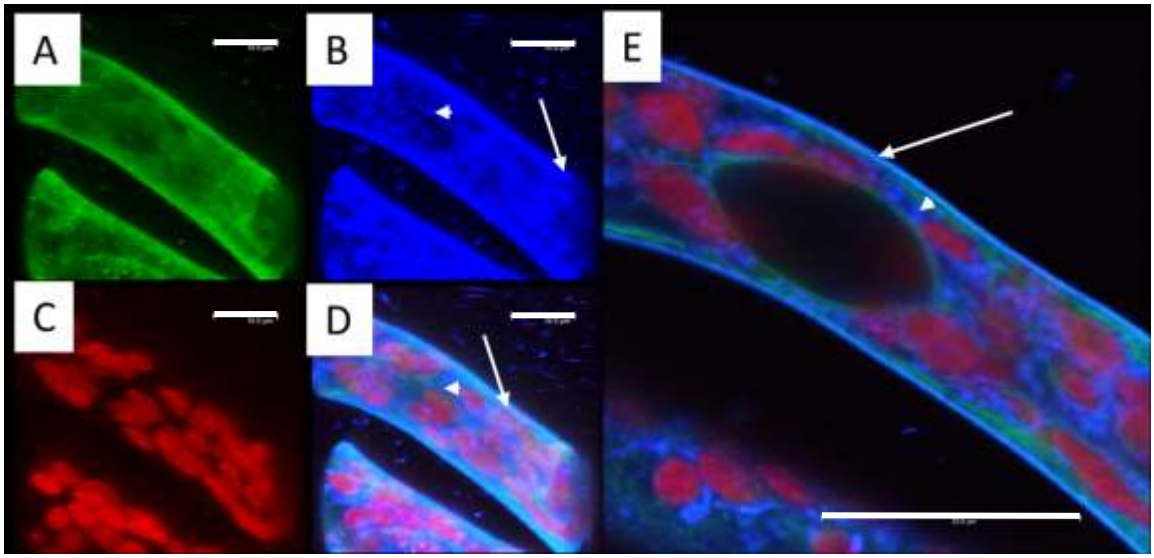

Fig. 90: *P. patens* ER cell line leaflet cells labelled with FM1-43, 3D Reconstruction of Maximum projection (A – D) of A) GFP channel B) FM1-43 channel; arrow: plasma membrane, arrowhead: vesicle C) chloroplast channel D) overlay of GFP, FM1-43 and chloroplast channel; arrow: plasma membrane, arrowhead: vesicle (scale bar 10 µm) E) Maximum projection of overlay of GFP, FM1-43 and chloroplast channel; arrow: plasma membrane; arrowhead: vesicle (scale bar 20 µm)

In a 3D reconstruction of a chloronema cell it is demonstrated that the dye is mostly accumulating in the plasma membrane (indicated by an arrow in fig. 90 B and D). In the interior of the cell the FM1-43 is only found in vesicles, this is marked with arrowheads in fig. 90 B and D. In fig. 90 E the mass of vesicles within the cell can be seen. Some vesicles seem to be near the nucleus and may have a connection to the ER around the nucleus (indicated with an arrowhead). The plasma membrane has in the overlay of the FM1-43 and GFP channel a turquoise colour, this can be used to be a prove that the ER is in the plasma membrane and not the cell wall (indicated by an arrow in fig. 90 D and E and in fig. 91).

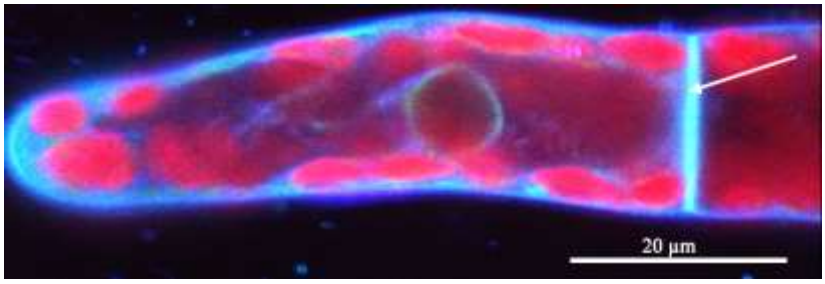

Fig. 91: *P. patens* ER cell line chloronema cell labelled with FM1-43 Maximum projection of overlay of GFP, FM1-43 and chloroplast channel; arrow: plasma membrane (scale bar 20 µm)

The chloronema cell in fig. 91 shows the expected fluorescence of the plasma membrane, with a higher fluorescence between the connection of the cells (indicated by an arrow). Even some structures within the cell can be perceived, maybe moving vesicles in the interior of the cell.

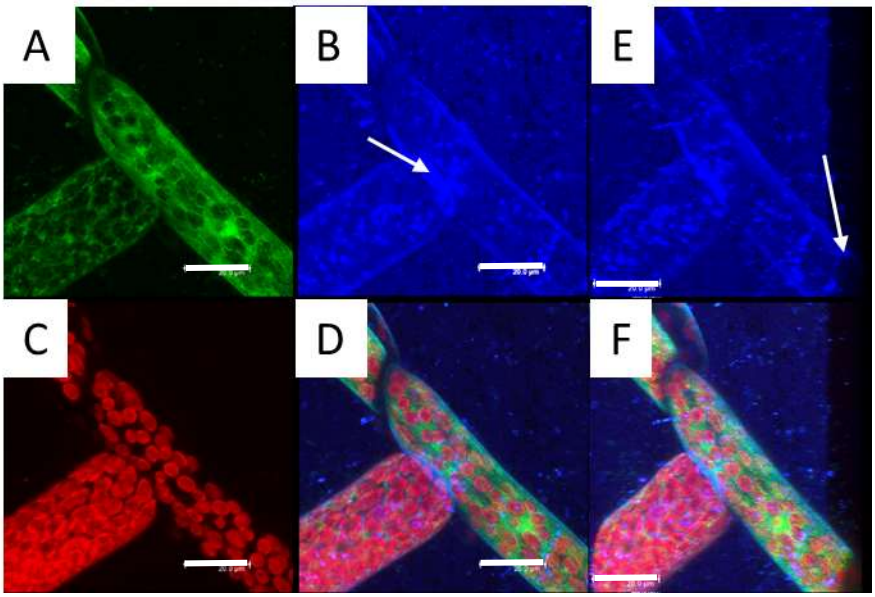

Fig. 92: *P. patens* ER cell line caulonema cell at a branching point labelled with FM1-43 Maximum projection of A) GFP channel B) FM1-43 channel; arrow: plasma membrane C) chloroplast channel D) overlay of GFP, FM1-43 and chloroplast channel E) 3D Reconstruction of Maximum projection of FM1-43 channel; arrow: plasma membrane F) 3D Reconstruction of Maximum projection of overlay of GFP, FM1-43 and chloroplast channel (scale bar 20 µm)

The caulonema cells revealed similar results like the chloronema cells, with less vesicles. In fig. 92 the fluorescence of the FM1-43 in the plasma membrane can be seen in the maximum projection (indicated by an arrow in fig. 92 B) and in the 3D reconstruction (indicated by an arrow in fig. 92 E). The points within the cell are probably no vesicles, because also in the outside of the cell these structures can be spotted and are an artefact of the not enough washed out dye.

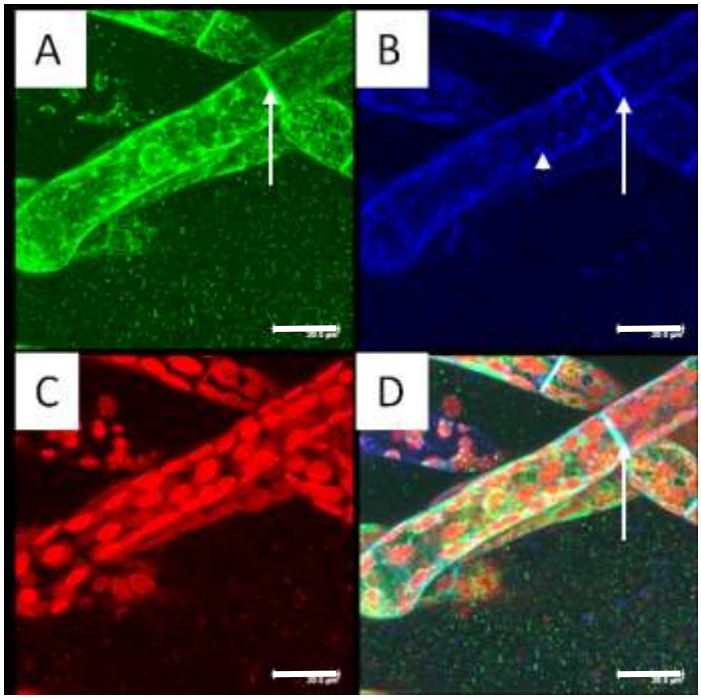

In this chloronema cell of fig. 93 the plasma membrane and vesicles are stained by the FM1-43, like in the cell shown before.

Fig. 93: *P. patens* ER cell line chloronema cells labelled with FM1-43, Maximum projection of A) GFP channel, arrow: plasma membrane B) FM1-43 channel; arrow: plasma membrane, arrowhead: vesicle C) chloroplast channel D) overlay of GFP, FM1-43 and chloroplast channel; arrow: plasma membrane (scale bar 20 µm)

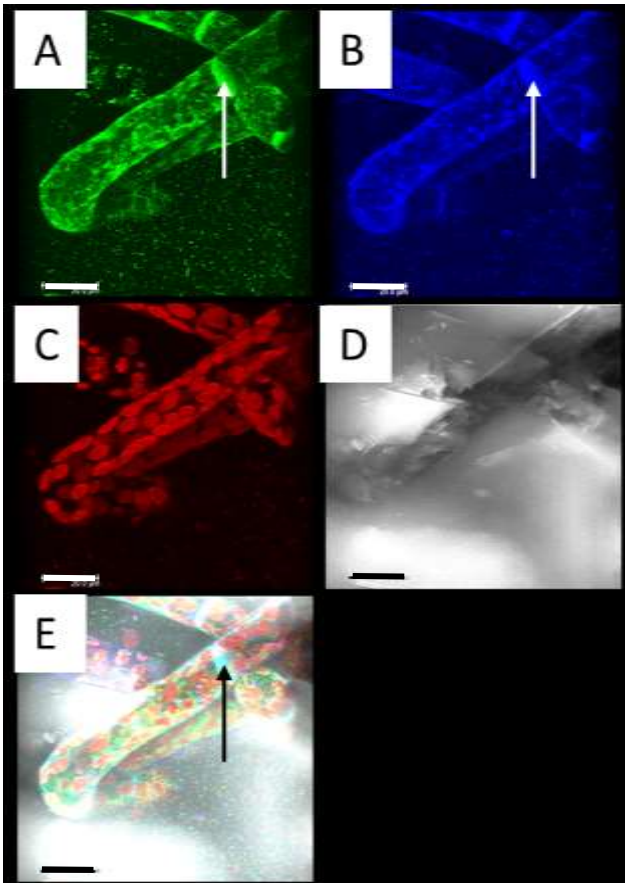

In the movie 18 of the 3D reconstruction of the maximum projection of fig. 93, the fluorescence of the dye in the plasma membrane around the whole cell and the vesicles within it can be depicted. In fig. 94 pictures out of the movie can be seen, here the plasma membrane is marked with an arrow.

Fig. 94: *P. patens* ER cell line chloronema cells labelled with FM1-43, 3D Reconstruction of Maximum projection of A) GFP channel; arrow: plasma membrane B) FM1-43 channel; arrow: plasma membrane C) chloroplast channel D) Transmission channel E) overlay of GFP, FM1-43, chloroplast channel and Transmission channel; arrow: plasma membrane (scale bar 20 µm)

M. elongata

In *M. elongata* the FM1-43 showed in all the different cell types the plasma membrane and some tiny vesicles in the leaflet. It also showed some netlike structures in the leaflet cells, which were maybe many vesicles connecting with each other. In the chloronema some tubulary structures can be seen. In comparison in the caulonema only the plasma membrane and some vesicles were showing the fluorescence of the FM1-43.

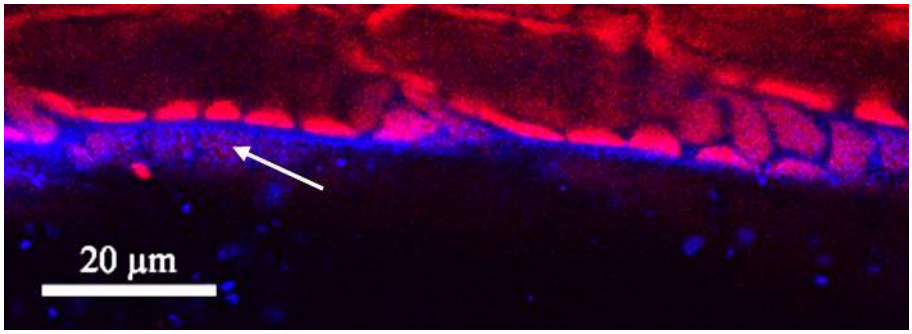

Fig. 95*: M. elongata* cell line leaflet cells labelled with FM1-43 Maximum projection of FM1-43 and chloroplast channel; arrow: vesicles (scale bar 20 µm)

The leaflet cell of *M. elongata* shows the fluorescence of the plasma membrane and in fig. 95 many tiny vesicles can be seen, they are forming a netlike structure through the cell.

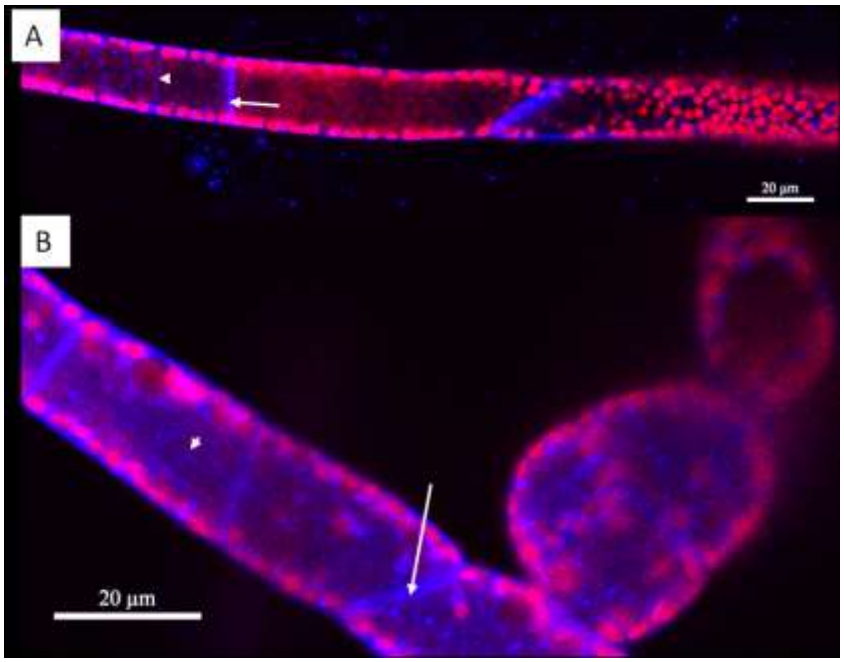

In fig. 96 it is shown that in the protonema cells the plasma membrane was labelled. Some fine strand like structure are stained too, they are in fig. 96 A vertical to the cell and in fig. 96 B horizontal, both marked with an arrowhead. Many vesicles are also present in the picture. Even the bulb formed cells revealed these structures.

Fig. 96*: M. elongata* cell line protonema cells labelled with FM1-43 Maximum projection of FM1-43 and chloroplast channel A) chloronema and caulonema cell after each other; arrow: plasma membrane; arrowhead: vesicles B) chloronema cell at a branching point with a roundish cell; arrow: plasma membrane; arrowhead: strand of FM1-43 (scale bar 20 µm)

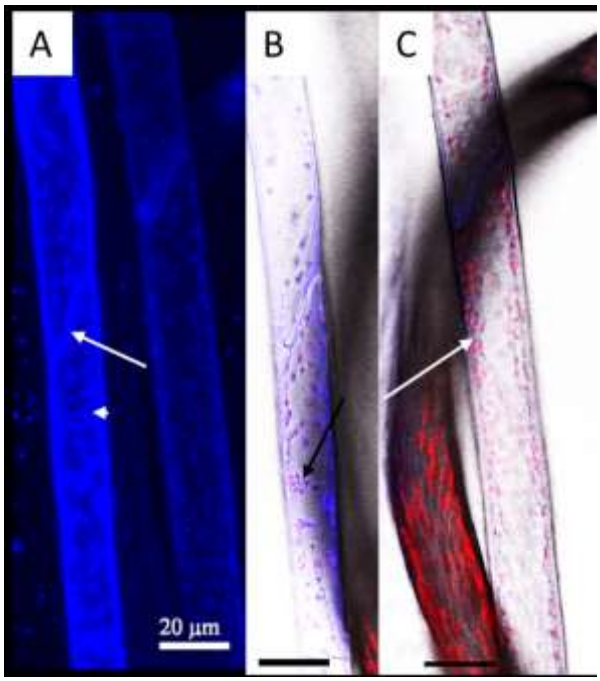

In fig. 97 caulonema cells of *M. elongata* showed like expected the FM1-43 in the plasma membrane and in vesicles (indicated by an arrowhead). The fluorescence in the plasma membrane between two connecting cells is higher than on the sides of the cell, because both cells contribute to it (marked with an arrow in fig. 97 A). In figs. 97 B and C the vesicles in the caulonema cells are marked with an arrow and the vesicles are around the chloroplasts.

Fig. 97*: M. elongata* cell line caulonema cell labelled with FM1-43 at different Z-positions A) FM1-43 channel; arrow plasma membrane; arrowhead: vesicle B) FM1-43, chloroplast and Transmission channel; arrow: vesicle C) FM1-43, chloroplast and Transmission channel; arrow: vesicles (scale bar 20 µm)

P. drummondii

In *P. drummondii* the FM1-43 dye stained in the leaflet, the plasma membrane and also the chloroplasts. In a caulonema cell the dye labelled the plasma membrane at a cell wall connection the plasmodesmata, where many vesicles were, and some open parts can be seen, but this were the openings of the plasmodesmata. In the chloronema of *P. drummondii,* a stained cell showed many vesicles and in the neighbouring caulonema cell the ER still showed some connections, but this cell has already plasmolysed.

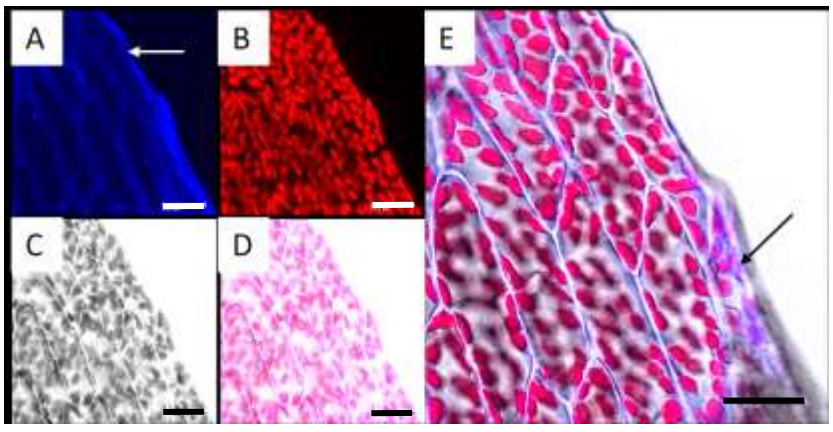

Fig. 98*: P. drummondii* cell line leaflet cells labelled with FM1-43 Maximum projection (A – D) A) FM1-43 channel; arrow: plasma membrane B) chloroplast channel C) Transmission channel D) overlay of FM1-43, chloroplast channel and Transmission channel E) overlay of FM1-43, chloroplast channel and Transmission channel; arrow: plasma membrane (scale bar 20 µm)

Fig. 98 shows a leaflet of *P. drummondii* stained with FM1-43 and showing the fluorescence of the dye in the plasma membrane (marked with an arrow in fig. 98 A and E). The chloroplasts also show a bit of a fluorescence, but vesicles are not stained.

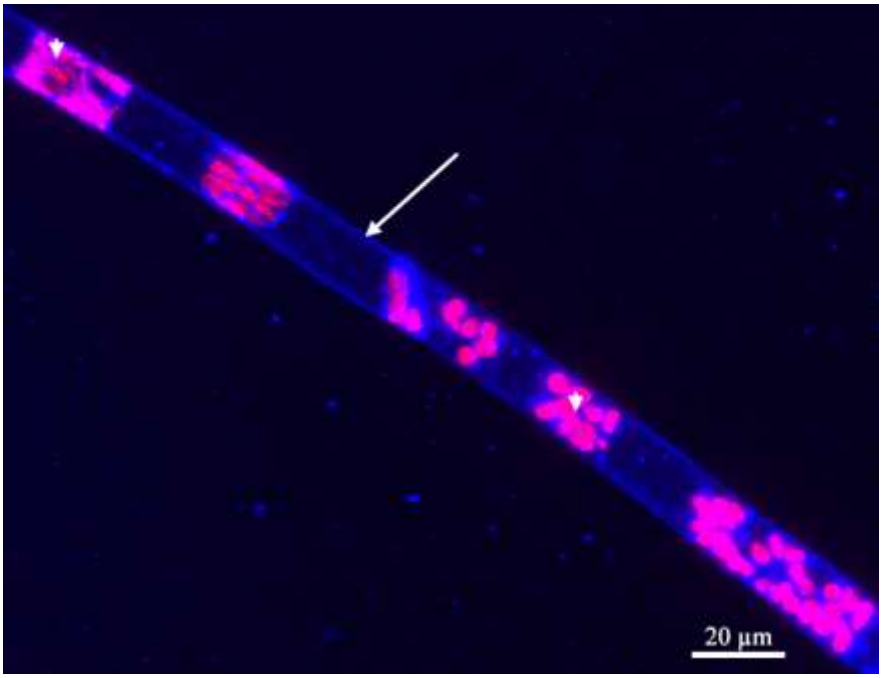

The protonema cell of *P. drummondii* in fig. 99 and movie 19 displays a fluorescenting plasma membrane (marked with an arrow) and vesicles (marked with an arrowhead) stained by FM1-43, the cell has plasmolysed and is not healthy anymore the dye also accumulated in the coagulated plasma.

Fig. 99*: P. drummondii* cell line protonema cells labelled with FM1-43 Maximum projection of overlay of FM1-43 and chloroplast channel; arrow: plasma membrane; arrowhead: vesicles (scale bar 20 µm)

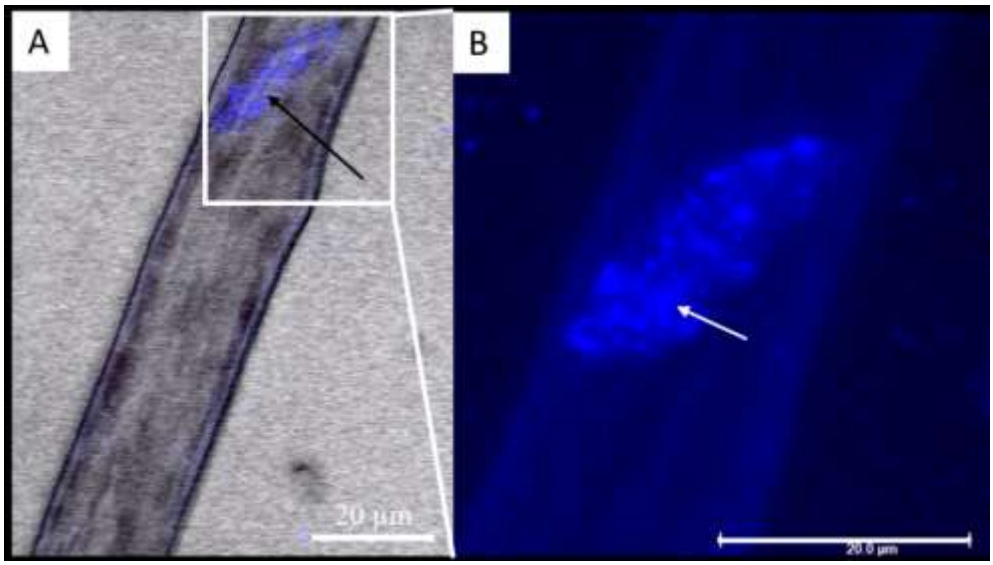

Fig. 100*: P. drummondii* cell line caulonema cell labelled with FM1-43 Maximum projection of A) FM1-43 channel and Transmission channel; arrow: plasma membrane between two cells B) Higher magnification of rectangle indicated part of A only FM1-43 channel; arrow: vesicles at plasmodesmata (scale bar 20 µm)

The caulonema cell displays a fluorescence of the plasma membrane on the outside of the cell, but also a high fluorescence in the plasma membrane between two cells (seen in movie 20). This may be a plasmodesmata with an accumulation of vesicles in the vicinity (marked with an arrow in fig. 100 B).

Rhodamine phalloidin

Cells of *P. patens* and *A. cepa* were used for labelling with Rhodamine phalloidin. To selectively stain the actin filaments with Rhodamine phalloidin (www.thermofisher.com) the plasma membrane has to be permeabilized with NP40 (www.sigmaaldrich.com), but this reagent also can destroy the cells. This was shown for the TRAAS buffer. So, the concentration should be low. To find the right combination of buffer and concentration of NP40 some experiments were made. The best result was received by using the PBS buffer and a concentration of NP40 of 0,001 %.

TRAAS buffer

At first the plant material was put in the buffer and then the cells were labelled with Rhodamine phalloidin. This application in the control cell line lead to dead cells with coagulated plasma, which showed a fluorescence of the cytoplasm. The GFP Life-act cell line did also not show the expected actin filaments, when the TRAAS buffer with NP40 (0,01 %) was applied before staining, because the cells likely died due to the high concentration of NP40. This means that the staining was not successful, we suspected the buffer was the main problem, therefore the staining without putting the plant material in the buffer first was tested and the TRAAS buffer alone was tested. When only the dye with the buffer was applied, the actin filaments of the GFP Life-act cell line could be recognized in the leaflet cells, but the dye did not show the structure and most of the protonema cells showed coagulated plasma. After applying the TRAAS buffer with a concentration of NP40 of 0,01 %, the cells of *P. patens* died even after an exposure time of only five minutes. Therefore, also other buffers were tested.

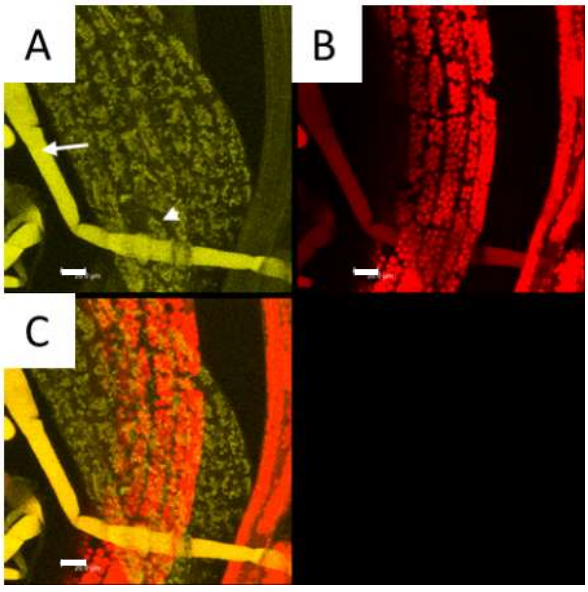

Before the application with Rhodamine phalloidin the cells were put in the TRAAS buffer and the dye was washed out with the buffer. After labelling the control cell line the leaflet cells plasmolysed (indicated by an arrowhead in fig. 101 B) and the protonema cells had a coagulated plasma (shown with an arrow in fig. 101 A) and no cell content was visible anymore.

Fig. 101: *P. patens* control cell line leaflet and protonema cells labelled with Rhodamine phalloidin in TRAAS buffer with NP40 before labelling; Maximum projection of A) Rhodamine phalloidin channel; arrow: coagulated plasma of chloronema cell; arrowhead: plasmolysed leaflet cell B) chloroplast channel C) overlay of Rhodamine phalloidin and chloroplast channel (scale bar 20 µm)

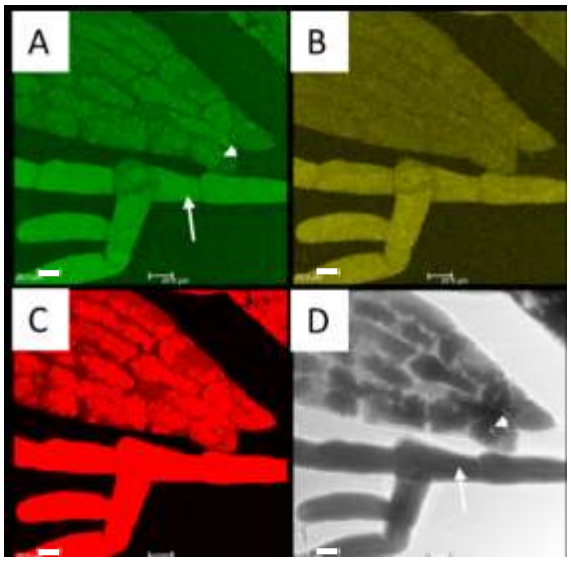

In the Life-act cell line similar results were shown like in the control cell line, the coagulated plasma of the protonema cells (indicated by an arrow in fig. 102 A and D) and the plasmolysed leaflet cells (marked with an arrowhead in fig. 102 A and D) are shown in fig. 102.

Fig. 102: *P. patens* Life-act cell line leaflet and protonema cells labelled with Rhodamine phalloidin in TRAAS buffer with NP40 before labelling Maximum projection of A) GFP channel; arrow: coagulated plasma of chloronema cell; arrowhead: plasmolysed leaflet cell B) Rhodamine phalloidin channel C) chloroplast channel D) Transmission channel; arrow: coagulated plasma of chloronema cell; arrowhead: plasmolysed leaflet cell (scale bar 20 µm)

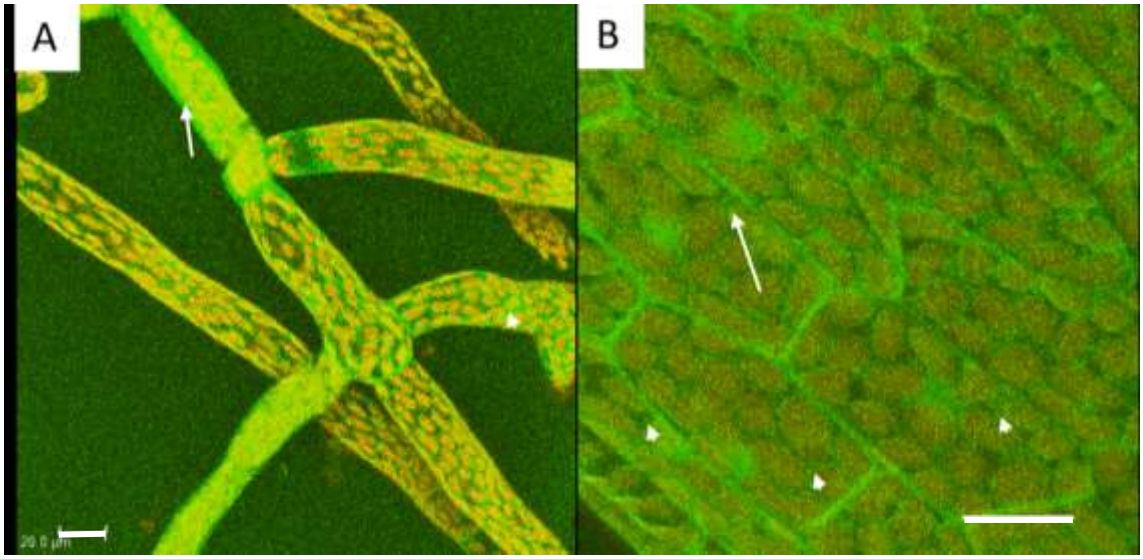

Fig. 103: *P. patens* Life-act cell line leaflet and protonema cells labelled with Rhodamine phalloidin Maximum projection of A) Protonema cells in overlay of GFP, Rhodamine phalloidin and chloroplast channel; arrow: coagulated plasma of chloronema cell; arrowhead: actin filaments only shown in green of GFP channel B) Leaflet cells in overlay of GFP, Rhodamine phalloidin and chloroplast channel; arrow: actin filaments only in green of GFP channel; arrowhead: G-Actin alone not bound in filament (scale bar 20 µm)

The dye was also applied without putting the cells first in the TRAAS buffer. This can be seen in fig. 103, the actin filaments of the GFP Life-act cell line could be recognized in the leaflet cells and partly in chloronema cells, but the dye did not show the structure of the actin filaments. A great part of the protonema cells shows coagulated plasma (marked with an arrow in fig. 103 A) and in the leaflet cells not bound G-actin is seen (indicated by arrowheads in fig. 103 B).

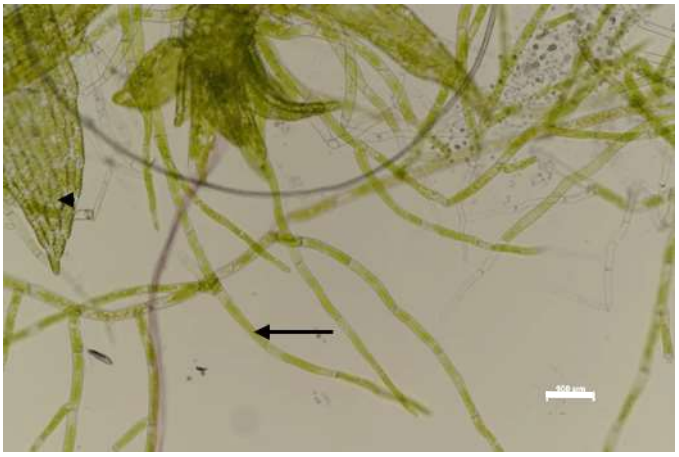

After five minutes of the application with the TRAAS buffer the leaflet cells plasmolysed (marked with an arrowhead in fig. 104) and the protonema cells show coagulated plasma and destroyed chloroplasts (marked with an arrow in fig. 104). This shows that the TRAAS buffer with NP40 was too strong permeabilizing the plasma membrane and through that destroying the cells.

Fig. 104: Bright field image of *P. patens* control cell line leaflet and protonema cells in TRAAS buffer with NP40; arrow: coagulated plasma of chloronema cell; arrowhead: plasmolysed leaflet cell (scale bar 100 µm)

PBS buffer

The PBS buffer alone did not affect the cells of *P. patens*, but when the buffer was applied with a concentration of NP40 of 0,01 %, the protonema cells died and the leaflet cells stayed unaffected. In comparison, the cells of *A. cepa* still lived, because they showed organelle movement, after such an application, even after an hour. When the concentration of NP40 was only 0,001 %, all of the cells still lived, because of that this concentration of NP40 was used for the staining with Rhodamine Phalloidin. The Rhodamine Phalloidin was unfortunately not able to penetrate the cell wall and stained actin filaments, but there was an accumulation at the cell wall. When applying the same combination on *A. cepa*, mostly vesicles in the plasma strings could be detected, in a time lapse even the movement of the vesicles, which contained the Rhodamine Phalloidin can be seen. This means the dye was not able to bind to the actin either due to unspecific labelling of G-actin or the dye did not work properly anymore.

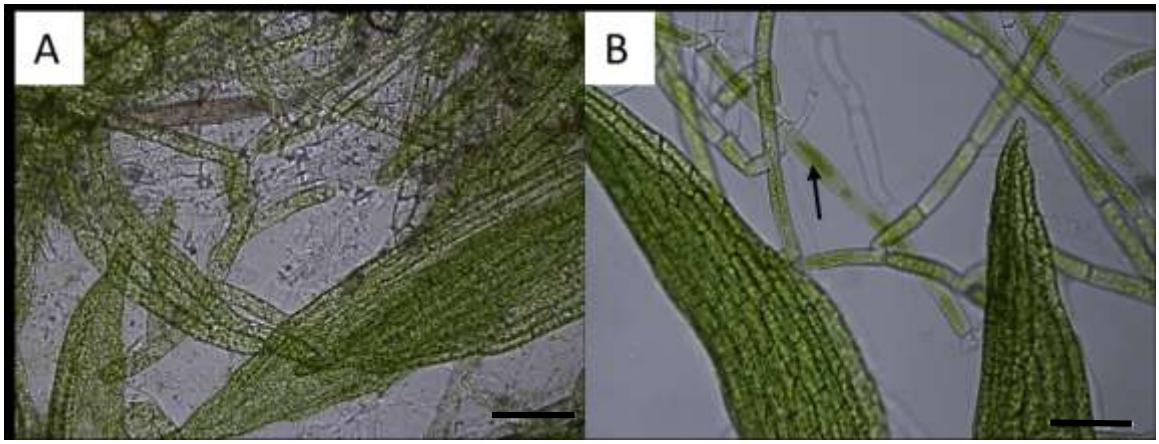

Fig. 105: Bright field image of *P. patens* control cell line leaflet and protonema cells in A) PBS buffer after 30 minutes of the application B) PBS buffer with NP40 (0,01 %); arrow: coagulated plasma of chloronema cell (scale bar 100 µm)

Just the PBS buffer alone had no effect on the cells (fig. 105 A), but with NP40 in the concentration of 0,01 % the chloronema cells showed coagulated plasma with degenerated chloroplasts (marked with an arrow in fig. 105 B).

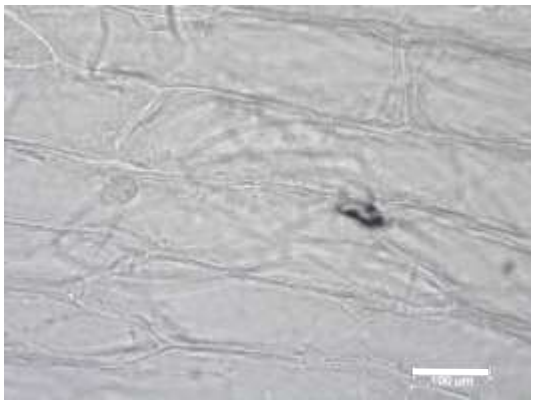

The same concentration of NP40 (0,01 %) with PBS buffer showed no effect on the cells of *A. cepa* (fig. 106), this means that the cells of *P. patens* are more sensitive to the permeabilization.

Fig. 106: Bright field image of *A. cepa* inner epidermis cells in PBS buffer with NP40 (0,01 %) (scale bar 100 µm)

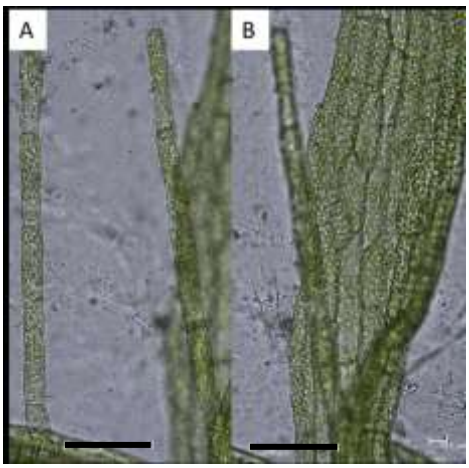

A lower concentration of NP40 did not affect the cells of *P. patens* anymore, the cells look like unpermeabilized cells (fig. 107).

Fig. 107: Bright field image of *P. patens* control cell line leaflet and protonema cells in PBS buffer with NP40 (0,001 %) A) chloronema cells B) leaflet cells (scale bar 100 µm)

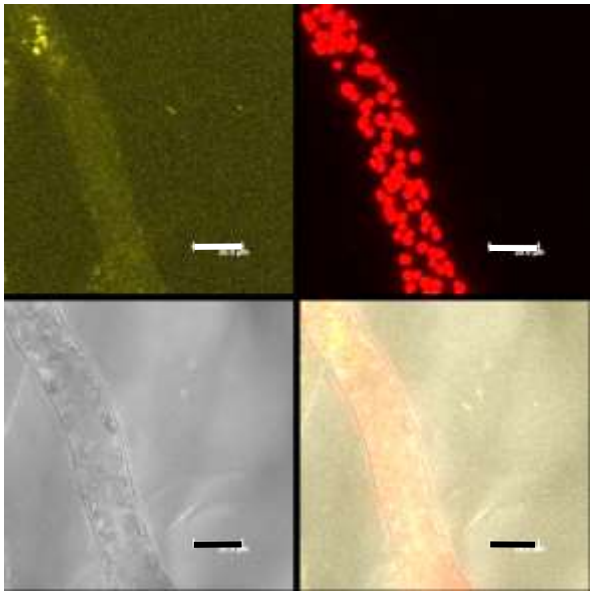

Therefore, this buffer with the Rhodamine phalloidin was used on the *P. patens* control cell line. Unfortunately, the dye did not show the actin filaments, it did not enter the cells and was just at the outer cell wall (fig. 108).

Fig. 108: *P. patens* control cell line protonema cell labelled with Rhodamine phalloidin in PBS buffer Maximum projection of A) Rhodamine phalloidin channel B) chloroplast channel C) Transmission channel D) overlay of Rhodamine phalloidin, chloroplast and Transmission channel (scale bar 20 µm)

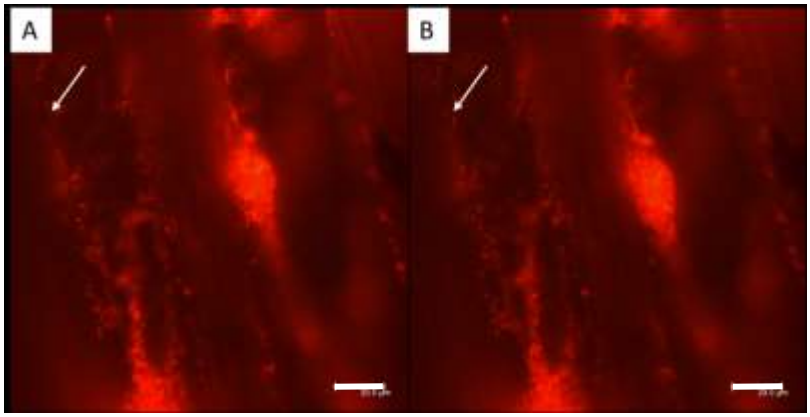

In *A. cepa* the dye could enter the cells but showed unspecific labelling due to G-actin, because it did not bind to the actin filaments. It was shown in the vesicles and around the nucleus, the cell did enclose the dye in the vesicles, through endocytosis.

Fig. 109: Fluorescence image of *A. cepa* inner epidermis cells labelled with Rhodamine phalloidin in PBS buffer with NP40 (0,001 %) A) start B) after 14 seconds; arrow: vesicle movement (scale bar 20 µm)

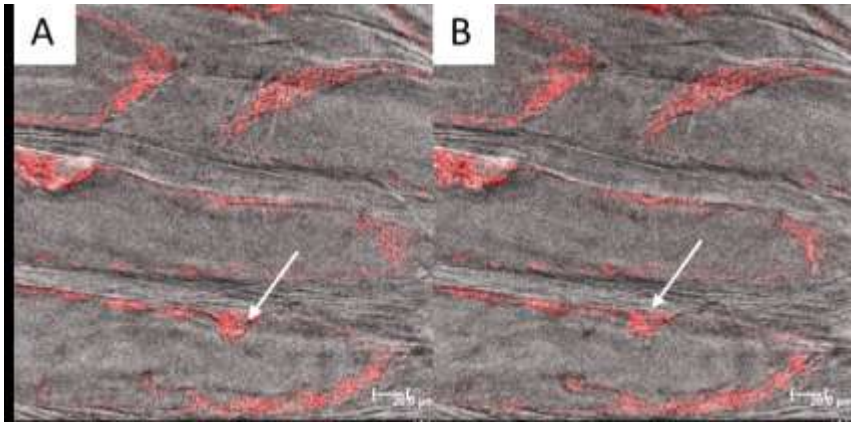

The movement of the vesicles containing the Rhodamine phalloidin can be seen in movies 21 and 22, in the fluorescence fig. 109 and in the confocal maximum projection image in fig. 110 indicated by arrows.

Fig. 110: *A. cepa* inner epidermis cells labelled with Rhodamine phalloidin in PBS buffer with NP40 (0,001%) Maximum projection overlay of Rhodamine phalloidin channel and Transmission channel A) start B) after 1 minute and 33 seconds; arrow: vesicle movement (scale bar 20 µm)

PM5E buffer

The cells of *P. patens* had no problem with the PM5E buffer alone, but with an application of the buffer with a concentration of NP40 of 0,01 %, it was lethal for the protonema cells and the leaflet cells plasmolysed. With a concentration of 0,001% of NP40 the cells still lived, and this combination was used for the labelling of Rhodamine Phalloidin. The Rhodamine phalloidin was not able to penetrate the cell wall and stain selectively the F-actin. The same combination was used in *A. cepa*, there the cell wall and some vesicles in the plasma strings showed fluorescence, here the dye accumulated.

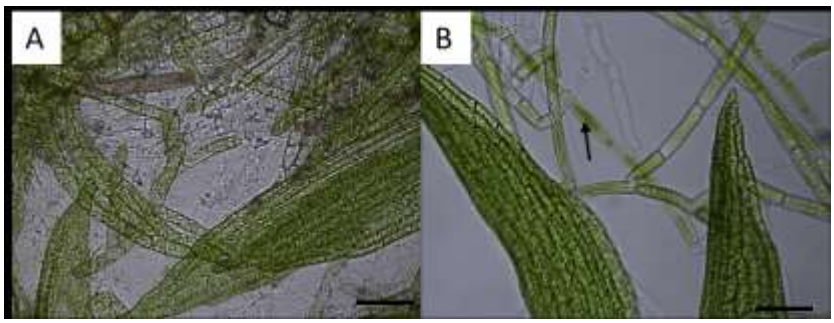

In fig. 111 the cells showed no effect due to the PM5E buffer, the chloroplasts and plasma are intact, and the cells did not plasmolyse.

Fig. 111: Bright field image of *P. patens* control cell line PM5E buffer after 30 minutes of the application A) leaflet cells B) chloronema cells (scale bar 100 µm)

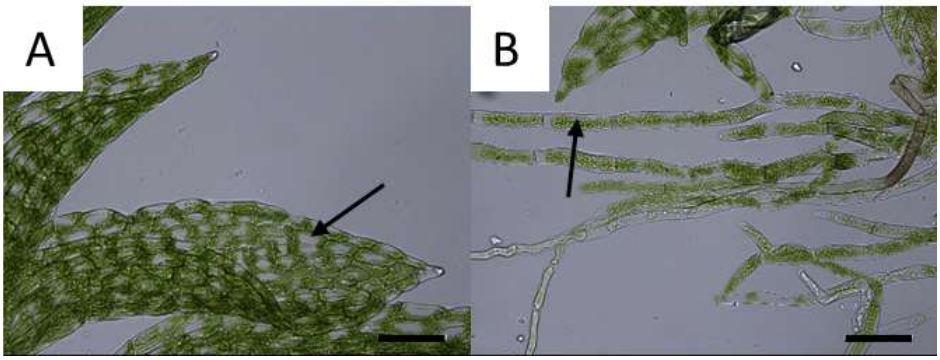

Fig. 112: Bright field image of *P. patens* control cell line PM5E buffer with NP40 (0,01 %) after 30 minutes of the application A) leaflet cells; arrow: plasmolysed cell B) chloronema cells; arrow: plasmolsed cell (scale bar 100 µm)

When the buffer contained the NP40 in a concentration of 0,01 %, the cells reacted to it and plasmolysed (indicated by arrows in fig. 112 A and B). The chloronema cells sometimes had a coagulated plasma. This meant that the concentration was too high for moss cells. With a lower concentration of NP40 (0,001 %) the cells did not show this effect and stayed healthy (fig. 113).

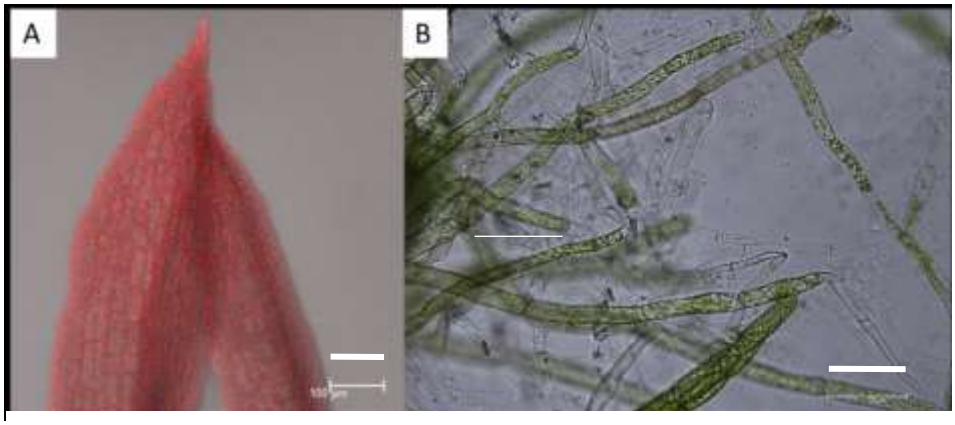

Fig. 113: *P. patens* control cell line PM5E buffer with NP40 (0,001 %) after 30 minutes of the application A) Maximum projection of chloroplast and Transmission channel of leaflet cells B) Bright field image of protonema cells (scale bar 100 µm)

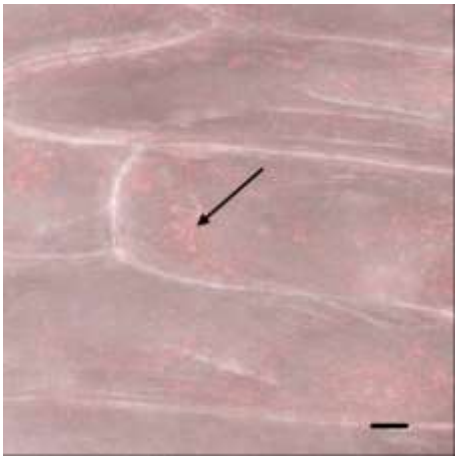

The *A. cepa* cells stained with Rhodamine phalloidin in the PM5E buffer with the NP40 (0,001 %) (fig. 114) showed the same results as the stained *A. cepa* cells with the PBS buffer and NP40 (0,001 %). Here the vesicles contained the dye too (indicated by an arrow in fig. 114), but no other structures were labelled.

Fig. 114: *A. cepa* inner epidermis cells labelled with Rhodamine phalloidin in PM5E buffer with NP40 (0,001 %) Maximum projection overlay of Rhodamine phalloidin channel and Transmission channel; arrow: vesicle (scale bar 20 µm)

3. 6 Plasmolysis

Plasmolysis was used to get an impression how the subcellular structures react to stress. In a solution of 0,4 M Mannitol the moss *P. patens* sometimes showed plasmolysis and other times not, this could be, because this concentration is on the edge of the osmotic value of *P. patens*. It also depended on the different cell types, even between chloronema and caulonema were differences. In the highest concentration the moss always showed plasmolysis right after applying the solution, the chloronema and caulonema almost immediately reacted to the 0,8 M Mannitol, but the leaves needed a few minutes to show the same reaction. In the lowest concentration sometimes only the leaflets showed plasmolysis. Cells which were already stressed, like being connected to a neighbouring dead cell, showed more likely plasmolysis. It also seemed to be important to first put the moss in distilled water, before applying the plasmolyticum. In the leaflet mostly concave plasmolysis was shown, the protonema cells showed concave plasmolysis and also sub-protoplast formation.

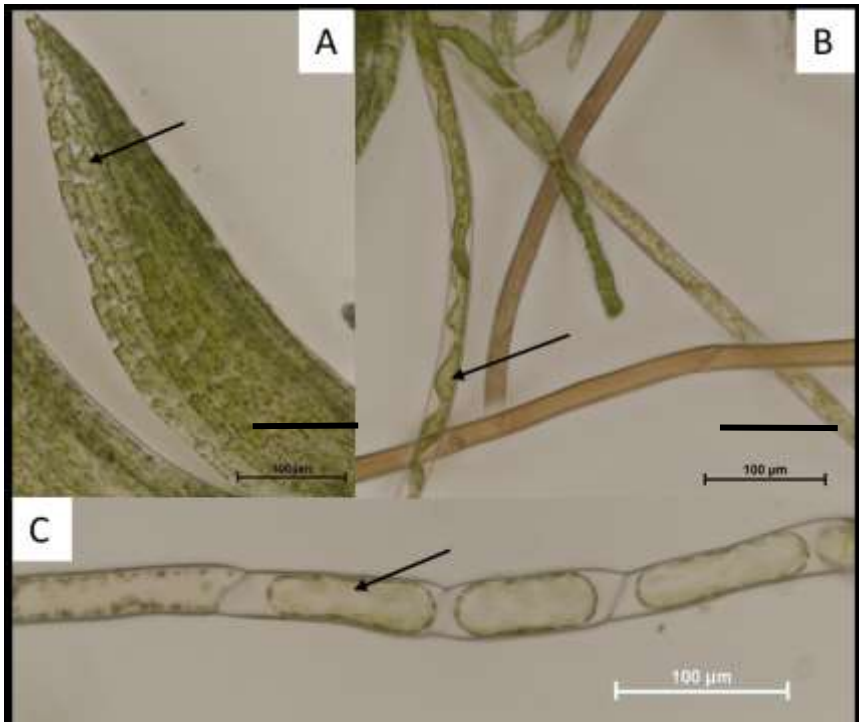

Fig. 115: Bright field image of A) *P. patens* Myosin VIII cell line leaflet cells in a Mannitol concentration of 0,4 M; arrow: concave plasmolysis B) *M. elongata* protonema cells in a Mannitol concentration of 0,8 M; arrow: plasmolysis C) *P. patens* Myosin VIII cell line protonema cells in a Mannitol concentration of 0,4 M; arrow: protoplast (scale bar 100 µm)

Plasmolysis with 0,4 M Mannitol

Not all of the GFP cell lines did always show plasmolysis at this concentration. The ER, actin and tubulin were seen in the Hechtian strands and plasma membrane. The ER showed the same structures as unplasmolysed cells, with their distinction between cisternae and tubules. Only the ER showed complete Hechtian strands, without a disruption in comparison in the Life-act cell line only a little part of the Hechtian strand remained at the protoplast. The tubulin was seen in protoplasmic strands and enclosed the chloroplasts between their tubules. The Life-act cell line did show more G-Actin due to

the osmotic stress. The Reticulon and Calnexin cell lines showed fluorescence of the GFP in the cell wall and in parts of the chloroplasts.

GFP-ER cell line

ER has many different functions also the maintenance of information transport between different cells, because of that we wanted to see how the cells respond to osmotic stress. When the plants were in the 0,4 M Mannitol solution, the moss reacted sometimes with a beginning plasmolysis and sometimes did not show a response, this could be the value for incipient plasmolysis for the plants.

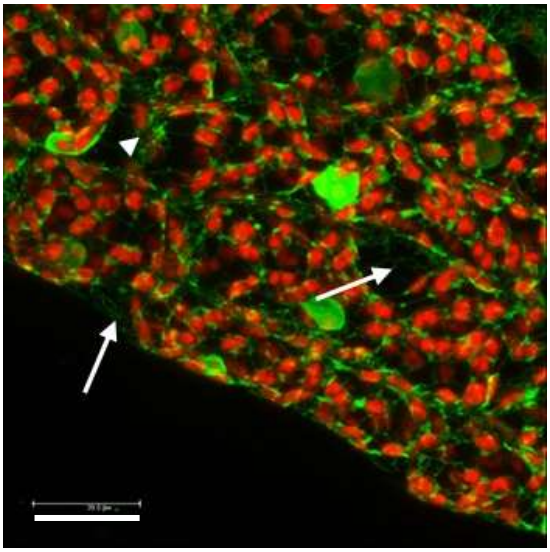

In fig. 116 the cells plasmolysed also in a concentration of 0,4 M Mannitol, Hechtian strands (marked with an arrow) can be perceived and the protoplast has retreated from the cell wall. Plasmolysis of another leaflet can be seen in the movie 23.

Fig. 116: *P. patens* ER cell line leaflet cells in a Mannitol concentration of 0,4 M, Maximum projection overlay of GFP and chloroplast channel (scale bar 20 µm)

Life-act cell line

The Life-act cell line showed the beginning of plasmolysis and an aggregation of G-actin in plasmolysis with 0,4 M Mannitol.

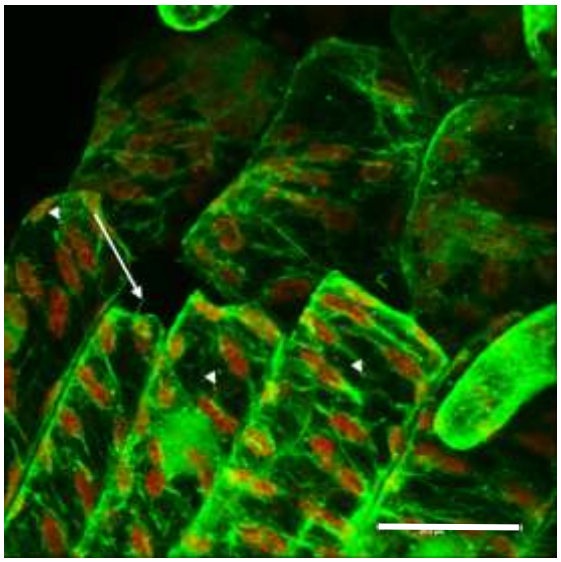

The leaflet cell in fig. 117 shows a beginning of plasmolysis, where on the edges of the cell the protoplast has retreated from the cell wall, also a part of a Hechtian strand can be seen (marked with an arrow). Furthermore, it is shown that more G-actin is present than in not plasmolysed cells (indicated by arrowheads).

Fig. 117: *P. patens* Life-act cell line leaflet cells in a Mannitol concentration of 0,4 M, Maximum projection overlay of GFP and chloroplast channel, arrow: Hechtian strand; arrowheads: G-Actin (scale bar 20 µm)

GFP-tubulin cell line

Most of the time the cells showed plasmolysis and the tubulin was also seen in Hechtian strands and protoplasmic strands. The microtubules tubules still enclosed the chloroplasts within them.

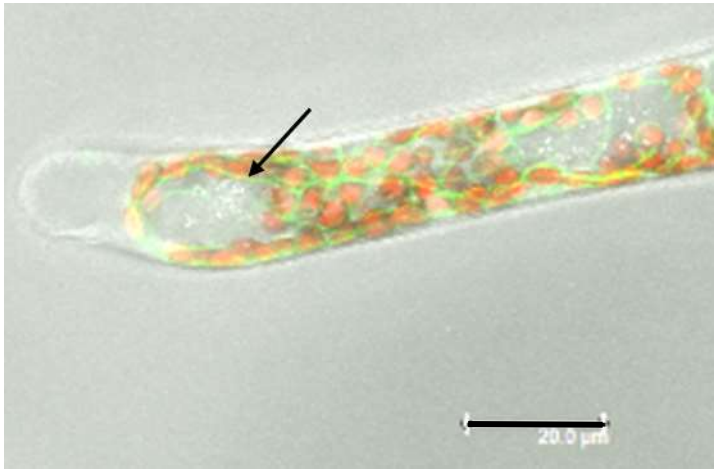

This chloronema end cell in fig. 118 shows how the protoplast has retracted from the cell wall, there is also the movie 24 of the 3D reconstruction, of this cell. The tubulin displays it tubulary structure and encloses the chloroplast between the microtubules (indicated by an arrow).

Fig. 118: *P. patens* GFP-Tub cell line bended chloronema cell in a Mannitol concentration of 0,4 M, Maximum projection overlay of GFP, chloroplast and Transmission channel, arrow: microtubule (scale bar 20 µm)

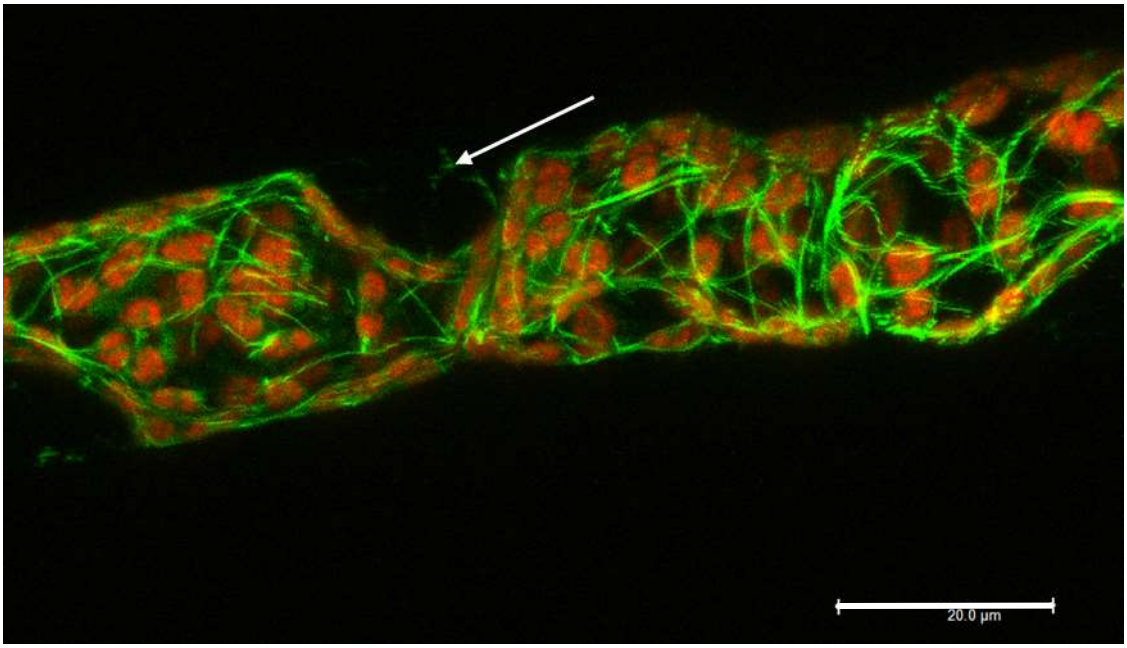

Fig. 119: *P. patens* Life-act cell line leaflet cells in a Mannitol concentration of 0,4 M, Maximum projection overlay of GFP and chloroplast channel, arrow: Hechtian strand; arrowhead: G-Actin (scale bar 20 µm)

The tubulin and therefore also the microtubules are enclosing the chloroplast and the protoplast in chloronema cells (fig. 119 and in the movie 25). Furthermore, some tubulary structures are seen, which follow the shape of the protoplast. Sometimes they show the Hechtian strands, indicated by an arrow in fig. 121 a connection from the cell wall to the protoplast.

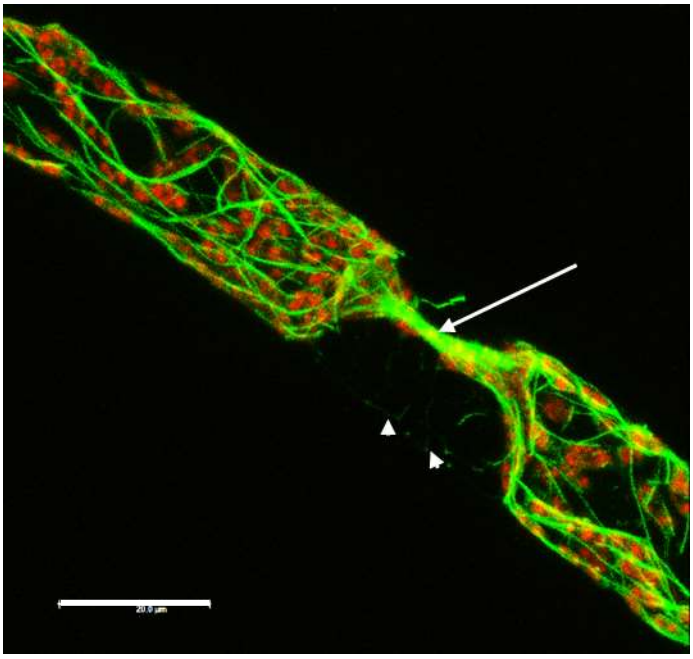

A thick bundle of microtubules, with chloroplasts between the microtubules, forms a protoplasmic strand and is marked in fig. 120 with an arrow. These microtubules connect the two parted protoplasts. Hechtian strands are also formed which are connecting the protoplasmic strand with the cell wall (connecting point with cell wall is marked with an arrowhead). In the movies 26 and 27 a 3D reconstruction of this cell can be seen.

Fig. 120: *P. patens* GFP-Tub cell line chloronema cell in a Mannitol concentration of 0,4 M, Maximum projection overlay of GFP and chloroplast channel, arrow: protoplasmic strand; arrowheads: connecting point of Hechtian strands to cell wall (scale bar 20 µm)

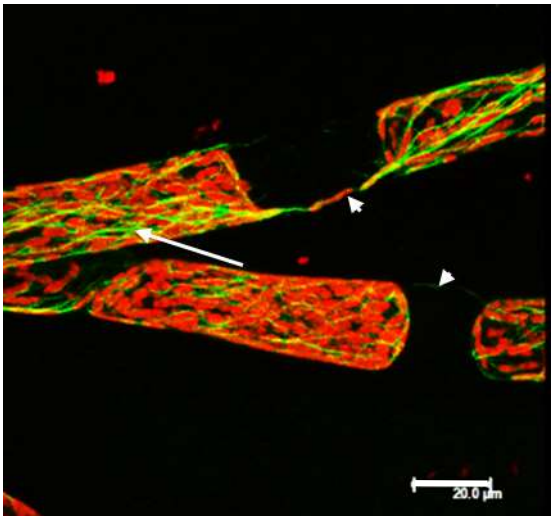

In the upper chloronema cell a sub-protoplast is shown with a protoplasmic strand at the cell wall with tubulin and within two enclosed chloroplasts (indicated by an arrowhead in fig. 121). The micortubules are enclosing the chloroplasts within them (marked with an arrow in the chloronema cell in fig. 121), this is seen in both cells. The lower caulonema cell displays a protoplasmic strand without chloroplasts and there just one microtubule is connecting the two sub-protoplasts (indicated by an arrowhead in fig. 121).

Fig. 121: *P. patens* GFP-Tub cell line chloronema cell above and caulonema cell below in a Mannitol concentration of 0,4 M, Maximum projection overlay of GFP and chloroplast channel, arrow: tubules between chloroplasts; arrowheads: protoplasmic strand (scale bar 20 µm)

Reticulon cell line

The Reticulon cell line displayed plasmolysis when put in a 0,4 M Mannitol concentration, the GFP revealed unspecific labelling with fluorescence in parts of the chloroplasts, near the cell wall and around the chloroplasts.

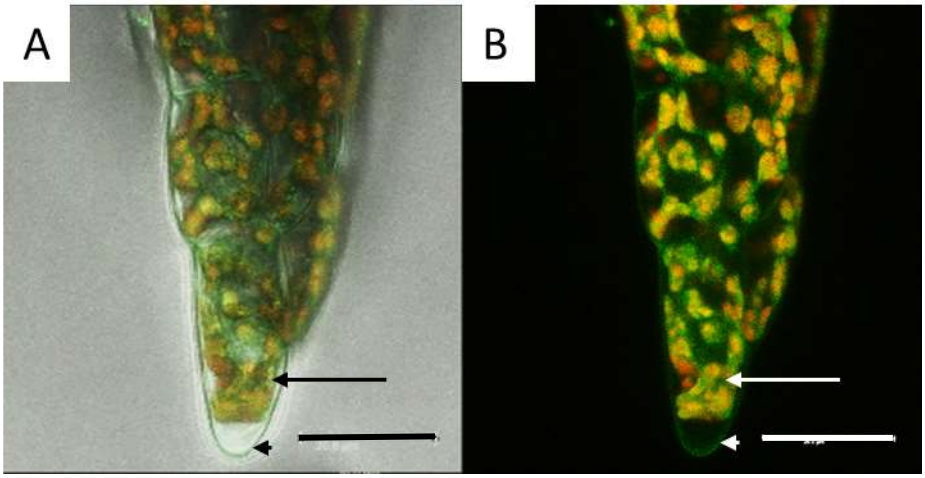

Fig. 122: *P. patens* Reticulon cell line leaflet cells in a Mannitol concentration of 0,4 M, Maximum projection A) overlay of GFP, chloroplast and Transmission channel; arrow: GFP between chloroplasts; arrowheads: cell wall; B) overlay of GFP and chloroplast channel; arrow: GFP between chloroplasts; arrowheads: cell wall (scale bar 20 µm)

The end cell of the leaflet in fig. 122 plasmolysed and a retracted protoplast is seen (movie 28). The GFP of Reticulon shows fluorescence near the cell wall (indicated by an arrowhead in fig. 122) and in some parts of the chloroplast and some connections between the chloroplasts (marked with an arrow in fig. 122).

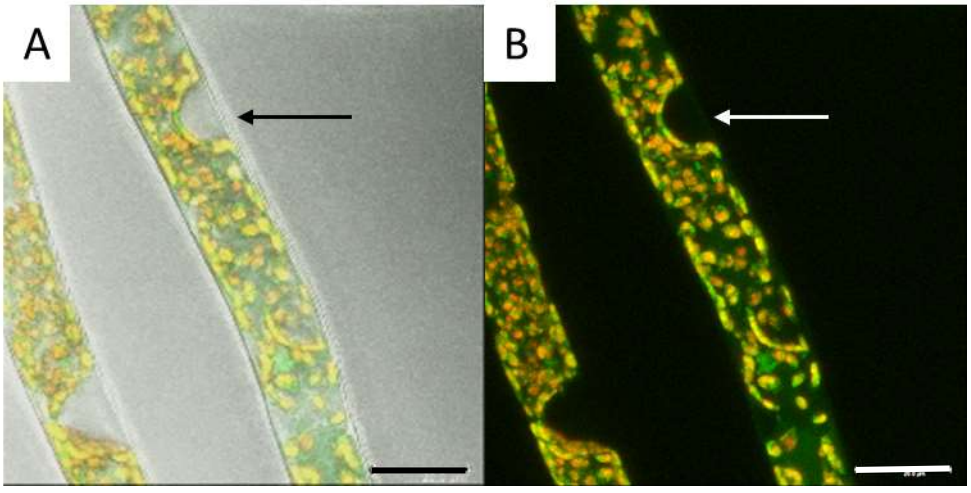

Fig. 123: *P. patens* Reticulon cell line chloronema cells in a Mannitol concentration of 0,4 M, Maximum projection A) overlay of GFP, chloroplast and Transmission channel; arrow: cell wall; B) overlay of GFP and chloroplast channel; arrow: cell wall (scale bar 20 µm)

In the chloronema cell in fig. 123, the Reticulon can be recognized in parts of the chloroplasts, a little bit in close vicinity to the cell wall (marked with an arrow in fig. 123) and even in the cytoplasm, because of unspecific labelling.

Calnexin cell line

The Calnexin cell line showed a signal of the GFP near the cell wall in the leaflet and chloronema cells and the cytoplasm seemed to show the fluorescence, due to unspecific labelling.

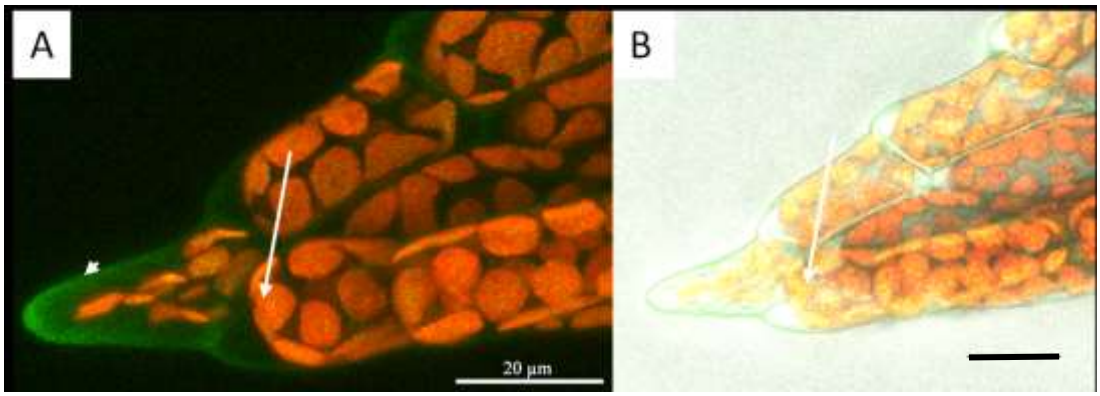

Fig. 124: *P. patens* Calnexin cell line leaflet cells in a Mannitol concentration of 0,4 M, Maximum projection A) overlay of GFP and chloroplast channel; arrow: protoplast; arrowhead: cell wall B) overlay of GFP, chloroplast and Transmission channel; arrow: protoplast; arrowhead: cell wall (scale bar 20 µm)

The leaflet cells in fig. 124 show plasmolysis, the protoplast has retreated from the cell wall (marked with an arrow), but the Calnexin unspecific labelling stayed near the cell wall (indicated by an arrowhead), and in the chloroplasts (shown in movie 29).

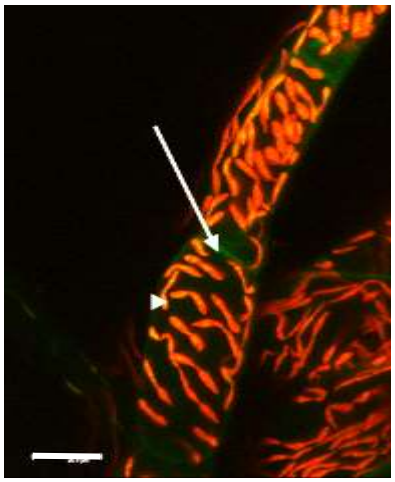

When the chloronema cells were in the 0,4 M Mannitol, they did not show plasmolysis and the GFP showed unspecific labelling near the cell wall (fig. 125). The chloroplast did change their form maybe due to the osmotic stress.

Fig. 125: *P. patens* Calnexin cell line chloronema cells in a Mannitol concentration of 0,4 M, Maximum projection overlay of GFP and chloroplast channel (scale bar 20 µm)

Plasmolysis with 0,5 M Mannitol

Using the concentration of 0,5 M Mannitol ensures that the cells begin to plasmolyse. The ER showed many Hechtian strands with a lot of connections to the cell wall. The ER formed ring like structures within chloroplasts. The Life-act cell line displayed normal actin filaments and the Hechtian strands between neighbouring cells. The GFP-Tub cell line did not show Hechtian strands so often only in a leaflet cell one was seen. The tubules revealed a wavier structure and did not enclose the chloroplasts so strictly anymore. The Myosin VIII showed fluorescence near the cell wall and in one chloronema cell it was seen in a protoplasmic strand.

GFP-ER cell line

The ER cell line always showed the Hechtian strands in all the cell types. Hechtian strands formed connections to cell walls of neighbouring cells and to cell wall of the cell. The cisternae and tubules were not always so good preserved, but in the leaflet cell they were good to see. Rings in the chloroplasts were shown, shaping them a bit like 'donuts'.

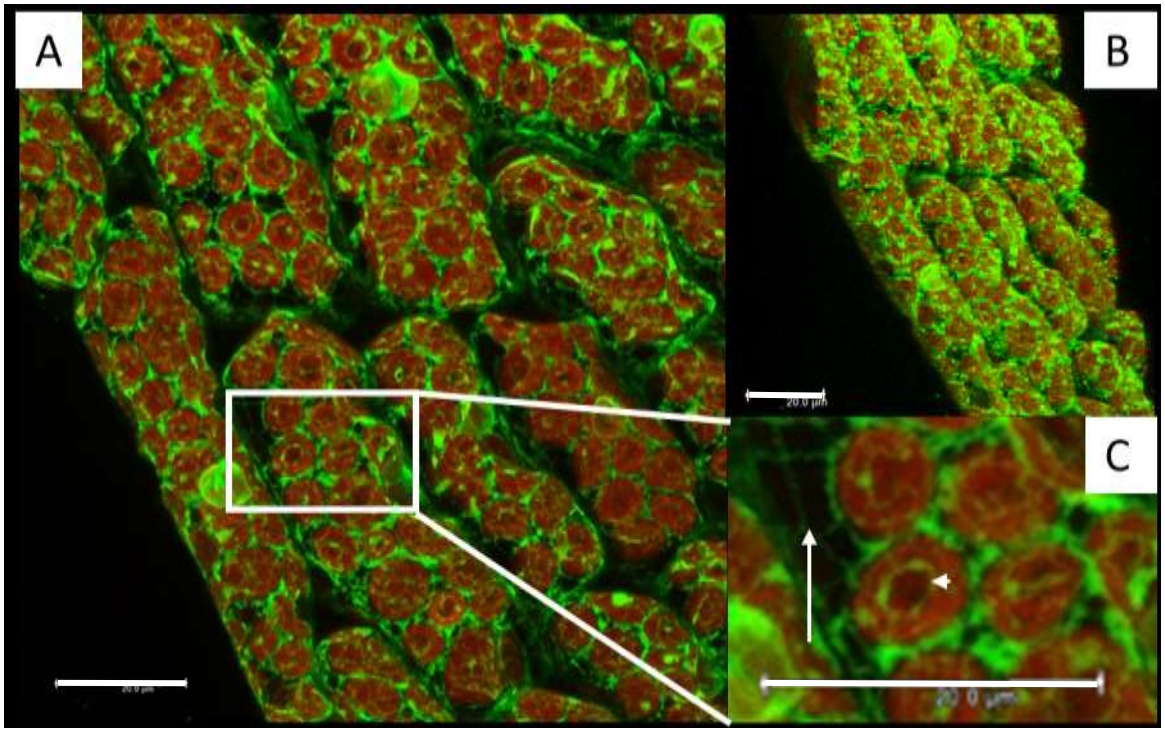

Fig. 126: *P. patens* GFP-ER cell line leaflet cells in a Mannitol concentration of 0,5 M, A) Maximum projection overlay of GFP and chloroplast channel B) 3D Reconstruction of Maximum projection overlay of GFP and chloroplast channel C) higher magnification of the rectangle indicated part of A; arrow: Hechtian strand; arrowhead: ER forming ring in chloroplast (scale bar 20 µm)

In a 0,5 M Mannitol concentration the leaflets showed that the ER is surrounding the chloroplast more than in un-plasmolysed cells, it formed rings in the chloroplasts (indicated by an arrowhead in fig. 126 C). The ER showed the Hecht reticulum and the Hechtian strands marked with an arrow in fig. 126 C, the plasmolysis just started, and the cell retreated only partly from the cell wall. The protoplast only retracted from the edges of the cell and not completely from every cell wall. In the maximum projection in the 3D it can be seen that the ER stretches through the whole cell and the protoplast has only retreated in the middle of the leaflet cells.

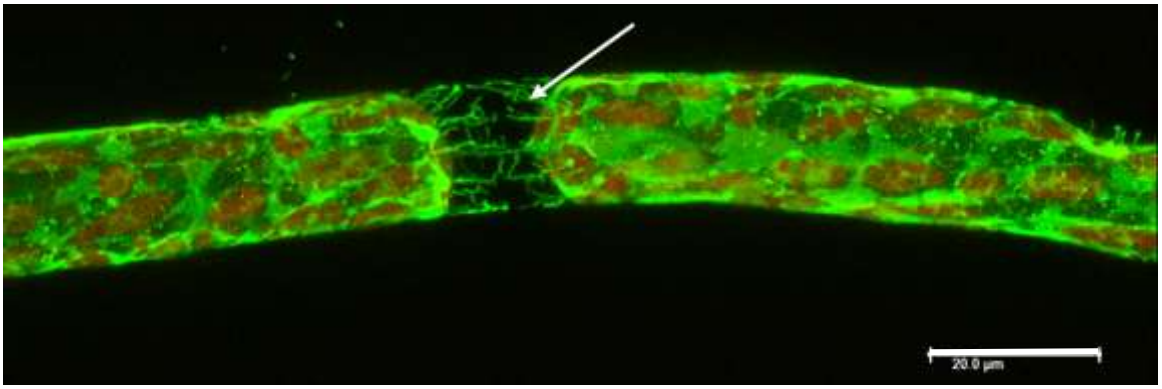

Fig. 127: *P. patens* GFP-ER cell line chloronema cells in a Mannitol concentration of 0,5 M Maximum projection overlay of GFP and chloroplast channel; arrow: Hechtian strand (scale bar 20 µm)

In this picture there are many Hechtian strands between the two formed protoplasts present (marked with an arrow in fig. 127). The ER still keeps a connection between the two protoplasts, but its structure in the cell is not so fine any more and more destroyed GFP can be seen.

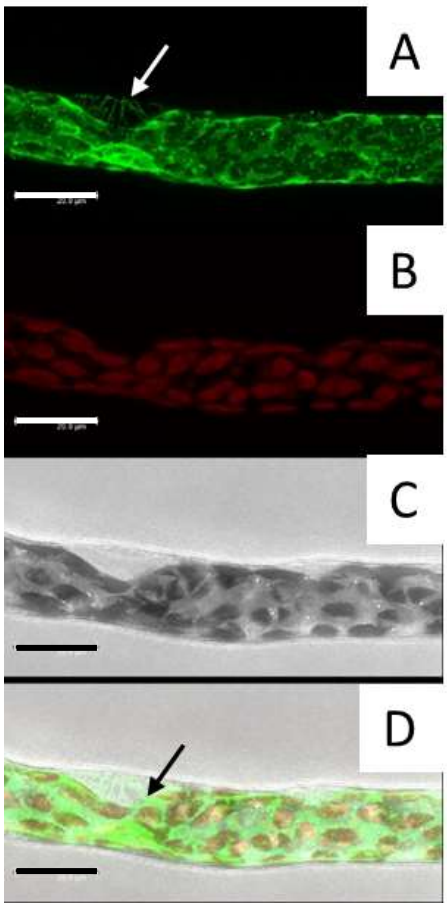

In this chloronema cell the protoplast has retreated from the upper cell wall, but still has a connection to it through the Hechtian strands (indicated by an arrow in fig. 128 A and C).

Fig. 128: *P. patens* GFP-ER cell line chloronema cell in a Mannitol concentration of 0,5 M Maximum projection A) GFP channel; arrow: Hechtian strand B) chloroplast channel C) Transmission channel D) overlay of GFP, chloroplast and Transmission channel; arrow: Hechtian strand (scale bar 20 µm)

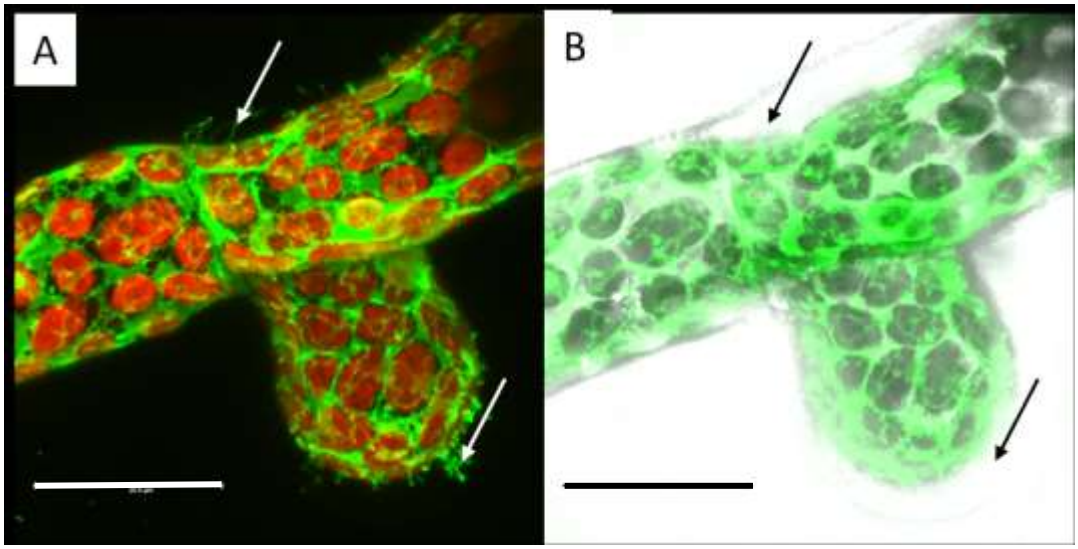

Fig. 129: *P. patens* GFP-ER cell line chloronema cells at a branching point with a newly formed cell in a Mannitol concentration of 0,5 M, Maximum projection A) overlay of GFP and chloroplast channel; arrows: Hechtian strands; B) overlay of GFP and Transmission channel; arrows: Hechtian strands; (scale bar 20 µm)

The newly formed chloronema cell in fig. 129 plasmolysed and showed many Hechtian strands to the cell wall (Hechtian strands indicated by an arrow in fig. 129). This looks like the connection to the cell wall is in newly formed cells more necessary than in older cells. The movie 30 of the 3D Reconstruction demonstrates that the strands are forming a network with tiny strands in the whole tip of the cell to the cell wall.

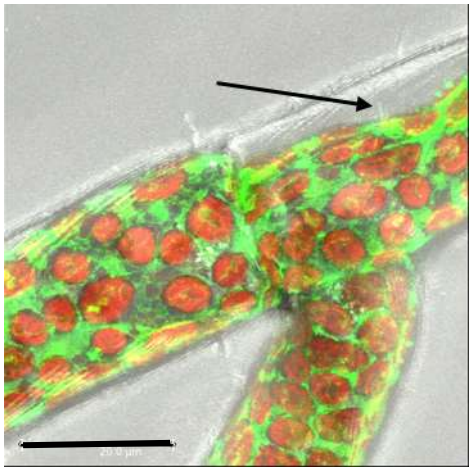

Sometimes cells plasmolyse, but no Hechtian strands are seen anymore, because they already vanished or lost their connection to the cell wall, in fig. 130 a tiny part of the Hechtian strand remained (indicated by an arrow).

Fig. 130: *P. patens* GFP-ER cell line chloronema cells at a branching point in a Mannitol concentration of 0,5 M, Maximum projection overlay of GFP, chloroplast and Transmission channel; arrow: remaining Hechtian strand; (scale bar 20 µm)

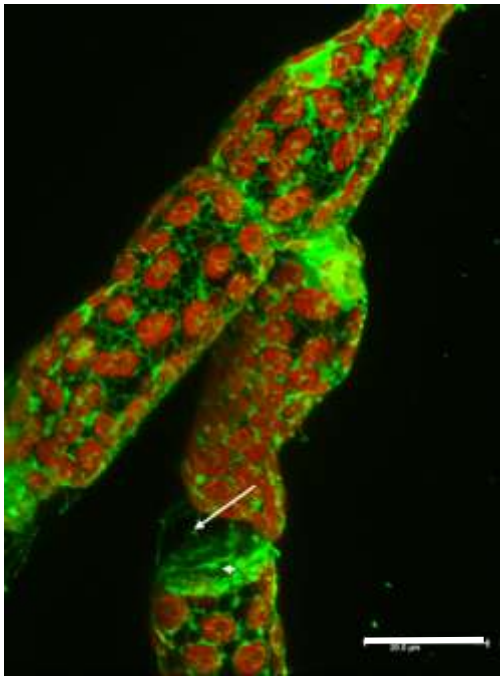

In fig. 131 the plasma membrane near the cell wall can be seen with the Hechtian strands (indicated by arrow) forming a connection between the plasma membrane (indicated by arrowhead) and the protoplast, this can also be perceived in movie 31 of the 3D reconstruction. Near the cell wall the ER is accumulating and the Hechtian strands are expanding there to the protoplast.

Fig. 131: *P. patens* GFP-ER cell line chloronema cells at a branching point with a newly formed cell in a Mannitol concentration of 0,5 M, Maximum projection overlay of GFP and chloroplast channel; arrow: Hechtian strands; arrowhead: plasma membrane (scale bar 20 µm)

Life-act cell line

The Life-act cell line showed the actin filaments and the fluorescence of the GFP in the Hechtian strands.

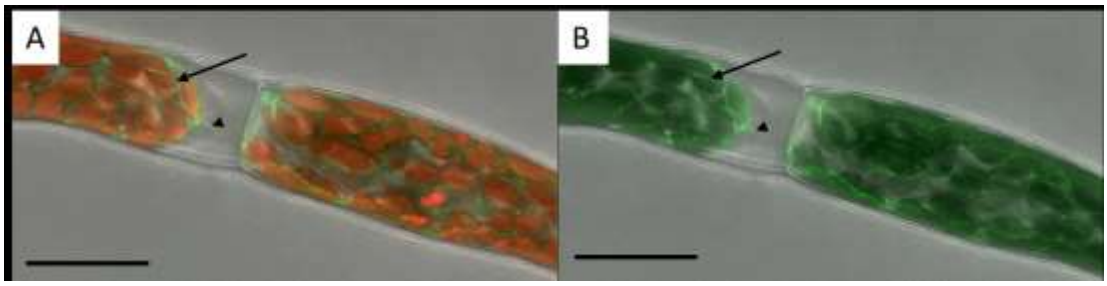

Fig. 132: *P. patens* Life-act cell line chloronema cells in a Mannitol concentration of 0,5 M, Maximum projection A) overlay of GFP, chloroplast and Transmission channel; arrow: actin filament; arrowhead: Hechtian strands B) overlay of GFP and Transmission channel; arrow: actin filament; arrowhead: Hechtian strand (scale bar 20 µm)

In the chloronema cell in fig. 132 the Hechtian strands are seen (indicated by an arrowhead) and actin filaments between chloroplasts can be distinguished (marked with an arrow in fig. 132).

GFP-tubulin cell line

The microtubule structure of the GFP-Tub is a little bit more diffuse and wavier than in non-plasmolysed cells. The tubules still enclosed the protoplast within its microtubules. At this concentration only in a leaflet cell a Hechtian strand was present.

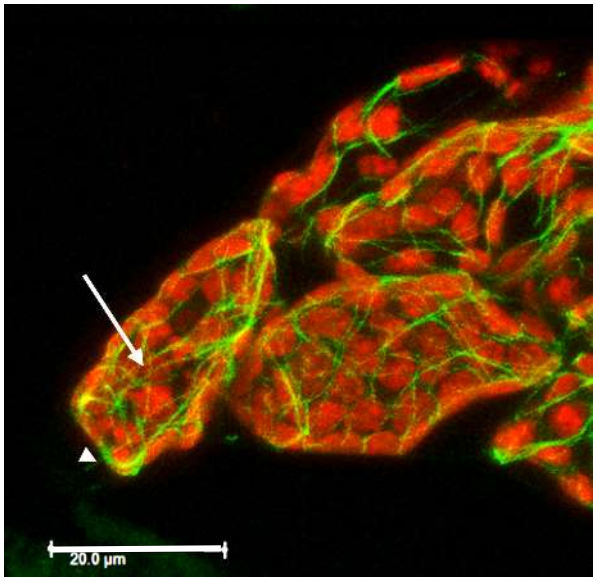

A single microtubule is forming a Hechtian strand to the tip of the cell in the leaflet in fig. 133 indicated by an arrowhead but is not reaching the cell wall anymore (movie 32). The microtubules are a little bit more unorganized and wavy (marked with an arrow in fig. 133) and still enclose chloroplasts, but not so strict anymore.

Fig. 133: *P. patens* GFP-Tub cell line leaflet cells in a Mannitol concentration of 0,5 M, Maximum projection overlay of GFP and chloroplast channel; arrow: tubule; arrowhead: Hechtian strand (scale bar 20 µm)

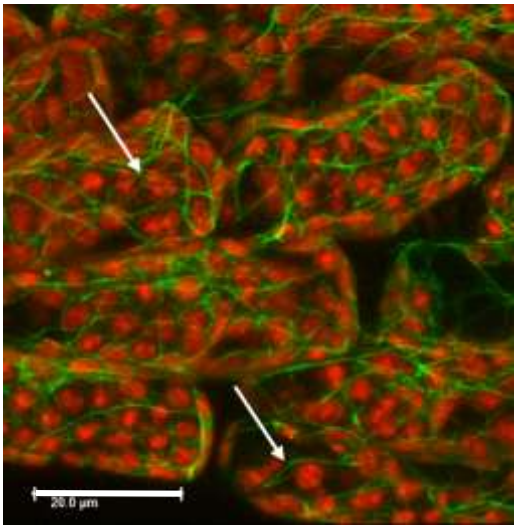

At the beginning of plasmolysis, a shrinkage from the cell wall is visible, in the leaflet cell the tubulin surrounds the protoplast. The microtubules display a wavy structure this is marked with arrows in fig. 134.

Fig. 134: *P. patens* GFP-Tub cell line leaflet cells in a Mannitol concentration of 0,5 M, Maximum projection overlay of GFP and chloroplast channel; arrow: tubules (scale bar 20 µm)

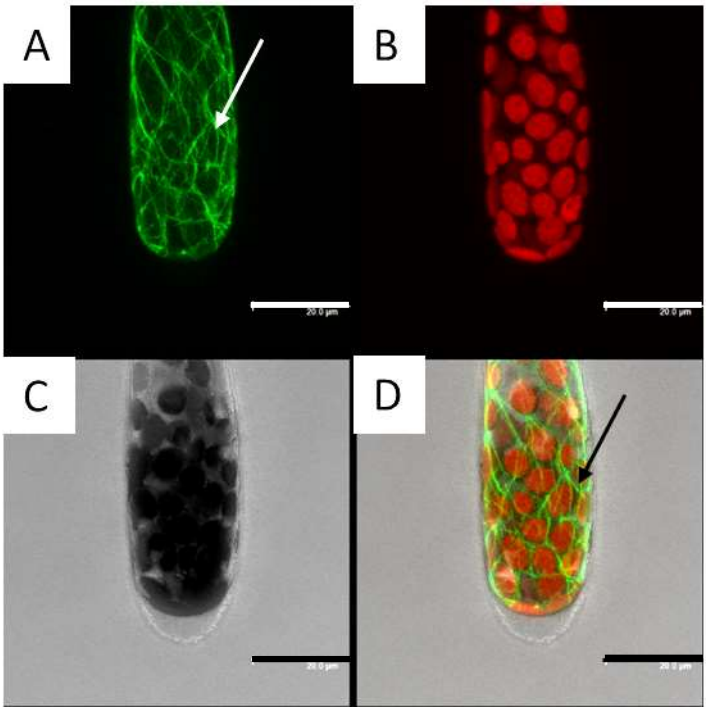

In the tip cell of chloronema cell in fig. 135 the tubulin forms a sheet around the protoplast but shows no Hechtian reticulum. The microtubules are formed between the chloroplasts (indicated by an arrow in fig. 135). Another chloronema cell at a branching point with starting plasmolysis can be seen in movie 33.

Fig. 135: *P. patens* GFP-Tub cell line leaflet cells in a Mannitol concentration of 0,5 M, Maximum projection A) GFP channel; arrow: tubule B) chloroplast channel C) Transmission channel D) overlay of GFP, chloroplast and Transmission channel; arrow: tubule (scale bar 20 µm)

Myosin VIII cell line

The Myosin VIII was fluorescenting mostly near the cell wall and in the chloroplasts. The cytoplasm also shows the GFP fluorescence. In one cell the GFP signal was seen in a protoplasmic strand between two sub-protoplasts, all these signals were due to unspecific labelling.

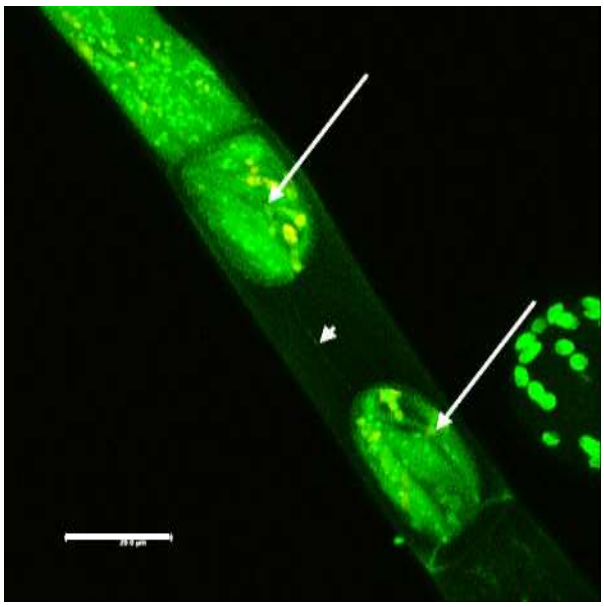

In fig. 136 the Myosin VIII is fluorescenting near the cell wall, in the cytoplasm and in a protoplasmic strand (marked with an arrowhead) between two sub-protoplasts (indicated by arrows). The sub-protoplasts also show a fluorescence of the GFP, but no distinguishable structures within them.

Fig. 136: *P. patens* Myosin VIII cell line chloronema cells in a Mannitol concentration of 0,5 M, Maximum projection overlay of GFP and chloroplast channel; arrows: sub-protoplasts; arrowhead: protoplasmic strand

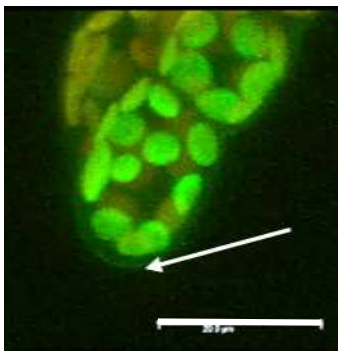

In the end cell of a leaflet (fig. 137) the Myosin VIII is seen near the cell wall (marked with an arrow) and around the chloroplasts (unspecific labelling).

Fig. 137: *P. patens* Myosin VIII cell line leaflet cells in a Mannitol concentration of 0,5 M, Maximum projection overlay of GFP and chloroplast channel; arrow: cell wall (scale bar 20 µm)

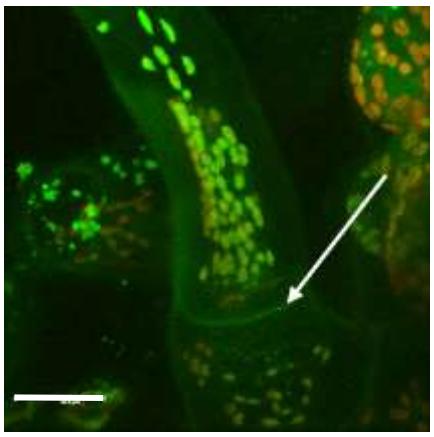

In this chloronema cell (fig. 138), which is growing out from a stem cell, a fluorescence of the Myosin VIII near the cell wall (marked with an arrow), around the chloroplasts and in the cytoplasm is detected.

Fig. 138: *P. patens* Myosin VIII cell line chloronema cell growing from the stem in a Mannitol concentration of 0,5 M, Maximum projection overlay of GFP and chloroplast channel; arrow: cell wall (scale bar 20 µm)

Plasmolysis with 0,6 M Mannitol

At a concentration of 0,6 M Mannitol the cells showed a stronger plasmolysis. Hechtian strands were seen in the ER, Life-act and GFP-Tub cell line.

GFP-ER cell line

In the 0,6 Mannitol concentration the ER cell line showed plasmolysis and many Hechtian strands in leaflet cells between sub-protoplasts.

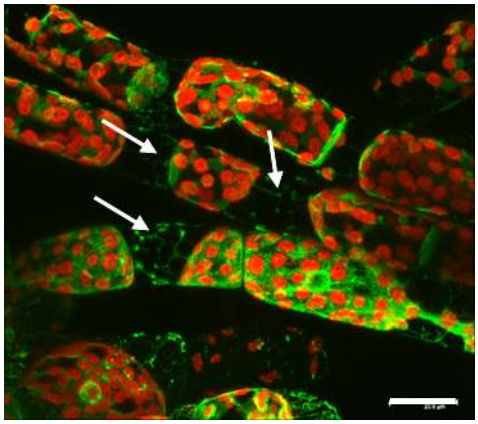

Between the cells in fig. 139 many Hechtian strands can be depicted (marked with arrows). They were between the protoplast and the cell wall of a neighbouring cell and between two separated sub-protoplasts and to the edge of the cell (also seen in movie 34).

Fig. 139: *P. patens* GFP-ER cell line chloronema cells in a Mannitol concentration of 0,6 M, Maximum projection of overlay of GFP and chloroplast channel; arrows: Hechtian strands (scale bar 20 µm)

Life-act cell line

The Life-act cell line plasmolysed in the 0,6 M Mannitol plasmolyticum and Hechtian strands were seen in leaflet and chloronema cells.

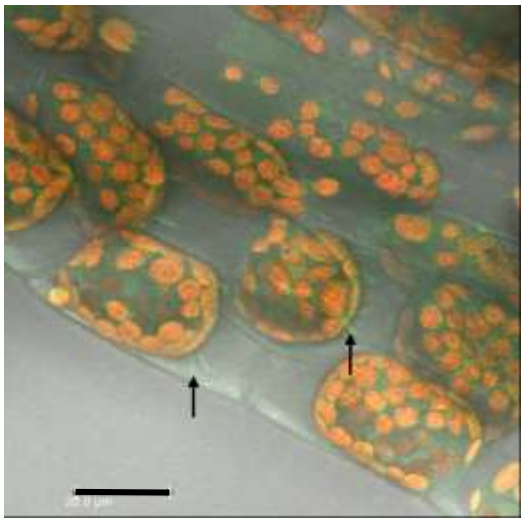

The Life-act cell line showed also the actin in the Hechtian strands (indicated by arrows in fig. 140). In the leaflet cells the protoplasts were mostly shrinking to one side and the Hechtian strands were connecting to the cell walls to all other sides.

Fig. 140: *P. patens* Life-act cell line leaflet cells in a Mannitol concentration of 0,6 M, Maximum projection of overlay of GFP, chloroplast and Transmission channel; arrows: Hechtian strands (scale bar 20 µm)

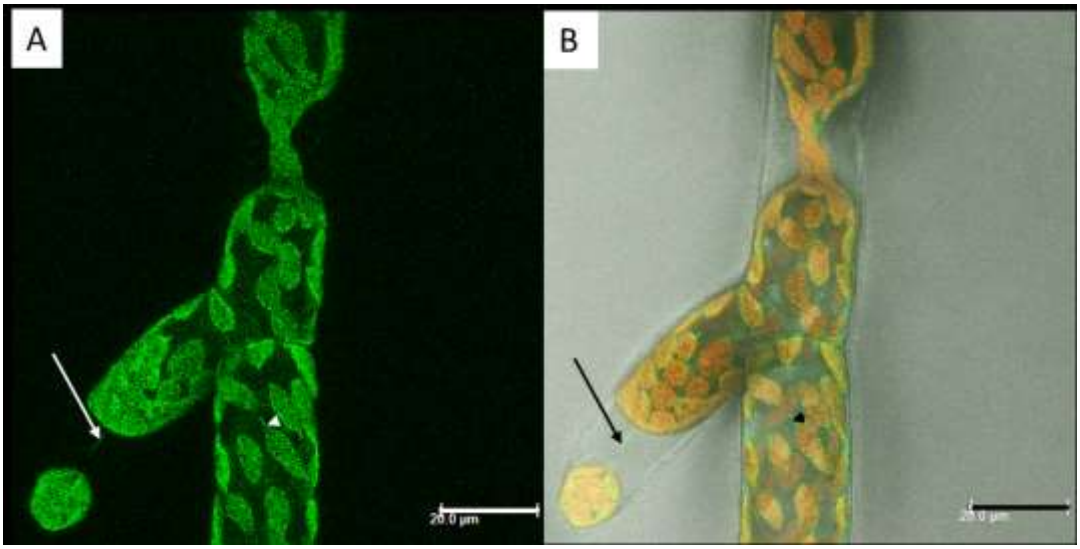

Fig. 141: *P. patens* Life-act cell line chloronema cells in a Mannitol concentration of 0,6 M, Maximum projection of A) GFP channel; arrow: Hechtian strand; arrowhead: microtubule near chloroplast B) overlay of GFP, chloroplast and Transmission channel; arrow: Hechtian strand; arrowhead: actin filament near chloroplast (scale bar 20 µm)

In fig. 141 a chloronema cell of a Life-act cell line showed that the actin is in the Hechtian strand between two sub-protoplasts in an end cell. There was just one Hechtian strand (marked with an arrow) connecting these two sub-protoplasts. An actin filament was stretching out from a chloroplast in a non-plasmolysed part of the cell (indicated by an arrowhead in fig. 141).

GFP-tubulin cell line

The GFP-Tub cell line showed plasmolysis and Hechtian strands in 0,6 M Mannitol concentration.

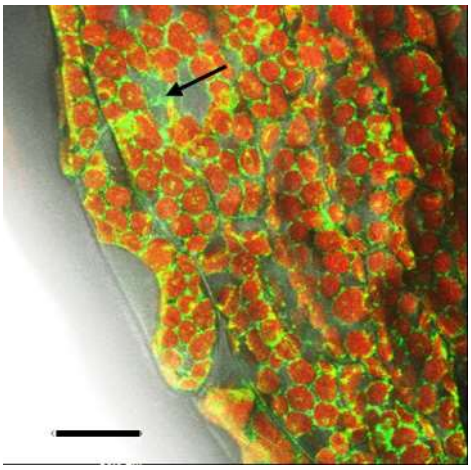

At the concentration of 0,6 M Mannitol the protoplast retracted more from the cell wall. An encapsulation of the chloroplast by the tubulin can be seen. The protoplast in the leaflet cell retreated from the outer cell wall to the inner part of the leaflet. Hechtian strands can be seen in one leaflet (marked with an arrow in fig. 142).

Fig. 142: *P. patens* GFP-Tub cell line leaflet cells in a Mannitol concentration of 0,6 M, Maximum projection of overlay of GFP, chloroplast and Transmission channel; arrow: Hechtian strand (scale bar 20 µm)

Plasmolysis with 0,8 M Mannitol

For the mosses 0,8 M Mannitol was a strong plasmolyticum and all the cells plasmolysed in this concentration. The ER, Life-act and GFP-Tub cell line showed their GFP structures in the Hechtian strands and the ER and actin were seen in protoplasmic strands. The ER cisternae responded to the high plasmolysis, they accumulated together. The Myosin VIII cell line showed plasmolysis, but the Myosin VIII showed unspecific labelling.

GFP-ER cell line

The GFP-ER cell line showed a stronger form of plasmolysis when treated with 0,8 M Mannitol. Many Hechtian strands are seen and protoplasmic strands also contained the GFP of the ER. The cisternae of the leaflet cells were measured and counted, it showed that the number of cisternae decreased, and its area increased. This means that the ER has aggregated together.

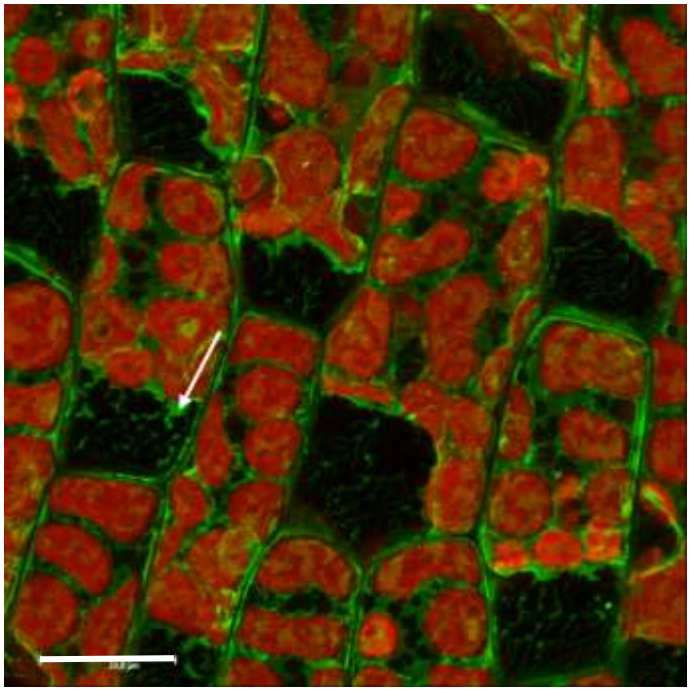

When using higher concentrations of Mannitol, the protoplast retreats more from the cell wall and seems to form more cisternae and less strands. All the cells in the leaflet cells retreat to the same direction. The Hechtian strands increase in number and also in size they form thicker strands marked with an arrow in fig. 143.

Fig. 143: *P. patens* GFP-ER cell line leaflet cells in a Mannitol concentration of 0,8 M, Maximum projection overlay of GFP and chloroplast channel; arrows: Hechtian strands; (scale bar 20 µm)

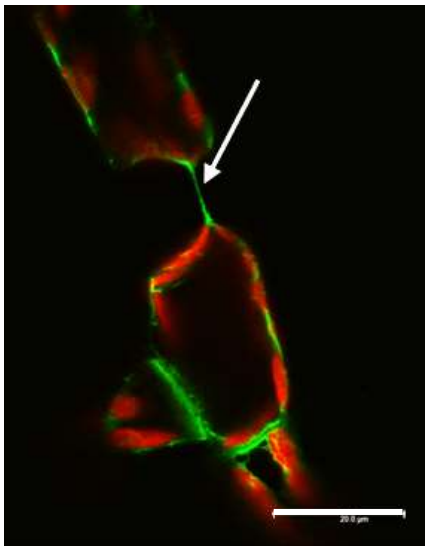

In fig. 144 a protoplasmic strand (indicated by an arrow) formed by ER can be seen between two sub-protoplasts in a chloronema cell. This strand seems to still connect the two sub-protoplasts with each other.

Fig. 144: *P. patens* GFP-ER cell line chloronema cell in a Mannitol concentration of 0,8 M, Maximum projection overlay of GFP and chloroplast channel; arrow: protoplasmic strand (scale bar 20 µm)

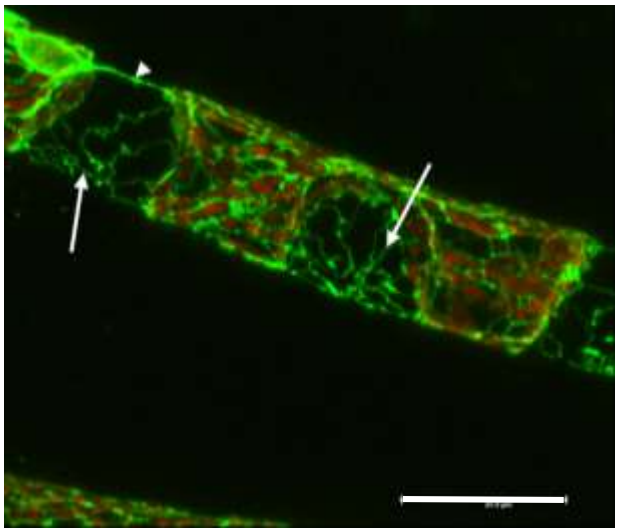

In this chloronema cell (fig. 145 and shown in movie 35) the nucleus forms a Hechtian strand to the sub-protoplast (indicated by an arrowhead). The sub-protoplasts retreated from the lower cell wall two times and both times they stayed connected to the cell wall through a lot of Hechtian strands (marked with arrows).

Fig. 145: *P. patens* GFP-ER cell line chloronema cells in a Mannitol concentration of 0,8 M, Maximum projection overlay of GFP and chloroplast channel; arrows: Hechtian strands; arrowhead: Hechtian strand from nucleus to sub-protoplast (scale bar 20 µm)

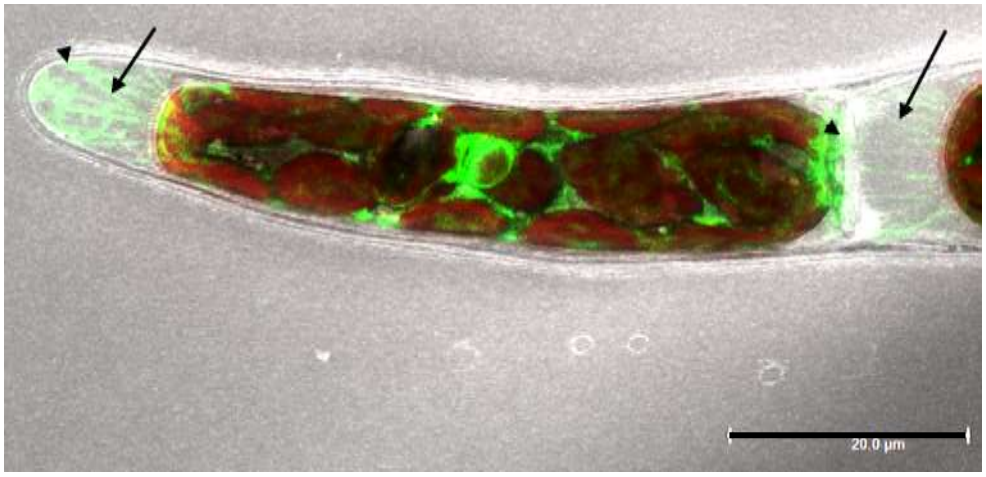

Fig. 146: *P. patens* GFP-ER cell line chloronema end cell in a Mannitol concentration of 0,8 M, Maximum projection overlay of GFP, chloroplast and Transmission channel; arrows: Hechtian strands; arrowheads: Hechtian strands connecting to cell wall (scale bar 20 µm)

In the tip cells of the chloronema cell in fig. 146 the Hechtian reticulum at the cell wall can be seen and Hechtian strands connecting the cells to each other were detected in this picture (marked with arrowheads). The ER cell line showed many Hechtian strands within the chloronema cells. The 3D reconstruction movie 36 shows this cell and the Hechtian strands at different angles.

Measurement of cisternae in leaflets for ER cell line

The cisternae of the ER were measured and counted at the beginning of plasmolysis and after 15 minutes. In the movie 37, the plasmolysed leaflet cells reveal the movement of the ER and how all the protoplasts retreated to the same side. The statistics showed that in all the cells a decrease in number of the cisternae can be clearly seen, also most of the cells have an increase in the area of cisternae. This would indicate that the ER shrinks together in plasmolysed cells and builds lesser cisternae with a higher area.

First measured leaflet cells

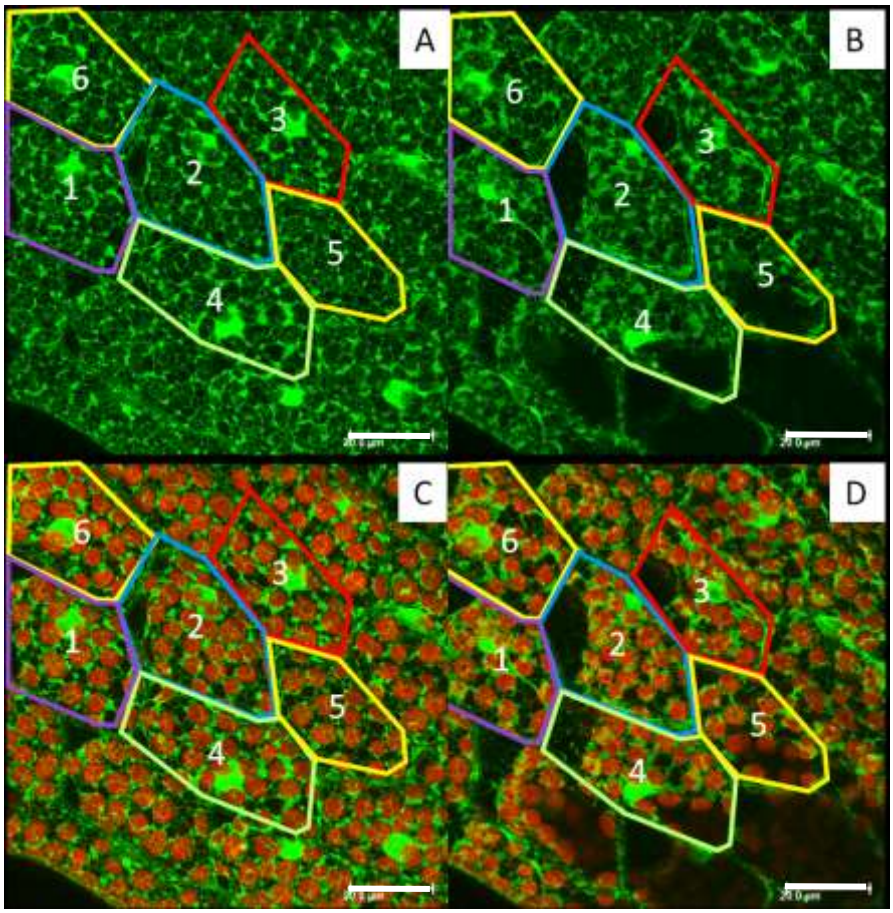

Fig. 147: *P. patens* GFP-ER cell line leaflet cells in a Mannitol concentration of 0,8 M, Maximum projection of A) GFP channel at beginning of plasmolysis B) GFP channel after 15 minutes in the plasmolyticum C) overlay of GFP and chloroplast channel at beginning of plasmolysis D) overlay of GFP and chloroplast channel after 15 minutes in the plasmolyticum; measured cells numbered and colourful surrounded (scale bar 20 µm)

In fig. 147 the six cells, which were used for measurement of cisternae area and number are marked. The cells one and two already showed plasmolysis at the beginning of the experiment after 15 minutes all measured cells show plasmolysis. The leaflet moved during the scan, because the plasmolyticum evaporated. The cells four and five lost some information of the GFP signal, because the scanning depth was not accurate anymore. In the picture alone, a change cannot be qualified, so it was measured with ImageJ. A significance between the begin and end of measurement was measured, and the cells were nonsignificant. All measured values including the T-test are shown in the Appendix (supplementary dara 3: table 6 and 7).

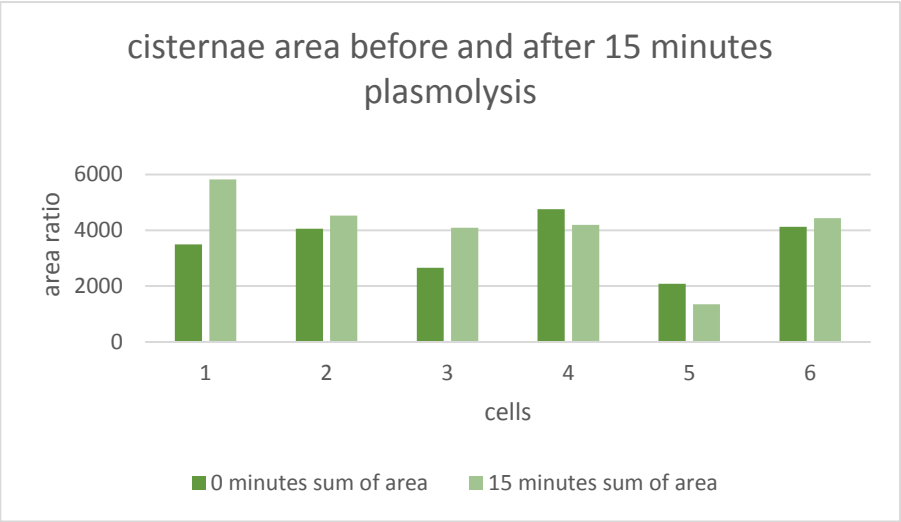

In the measurement of the area of the cisternae (fig. 148) an increase for the cells can be seen for one to three and six after 15 minutes. In comparison the cells four and five showed a decrease.

Fig. 148: area ratio of cisternae of *P. patens* GFP-ER cell line leaflet cells in a Mannitol concentration of 0,8 M at the beginning of plasmolysis and after 15 Minutes measured cells are indicated in fig. 152; error bar indicates standard deviation, significance indicated by a star

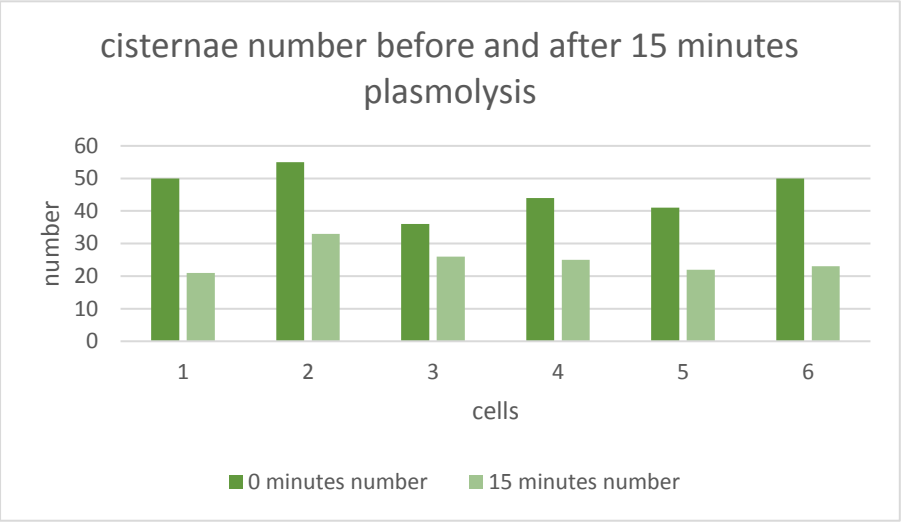

All the cells showed a decrease in number of the cisternae (fig. 149).

Fig. 149: number of cisternae of *P. patens* GFP-ER cell line leaflet cells in a Mannitol concentration of 0,8 M at the beginning of plasmolysis and after 15 Minutes measured cells are indicated in fig. 152; error bar indicates standard deviation, significance indicated by a star

Second measured leaflet cells

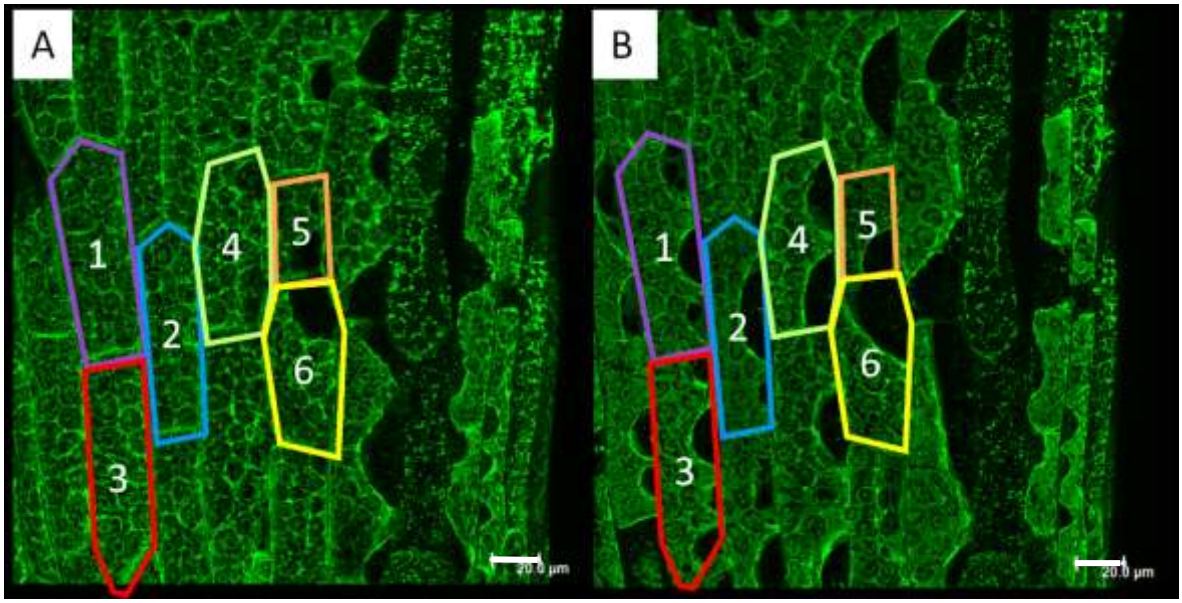

Fig. 150: *P. patens* GFP-ER cell line leaflet cells in a Mannitol concentration of 0,8 M, Maximum projection of A) GFP channel at beginning of plasmolysis B) GFP channel after 32 minutes in the plasmolyticum; measured cells numbered and colourful surrounded (scale bar 20 µm)

In fig. 150 only the GFP channels is shown, a change in the ER from the start (cero minutes) of the experiment and after 32 minutes can be recognized. A time lapse movie (movie 37) displays the movement of the ER in the plasmolysed cell. The ER accumulated and retracted from one side. The cells five and six showed already plasmolysis at the beginning, after 32 minutes all measured cells showed plasmolysis. The cells respond to the plasmolysis with mannitol with an increased area and a decrease of the number of cisternae. A significance between the begin and end of the measurement was shown for the cell six, the others were nonsignificant. All measured values including the T-test are shown in the Appendix (supplementary dara 3: table 8 and 9).

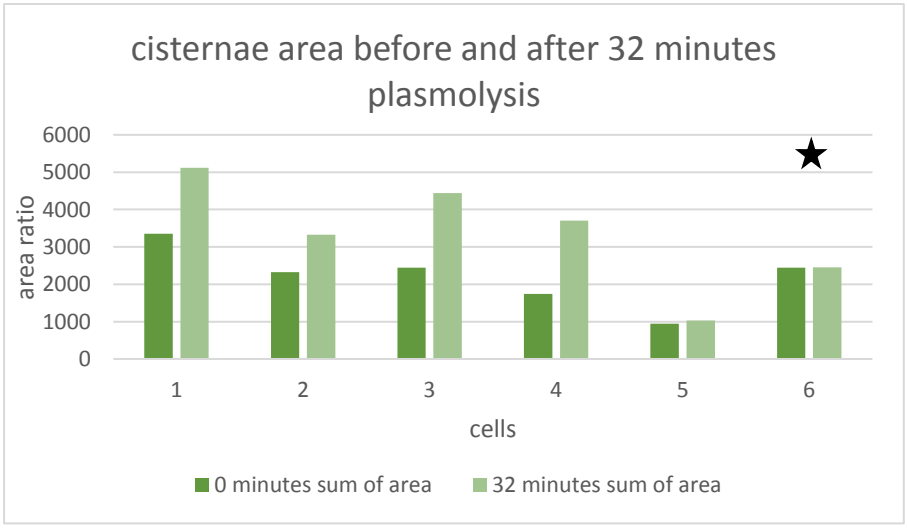

In these six cells all have an increased area of cisternae (fig. 151) and a decrease in their number (fig. 152).

Fig. 151: area ratio of cisternae of *P. patens* GFP-ER cell line leaflet cells in a Mannitol concentration of 0,8 M at the beginning of plasmolysis and after 32 minutes measured cells are indicated in fig. 152; error bar indicates standard deviation, significance indicated by a star

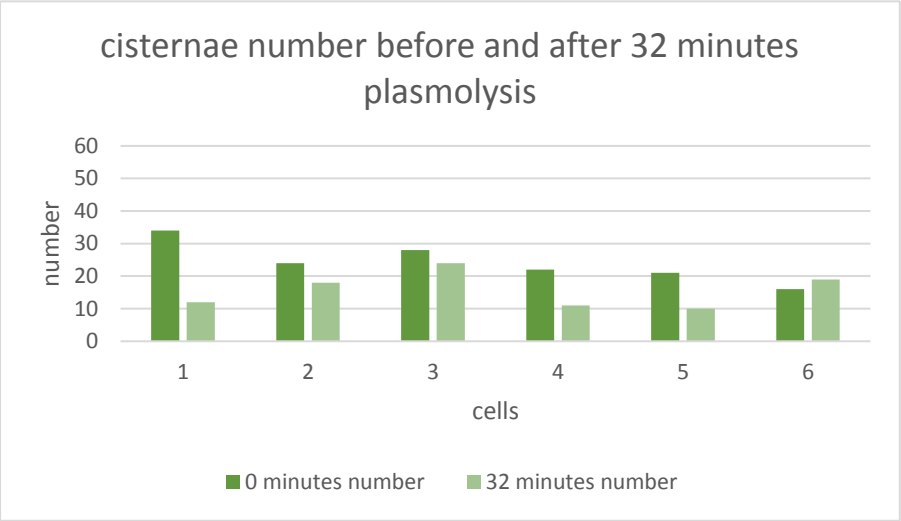

Fig. 152: number of cisternae of *P. patens* GFP-ER cell line leaflet cells in a Mannitol concentration of 0,8 M at the beginning of plasmolysis and after 32 minutes measured cells are indicated in fig. 152; error bar indicates standard deviation, significance indicated by a star

Life-act cell line

The cell responded to the 0,8 M Mannitol and plasmolysed. In both leaflet and protonema cells the actin surrounded the chloroplasts. The actin filaments formed ring like structures within the chloronema cells. Actin was found in Hechtian strands and in protoplasmic strands.

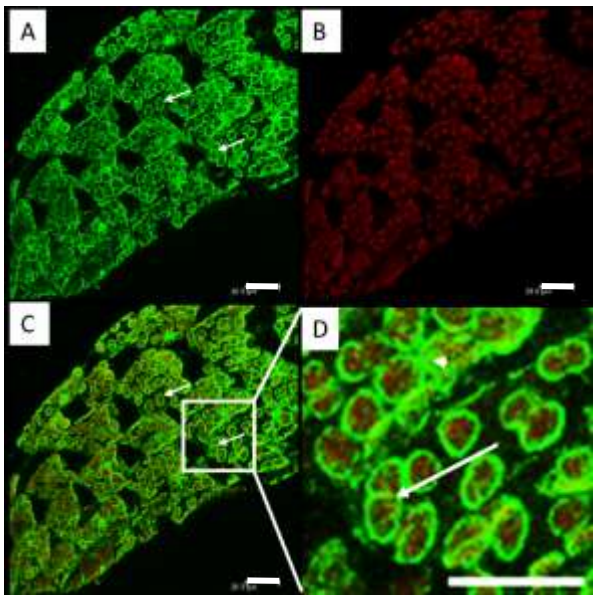

At higher concentrations of mannitol (0,8 M), the actin in the leaflet cells is gathering around the chloroplast (fig. 153). The protoplast retreats from the cell wall and the actin moves with it at the edge. The actin is forming ring like structures around the chloroplasts (indicated by an arrow in fig 153 D). A star shaped structure formed by actin can be seen in fig. 153 D marked with an arrowhead. The circles within the chloroplasts can be seen in the movie 38 (an average 3D reconstruction).

Fig. 153: *P. patens* Life-act cell line leaflet cells in a Mannitol concentration of 0,8 M, Maximum projection A) GFP channel; arrows: actin rings around chloroplasts B) chloroplast channel C) overlay of GFP and chloroplast channel; arrows: actin rings around chloroplasts D) higher magnification of the rectangle indicated part of C; arrow: actin ring around chloroplast; arrowhead: star shaped actin (scale bar 20 µm)

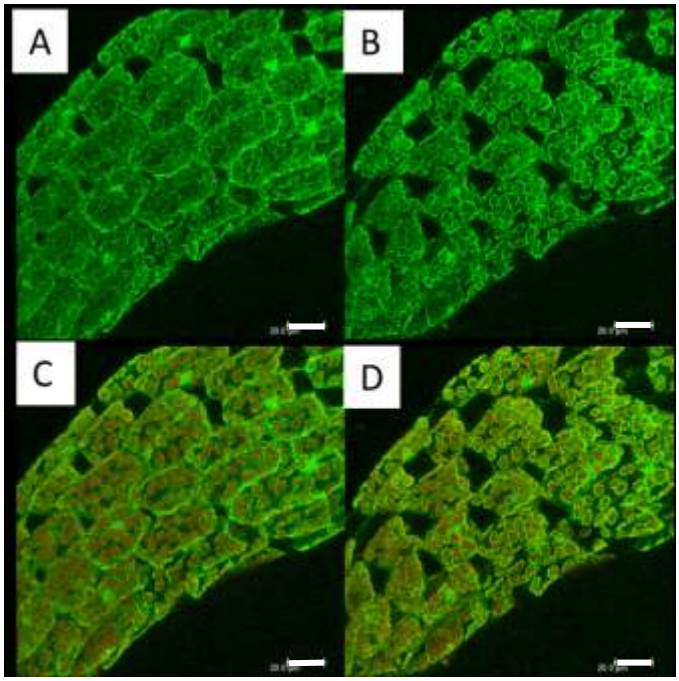

In a movie the change of the actin filaments according to the plasmolyticum shows that the protoplast retreats and the actin filaments retract and forms circles around the chloroplasts and accumulate around them. In fig. 154 A and C only mild plasmolysis can be seen after 22 minutes nearly all the cells show a stage of plasmolysis in fig. 154 B and D. The movement of the actin filaments through plasmolysis is demonstrated in the time lapse movie 39.

Fig. 154: *P. patens* Life-act cell line leaflet cells in a Mannitol concentration of 0,8 M, Maximum projection of A) GFP channel at beginning of plasmolysis B) GFP channel after 22 minutes in the plasmolyticum C) overlay of GFP and chloroplast channel at beginning of plasmolysis D) overlay of GFP and chloroplast channel after 22 minutes in the plasmolyticum (scale bar 20 µm)

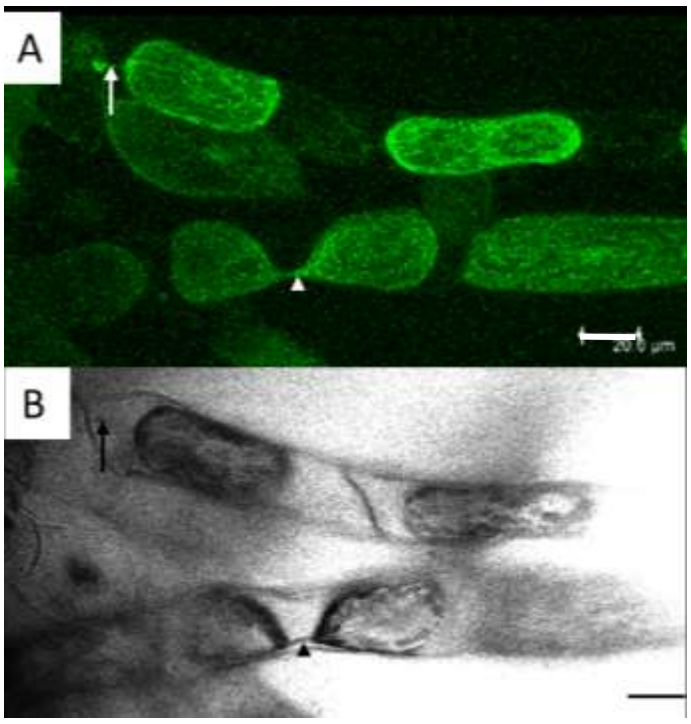

In the caulonema cells the actin shrinks with the protoplast but also forms Hechtian strands (fig. 155). Protoplasmic strands from the protoplast to cell wall (indicated by an arrow in fig. 155) and between sub-protoplast are also shown (marked with an arrowhead in fig. 155).

Fig. 155: *P. patens* Life-act cell line caulonema cells in a Mannitol concentration of 0,8 M, A) Maximum projection GFP channel; arrow: protoplasmic strand to cell wall; arrowhead: protoplasmic strand between two sub-protoplasts B) Transmission channel; arrow: protoplasmic strand to cell wall; arrowhead: protoplasmic strand between two sub-protoplasts (scale bar 20 µm)

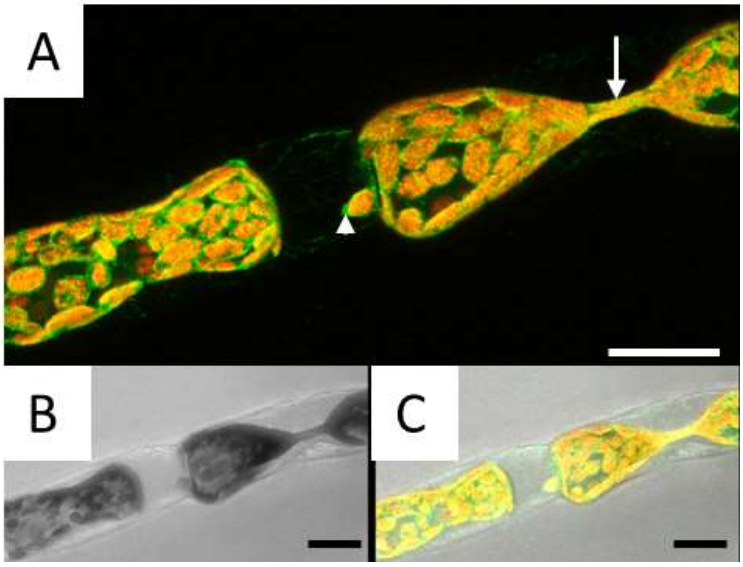

In fig. 156 a chloronema cell with the Hechtian reticulum to the cell wall to another cell is shown. Furthermore, a protoplasmic strand between two sub-protoplasts is present (marked with an arrow in fig. 156 A). In the left cell a single chloroplast is still attached to the cell wall through a protoplasmic strand and is surrounded by actin (indicated by an arrowhead in fig. 156 A). This cell is also shown in the 3D reconstructions movies 40 and 41.

Fig. 156: *P. patens* Life-act cell line chloronema cells in a Mannitol concentration of 0,8 M, Maximum projection A) overlay of GFP and chloroplast channel; arrow: protoplasmic strand; arrowhead: chloroplast encircled by actin in protoplasmic strand B) Transmission channel C) overlay of GFP, chloroplast and Transmission channel (scale bar 20 µm)

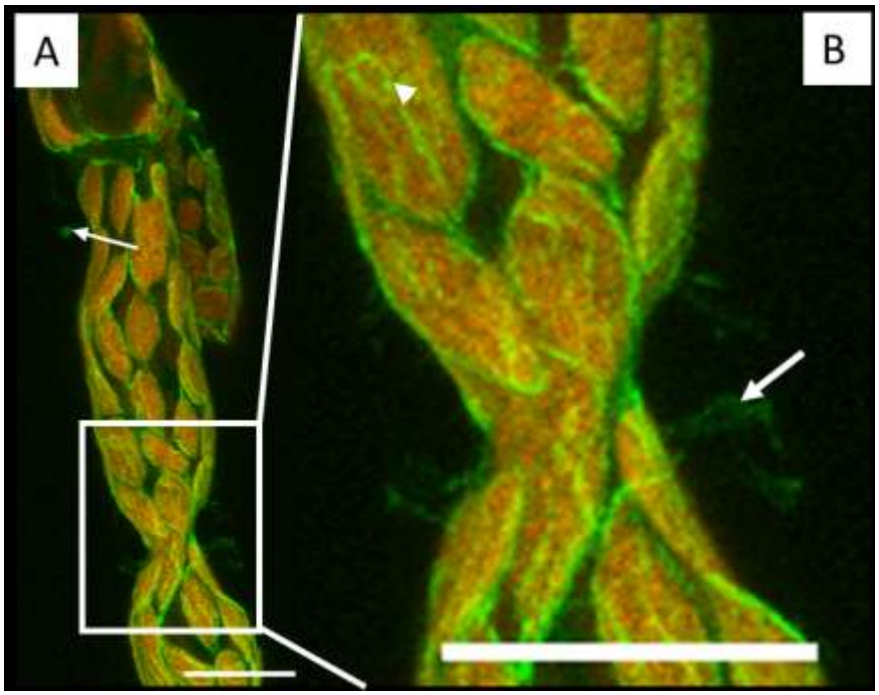

Fig. 157: *P. patens* Life-act cell line chloronema cell in a Mannitol concentration of 0,8 M, Maximum projection A) overlay of GFP and chloroplast channel; arrow: Hechtian reticulum B) higher magnification of the rectangle indicated part of A; arrow: Hechtian strand; arrowhead: actin ring structure around chloroplast (scale bar 20 µm)

The actin around the chloroplasts is shown in fig. 157 B, it formed ring structures around the chloroplasts (marked with an arrowhead). The protoplast has not fully detached from the neighbouring cell wall and at this point actin still has connections to the cell wall. Hechtian strands are also seen which are connecting the cell wall and the protoplast (marked with an arrow in fig 157 B). The Hechtian reticulum can be seen in fig. 157 A (marked with an arrow). Two 3D reconstruction movies (42 and 43) are showing this cell.

GFP-tubulin cell line

When the cells of the GFP-Tub cell line were treated with a high concentration (0,8 M) of Mannitol many Hechtian strands were seen in the leaflet cells. Furthermore, the tubulin showed ring like structures within the chloroplasts and encircled them. In the chloronema cells an accumulation of the tubulin was seen.

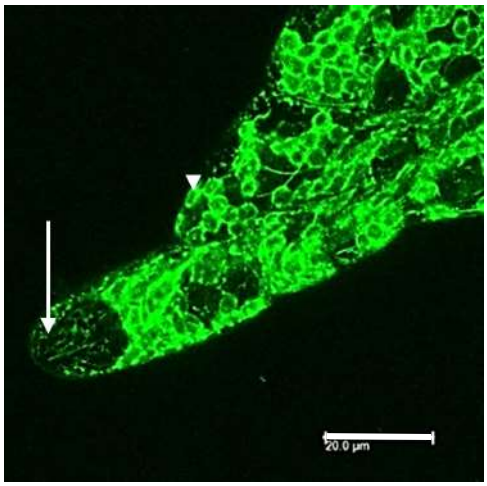

In the tip of the leaflet cell the Hechtian reticulum is very good expressed (marked with an arrow in fig 158 and shown in the movie 44). The microtubules in the cell have gathered around the chloroplasts (marked with an arrowhead) with just some microtubules left between the chloroplasts.

Fig. 158: *P. patens* GFP-Tub cell line leaflet cells in a Mannitol concentration of 0,8 M, Maximum projection GFP channel; arrow: Hechtian reticulum (scale bar 20 µm)

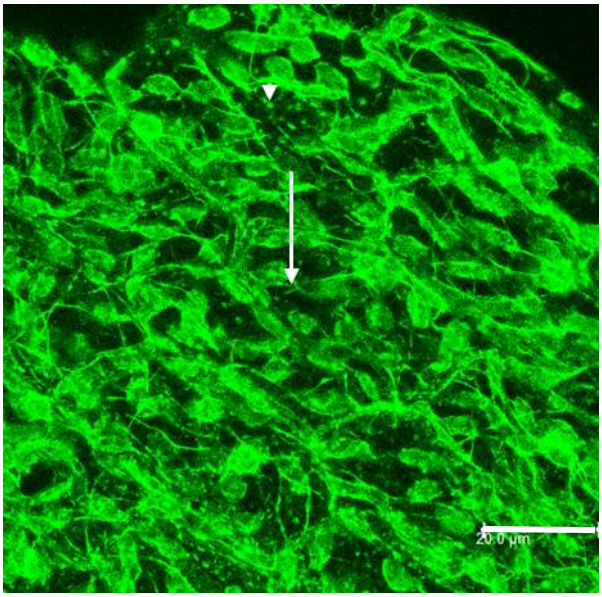

The leaflet in fig. 159 does show some globulary tubulin (marked with an arrowhead), some microtubules (indicated by an arrow) and an accumulation of tubulin around the chloroplast, but no plasmolysis of the cell. The degradation of the tubulin seems to be a response to the osmotic stress.

Fig. 159: *P. patens* GFP-Tub cell line leaflet cells in a Mannitol concentration of 0,8 M, Maximum projection GFP channel; arrow: tubule; arrowhead: G-Tubulin (scale bar 20 µm)

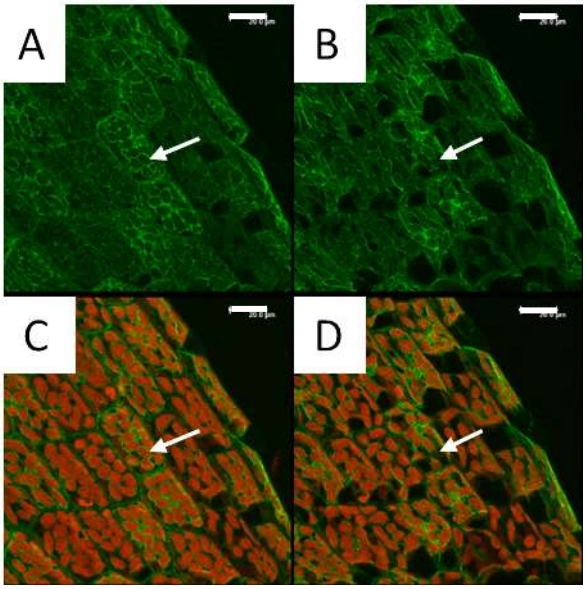

In a movie the change of the tubulin according to the plasmolyticum shows that the protoplast retreats and the tubulin retracts and also forms circles around the chloroplasts and accumulate around them. In the first pictures of fig. 160 A and C only mild plasmolysis can be seen after 32 minutes nearly all the cells show a stage of plasmolysis (fig. 160 B and D). The movement of the microtubules can be seen in the time lapse movie 45.

Fig. 160: *P. patens* GFP-Tub cell line leaflet cells in a Mannitol concentration of 0,8 M, Maximum projection of A) GFP channel at beginning of plasmolysis B) GFP channel after 32 minutes in the plasmolyticum C) overlay of GFP and chloroplast channel at beginning of plasmolysis D) overlay of GFP and chloroplast channel after 32 minutes in the plasmolyticum (scale bar 20 µm)

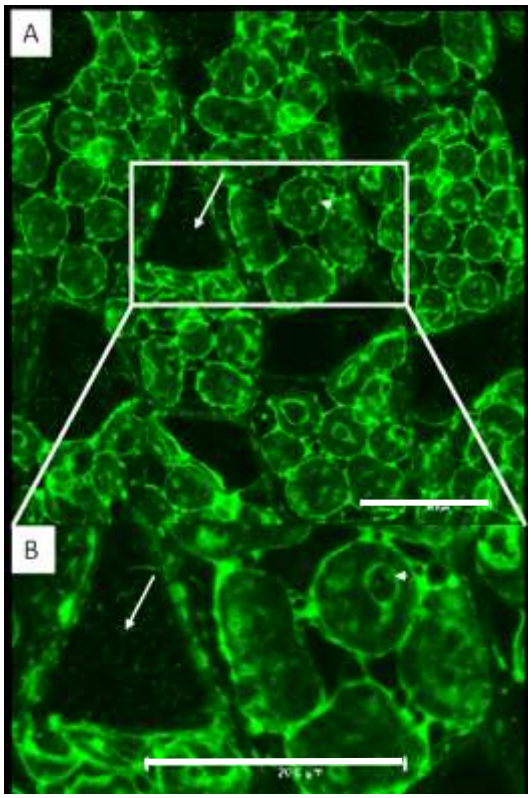

In the leaflet cells many Hechtian strands formed by the tubulin can be seen, which formed connections to the cell wall and the retracted protoplast (indicated by an arrow in fig. 161). The movie 46 demonstrates the 3D reconstruction of this cell and the microtubules at different angles. The tubulin also formed ring structures around the chloroplast and also within the chloroplasts (marked with an arrowhead in fig. 161).

Fig. 161: *P. patens* Life-act cell line leaflet cells in a Mannitol concentration of 0,8 M, Maximum projection A) GFP channel; arrow: Hechtian reticulum; arrowhead ring structure of Tubulin in chloroplast B) higher magnification of the rectangle indicated part of A; arrow: Hechtian strand; arrowhead: tubulin ring structure in chloroplast (scale bar 20 µm)

The chloronema cells showed in high concentrations of Mannitol more curved protoplasts and also parted protoplasts and the tubulin followed the form of the protoplast. The tubulin also accumulated together indicated by an arrow in fig. 162. Another plasmolysed cell is shown in the movie 47, there Hechtian strands are present.

Fig. 162: *P. patens* GFP-Tub cell line chloronema cells in a Mannitol concentration of 0,8 M, Maximum projection GFP and Transmission channel; arrow: accumulation of tubulin (scale bar 20 µm)

Myosin VIII cell line

The Myosin VIII cell line showed plasmolysis when treated with 0,8 M Mannitol, but the GFP-Myosin signal was detected both in leaflet cells and in protonema cells only in the chloroplasts and no specific fluorescence of the Myosin VIII was revealed (unspecific labelling).

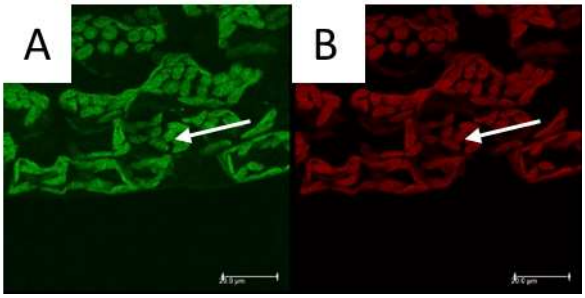

The leaflet cell shows plasmolysis in a Mannitol concentration of 0,8 M, but the Myosin VIII displays the same fluorescence as the chloroplasts (indicate by an arrow in fig. 163) and fluorescence of the cytosol and the cell wall.

Fig. 163: *P. patens* Myosin VIII cell line leaflet cells in a Mannitol concentration of 0,8 M, Maximum projection A) GFP channel; arrow: chloroplast B) chloroplast channel; arrow: chloroplast (scale bar 20 µm)

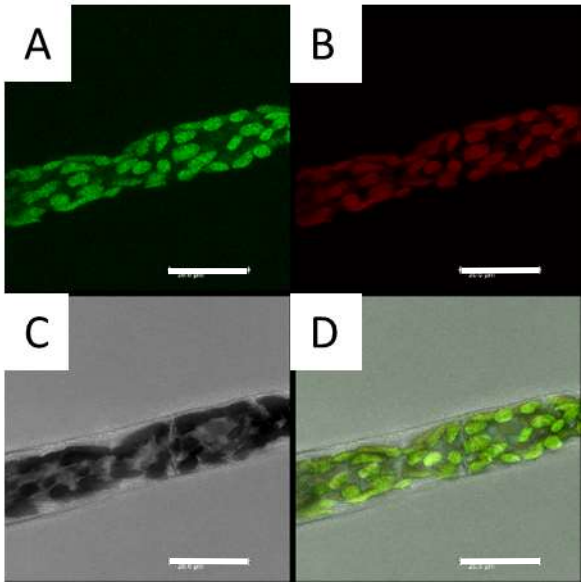

In fig. 164 the GFP of the Myosin VIII showed the same response to the plasmolyticum as in the leaflet cells. The GFP signal indicaeted only the chloroplasts, this can also be seen in the movie 48.

Fig. 164: *P. patens* Myosin VIII cell line chloronema cell in a Mannitol concentration of 0,8 M, Maximum projection A) GFP channel B) chloroplast channel C) Transmission channel D) overlay of GFP, chloroplast and Transmission channel (scale bar 20 µm)

4 Discussion

4. 1 Preservation of the cell lines

The preservation of the subcellular structures was most of the time very good, but not always. This was because the mosses lived under laboratory conditions and sometimes there was an invasion of fungi in the plate and this moss could not be used anymore. The preparation also sometimes killed parts of the protonema, when there was pressure on them during preparation with the tweezer or through the cover slide.

4. 2 Preservation of subcellular structures

Most of the cells showed the subcellular structures very well, with all the expected structures. The ER, Life-act and GFP-Tub cell line showed all the expected structures and were therefore more precisely investigated than the other cell lines. Through the other structures (ER, actin and tubulin) the location of the nucleus was shown. The cell wall was visualized in the Transmission mode. Chloroplast were seen in every cell and showed their autofluorescence in red. Mitochondria were not seen with the CLSM or the light microscope. Oil bodies were seen in the leaflet cells of *P. drummondii*.

The **ER** cell line showed the ER near the plasma membrane, the ER around the nucleus (the nuclear envelope) and its dynamic changing cisternae and tubules. The cisternae are not stable and change their shape and size, also 'holes' within the cisternae can be seen in higher magnification. The ER showed a network through the cell with connections to the chloroplasts. The ER looked like a sheath on the tip of a protonema cell.

A fine network of **actin filaments** was seen in the leaflets of the Life-act cell line, it was seen between the chloroplasts and around the nucleus. The cell cortex near the plasma membrane contained actin in the leaflet and protonema cells. In the chloronema cells, some actin filaments were spanning through the cell and were seen around the chloroplasts. The actin filaments were mostly found near the cell wall, this was shown in a 3D reconstruction.

In the GFP-Tub cell line, the **tubulin** is making ring structures in the leaflets, this were possibly microtubules in cross section. In the chloronema cells, the tubulin encloses the chloroplasts. Furthermore, the tubulin was detected near the nucleus. The microtubules made by the tubulin were only at the periphery of the cell, so near the cell wall and not so much in the interior of the cell. Tubulin is essential for cell division and is present in the spindle apparatus (Plattner and Hentschel 2017).

With the confocal microscope it was not easy to see specific fluorescence of the **Myosin VIII**, but in other studies it was shown (Vidali et al. 2009). This protein can be seen in close vicinity to the plasma and sometimes surrounding the chloroplasts partly or the whole chloroplast. It should be detectable in newly generated protonema cells near the cell wall (Wu and Bezanilla 2014). Maybe because of the higher gain there was too much noise to detect specifically the fluorescence of the Myosin VIII. But in the conventional fluorescence microscope there could be seen some differences. There was an accumulation of the Myosin VIII unspecific labelled GFP in the vacuole and near the cell wall, this could be because the plant wants to get rid of it and accumulates it there. Maybe the plant cannot

recognize the protein and thinks it is harmful and tries to put it away, like toxic compounds or foreign proteins they are stored in the vacuole and later degraded.

The **Reticulon and Calnexin** cell did not show any fluorescence of the expected structures, in *A. thaliana* leaf epidermal cells Calnexin resembled the cortical ER (Liu et al. 2017) and Reticulon in leaf epidermal cells of *Nicotiana tabacum* (Tolley et al. 2008) and *A. thaliana* (Tolley et al. 2010) showed ER tubules. A signal was found near the plasma membrane and in the cytoplasm and sometimes showed the same fluorescence as the chloroplasts. They expressed the GFP in parts of the chloroplast, so this could mean the GFP was integrated in the chloroplast DNA and not the nucleus, but more likely it was just unspecific labelling. In one picture also, an accumulation in the cytoplasm can be seen. This could mean that the Clock promoters in the cytoplasm were shown. Maybe the cell line cannot express anymore the GFP of Reticulon and Calnexin, because the GFP is not anymore bound to the protein. Another possibility would be that the protein, which was taken from *A. thaliana*, and was incorporated in *P. patens* through a vector, is not the same protein for both species. *A. thaliana* and *P. patens* have some common Reticulons, but this one in particular is not found (Blast) in *P. patens* so far. Maybe the protein got lost during evolution, because it was not needed in *P. patens* and was invented another time in *A. thaliana*. The plant degrades it because it cannot be used, or it is seen as poisonous to them.

4. 3 Subcellular structures of *P. patens* and vascular plants

In vascular plants the **ER** forms a three-dimensional network with a connection to the nucleus and building cisternae and tubules (Staehelin 1997), this was also seen in *P. patens*. The ER is known to show a network in the cells and the differentiation between cisternae and tubules (Goyal and Blackstone 2013). The Reticulon and Calnexin cell lines should have shown the same structure as the ER. This was shown in other studies for Reticulon, tubules of ER in leaf epidermal cells, in *Nicotiana tabacum* (Tolley et al. 2008) and in *A. thaliana* (Tolley et al. 2010); and in animals and yeast (Nziengui and Schoefs 2009). For Calnexin it was seen in *A. thaliana* leaf epidermal cells, which showed a network of tubules *(Liu et al. 2017)*.

In pollen tubes from *Lilium formosanum* and *Nicotiana tabacum* a cortical mesh-work of **actin** and a network around chloroplasts (Vidali et al. 2009), the similar structures were seen in the protonemata of *P. patens*. In tobacco guard cells, the actin did not form such network structures, they looked more directed (Yu et al. 2018), in comparison in leaflet cells of *P. patens* a ER network was seen.

Similar structures of **microtubules** as in protonema cells were seen in (outgrowing) root hairs of *A. thaliana.* There the cortical microtubules form a longitudinal or helical structure. In *A. thaliana* the trichoblasts and atrichoblasts have transversely oriented microtubules, during root hair outgrowth the trichoblasts disorganize themselves (van Bruaene et al. 2004). In leave cells of *A. thaliana* the microtubules are grouped together and ran parallel to each other, in comparison in leaflet cells of *P. patens* the microtubules look more netlike. The guard cells between the leave cells showed radial oriented microtubules (Ueda et al. 1999).

4. 4 Growth experiment: different increase in biomass

The difference in growth between 3M and Parafilm could be, because in the 3M tape the mosses can get better access to air without being affected of fungi and bacteria. But after 3 weeks sometimes an infection with fungi or bacteria occurs. For longer preservation of the cell lines the Parafilm would be better. The GFP cell lines seem to have more issues, when growing so they cannot invest all their energy in growth. All of them grow much better in 3M tape dishes, for the mosses its seems very important to have enough access to oxygen. Reticulon, Calnexin and Myosin VIII cell lines grow better in petri dishes enclosed with 3M tape. These three grow better than the control, the other GFP cell lines have less increase in mass than the control. The other lineages probably have to invest more of their energy in developing the GFP proteins, but Calnexin, Myosin VIII and Reticulon did not express the GFP.

4. 5 Labelling protocols and possible improvements

To get rid of the dye, so it does not show in the background, it helped to take a new slide after staining. When using buffers or solution for permeabilization to label the specimen with a fluorescent dye, it can be good to test the concentrations and buffers first alone before mixing them. Because than just the interaction of the buffer with the object can be observed and possible problems can be detected.

4. 6 Specific labelling

For staining the subcellular structures three dyes were used, two styryl dyes to label the plasma membrane and Rhodamine phalloidin to label the Actin filaments.

styryl dyes

Both of the styryl dyes **FM 1-43 and FM4-64** stained the plasma membrane and were most of the time able to label the vesicles, because endocytosis takes place after a while and then the vesicles became visible. The ER cell line showed all the plasma membranes like the styryl dyes were able to. Through the double labelling with GFP-ER and the styryl dyes it was possible to distinguish between the cell wall and plasma membrane in ER cell line. For staining of the plasma membrane in mosses, both dyes are equally staining the plasma membrane. When the examination is only looking for vesicle trafficking both dyes can be used. Between 30 minutes and an hour after application the styryl dyed FM1-43 showed the most vesicles. For the styryl dye FM4-64 30 minutes are better, but also after about 2 hours sometimes vesicles were seen. In this study the best way to show the ER was the GFP-marked cell line, because it was able to show the cisternae and tubules of the ER and most of the time the ER around the nucleus.

In human and mouse cells it was reported that the fluorescent dye FM4-64 was able by a spectral shift of the fluorescent to reveal a distinct microenvironment within the nuclear envelope (NE) in living cells (Zal et al. 2006).

The dyes were mostly used to investigate Endo-Exocytosis in plants cells. After some time, the vesicles seem to disappear, this is because stained secretory granules or vesicles

undergo exocytosis in a dye-free medium, due to concentration gradient, the FM1-43 molecules dissociate from the membrane and lose their fluorescence (Amaral et al. 2011).

For selectively staining the endoplasmic reticulum the ER-Tracker Blue-White DPX dye (www.thermofischer.com) could be a good way, it is photostable and can be used invitrogen, its excitation is at ~374 nm and exhibits an emission between 430 and 640 nm. Maybe this dye could show better the tubes and sheets of the ER, but this dye is not usable for the CLSM from Leica TCS SP5 DM-6000 CS, because its excitation wavelength is too low.

For staining all the membranes in the mosses, the DIOC would be the best way and a comparison with GFP labelled cell lines would be possible too.

Comparison of the styryl dyes labelling in other mosses

In *P. drummondii* even a plasmodesmata of the caulonema cell was recognizably labelled by the dye. There some open parts can be seen, which can be interpreted as some pores of the cell wall for communicating with the other cells. Or it could be that vesicles have accumulated there. In *M. elongata* the FM1-43 dye stained some netlike structures in the leaflets and in the chloronema also some tubulary structures. Some tiny tubulary structures were sometimes seen when labelling with the styryl dye FM4-64 in the protonema of the ER-GFP cell line, *M. elongata* and *P. drummondii.* It seemed like the FM1-43 and the FM4-64 were able to show some tubules of the ER in *M. elongata*. The stain was applied for the same time like for *P. patens* and the pictures were taken about the same times as for *P. patens*.

Rhodamine phalloidin, membrane permeabilization and buffers

The Rhodamine phalloidin is not able to penetrate the plasma membrane without disrupting it first so a membrane permeabilization is necessary. Furthermore, the plants need buffers to cope with the permeabilization.

It was shown that actin filaments in the onion cell could be stained (Invitrogen) with **Rhodamine phalloidin** and show the same configuration as a GFP-labelled cell, but the cells were fixed with formaldehyde, before staining (Umezu et al. 2011). Also, in the protocol for staining of actin filaments from the website of ThermoFischer (www.thermofischer.at) and other labelling protocols (Chazotte 2010) a fixation of the probe is recommended. Either the probe can be fixated with formaldehyde before staining or fixated simultaneously with permeabilization and staining with a fluorescent phallotoxin.

Unfortunately, not all of the dyes worked like expected, maybe because they were too old, or they could not enter the cells properly. In the onion the dye could enter the cells, but the dye did not bind to actin filaments, but was seen in the vesicles in plasma strings and in the cell wall. Or more a more sensible explanation would be that due to unspecific labelling of actin, because of its G and F-actin, the dye could not bind, and the stain stayed in the plasma in the vesicles.

But we wanted to stain the actin filaments in still living cells, in a further study it would be good to fix the cells before staining them.

The Rhodamine phalloidin needs **NP-40** as a detergent to **permeabilize** the cell walls, so that the dye can enter the cell. But the moss cells died when the concentration of it was too high (0,01%). The chloroplast degenerated, and they showed Brownian movement and coagulated plasma. With a lower concentration (0,01%) the mosses had no problem and this concentration was then used for labelling. The **buffers** should help the cells, so they are not destroyed so easily. For *P. patens* the PBS buffer worked the best. In the control with the PBS buffer, a low concentration of NP40 (0,01%) and the Rhodamine phalloidin showed in the chloronema an accumulation of the dye outside. Maybe the concentration of the NP40 was too low, so the plasma membrane could not be penetrated by the dye. The dye could enter the onion cells, the dye was seen in the vesicles, but it did not label the actin filaments.

4. 7 Osmotic stress – plasmolysis

Plasmolysis is the reaction of the plant to osmotic stress. When the osmotic value of the outside of the cell changes the plant cell responds to it, because its membranes are semipermeable. A plant cell plasmolyses when the outer medium of the cell is hypertonic, then water leaves the cell, this causes the protoplast to detach from the cell wall. This process is reversible, when the outer medium is hypotonic, the cell deplasmolyses. There are many forms of plasmolysis e.g. cap, concave, convex plasmolysis in plant cells. In mosses concave plasmolysis and in *Hookeria lucens* Zytorrhyse can be seen, concave plasmolysis was seen for the mosses in this study.

Some mosses started to plasmolyse at a concentration of 0,4 M Mannitol, but all of the mosses showed full plasmolysis at a concentration of 0,8 M Mannitol. The cells showed the detachment of the plasma membrane from the cell wall.

“Donut” shaped chloroplasts were sometimes seen in the cells, in ER and GFP-Tub cells. The ER and tubulin formed ring like structures within the cells, the tubulin could be the reason for the “donut” shape of the chloroplasts and the ER follows the shape. It was shown that FtsZ, an ancestral tubulin, plays a role in plastid shape and division in *P. patens (Kiessling et al. 2000)*. Smaller rings were seen near chloroplast in the Life-act cell line, caused by actin filaments. But in non-plasmolysed cells of GFP-Tub similar structures for the chloroplasts were seen, as the chloroplasts were folding in.

ER, Life-act and GFP-Tub cell lines showed Hechtian strands and protoplasmic strands fluorescently labelled. In the protoplasmic strands sometimes chloroplasts were incorporated. The tubulin and actin filaments formed rings around the chloroplasts and enclosed them. The microtubules in chloronema cells got wavier in their structure, but still enclosed the chloroplasts within them. In hypocotyl cells of *A. thaliana* the microtubules got as well wavier and formed thick bundles (Lang et al. 2014). Plasmolysis affects the subcellular structures, the actin filaments make more circles and enclose the chloroplasts, maybe to “protect” them. In *A. thaliana* the actin filaments followed the shape of the plasma membrane and the network of actin filaments accommodated to the new cell size (Lang et al. 2014). The tubulin does the same but makes in leaflets bigger circles within the chloroplasts. It was shown that plant phytohormones, environmental stresses (osmotic changes) and differentiation during growth can affect the microtubules (Hashimoto 2015).

Hechtian strands (Hecht K. 1912) were found in all the different cell types of the ER, Life-act and GFP-Tub cell lines, not always in all the same concentrations, but seen throughout all the experiments. More Hechtian strands were seen in leaflet cells in higher

concentrations of 0,8 M Mannitol. This Hechtian strands are the anchors for the cell (Lang et al. 2004) and try to keep connections to the cell wall. It could be possible that the cells also communicate through Hechtian strands, because neighboring cells almost every time had still a Hechtian strand to connect. The microtubules are maybe used to stabilize the Hechtian strands. It was shown that in Hechtian strands microtubules and actin filaments exist (Lang-Pauluzzi and Gunning 2000; Lang et al. 2014), but they do not build the Hechtian strands (Lang-Pauluzzi 2000), they are more likely needed later for the stabilization.

The only cell lines which did show the cell wall and not the plasma membrane were **Myosin VIII, Calnexin and Reticulon**. These cells did show plasmolysis, but the GFP signal did not show any structures as in the un-plasmolysed cells.

Osmotic change of ER cisternae

The majority of the cells showed an increase in size for the cisternae and every cell showed a decrease in number of the cisternae. The movement of the scanning area in the first leaflet experiment could explain why the cells four and five did have a loss in area of the cisternae and not an increase like the others. Because in the second experiment all cells showed an increase in area of cisternae. This experiment showed that the ER changes during plasmolysis, it retreats from the cell wall and the cisternae aggregate possibly due to the loss of space in the cell. Similar cisternalization was already shown in plasmolysed cells (Cheng et al. 2017).

5 Websites

P. drummondii

http://www.swissbryophytes.ch/index.php/de/beschreibung?taxon_id=nism-1907

M. elongata

http://www.swissbryophytes.ch/index.php/de/verbreitung?taxon_id=nism-1681

FM™ 4-64 Dye (*N*-(3-Triethylammoniumpropyl)-4-(6-(4-(Diethylamino) Phenyl) Hexatrienyl) Pyridinium Dibromide):

https://www.thermofisher.com/order/catalog/product/T13320

FM™ 1-43 Dye (*N*-(3-Triethylammoniumpropyl)-4-(4-(Dibutylamino) Styryl) Pyridinium Dibromide): https://www.thermofisher.com/order/catalog/product/T35356

Rhodamine Phalloidin:

https://www.thermofisher.com/order/catalog/product/R415

Nonident P40 Substitute:
https://www.sigmaaldrich.com/catalog/product/roche/11332473001?lang=de&region=AT&gclid=EAIaIQobChMI_fLf1tzF2QIVEbobCh0G7wvGEAAYASAAEgKTHfD_BwE

Confocal microscopy

http://www.univie.ac.at/mikroskopie/3_fluoreszenz/clsm/1_einleitung.htm

http://www.univie.ac.at/mikroskopie/3_fluoreszenz/clsm/3e_noisred.htm

6 References

Amaral E, Guatimosim S, Guatimosim C (2011) Using the fluorescent styryl dye FM1-43 to visualize synaptic vesicles exocytosis and endocytosis in motor nerve terminals. Methods in molecular biology (Clifton, N.J.) 689:137–148

Bezanilla M, Horton AC, Sevener HC, Quatrano RS (2003) Phylogenetic analysis of new plant myosin sequences. Journal of molecular evolution 57:229–239

Bolsover SR (2004) Cell biology: A short course, 2nd edn. Wiley-Interscience, Hoboken, NJ

Buer CS, Weathers PJ, Swartzlander GA (2000) Changes in Hechtian Strands in Cold-Hardened Cells Measured by Optical Microsurgery. Plant Physiol. 122:1365–1378

Chazotte B (2010) Labeling cytoskeletal F-actin with rhodamine phalloidin or fluorescein phalloidin for imaging. Cold Spring Harbor protocols 2010:pdb.prot4947

Chen H-W, Persson S, Grebe M, McFarlane HE (2018) Cellulose synthesis during cell plate assembly. Physiologia plantarum 164:17–26

Cheng X, Lang I, Adeniji OS, Griffing L (2017) Plasmolysis-deplasmolysis causes changes in endoplasmic reticulum form, movement, flow, and cytoskeletal association. Journal of experimental botany 68:4075–4087

Cleary AL (2001) Plasma membrane-cell wall connections: Roles in mitosis and cytokinesis revealed by plasmolysis of Tradescantia virginiana leaf epidermal cells. Protoplasma 215:21–34

Cove D (2005) The moss Physcomitrella patens. Annual review of genetics 39:339–358

Deeks MJ, Hussey PJ (2001) Plant Actin Biology. In: Ltd JW&S (ed) eLS. John Wiley & Sons, Ltd, Chichester, UK, pp 1–9

Di Sano F, Fazi B, Tufi R, Nardacci R, Piacentini M (2007) Reticulon-1C acts as a molecular switch between endoplasmic reticulum stress and genotoxic cell death pathway in human neuroblastoma cells. Journal of neurochemistry 102:345–353

Ehtesham NZ, Phan TN, Gaikwad A, Sopory SK, Tuteja N (1999) Calnexin from Pisum sativum: cloning of the cDNA and characterization of the encoded protein. DNA and cell biology 18:853–862

Frahm J-P, Frey W, Döring J (2004) Moosflora, 4th edn. Ulmer, Stuttgart

Goyal U, Blackstone C (2013) Untangling the web: mechanisms underlying ER network formation. Biochimica et biophysica acta 1833:2492–2498

Hamada T, Ueda H, Kawase T, Hara-Nishimura I (2014) Microtubules contribute to tubule elongation and anchoring of endoplasmic reticulum, resulting in high network complexity in Arabidopsis. Plant physiology 166:1869–1876

Hashimoto T (2015) Microtubules in plants. The arabidopsis book 13:e0179

Hecht K. (1912) Studien über Vorgänge der Plasmolyse. Beiträge zur Biologie der Pflanze:133–189

Heß D (2004) Allgemeine Botanik, 1st edn. Ulmer, Stuttgart

Hodge T, Cope MJ (2000) A myosin family tree. Journal of cell science 113 Pt 19:3353–3354

Hu J, Shibata Y, Voss C, Shemesh T, Li Z, Coughlin M, Kozlov MM, Rapoport TA, Prinz WA (2008) Membrane proteins of the endoplasmic reticulum induce high-curvature tubules. Science (New York, N.Y.) 319:1247–1250

Kiessling J, Kruse S, Rensing SA, Harter K, Decker EL, Reski R (2000) Visualization of a Cytoskeleton-like Ftsz Network in Chloroplasts. The Journal of Cell Biology 151:945–950

Lang I, Barton DA, Overall RL (2004) Membrane-wall attachments in plasmolysed plant cells. Protoplasma 224:231–243

Lang I, Sassmann S, Schmidt B, Komis G (2014) Plasmolysis: Loss of Turgor and Beyond. Plants (Basel, Switzerland) 3:583–593

Lang-Pauluzzi I (2000) The behaviour of the plasma membrane during plasmolysis: a study by UV microscopy. J Microsc 198:188–198

Lang-Pauluzzi I, Gunning BES (2000) A plasmolytic cycle: The fate of cytoskeletal elements. Protoplasma 212:174–185

Leach MR, Williams D. B. (2000 - 2013) Madame Curie Bioscience Database: Calnexin and Calreticulin, Molecular Chaperones of the Endoplasmic Reticulum. Landes Bioscience, Austin (TX)

Liu DYT, Smith PMC, Barton DA, Day DA, Overall RL (2017) Characterisation of Arabidopsis calnexin 1 and calnexin 2 in the endoplasmic reticulum and at plasmodesmata. Protoplasma 254:125–136

Mueller SJ, Reski R (2015) Mitochondrial Dynamics and the ER: The Plant Perspective. Frontiers in cell and developmental biology 3:78

Nabi IR (2011) Cellular Domains. John Wiley & Sons, Inc, Hoboken, NJ, USA

Niehl A, Amari K, Gereige D, Brandner K, Mély Y, Heinlein M (2012) Control of Tobacco mosaic virus movement protein fate by CELL-DIVISION-CYCLE protein48. Plant physiology 160:2093–2108

Nziengui H, Schoefs B (2009) Functions of reticulons in plants: What we can learn from animals and yeasts. Cellular and molecular life sciences : CMLS 66:584–595

Oertle T, Schwab ME (2003) Nogo and its paRTNers. Trends in Cell Biology 13:187–194

Oparka KJ (1994) Plasmolysis: new insights into an old process. New Phytol 126:571–591

Ortiz-Ramírez C, Hernandez-Coronado M, Thamm A, Catarino B, Wang M, Dolan L, Feijó JA, Becker JD (2016) A Transcriptome Atlas of Physcomitrella patens Provides Insights into the Evolution and Development of Land Plants. Molecular plant 9:205–220

Pierce BA (2006) Genetics: A conceptual approach, 2nd edn. Freeman and Company, New York, NY

Plattner H, Hentschel J (2017) Zellbiologie, 5th edn. Georg Thieme Verlag, Stuttgart, New York

Quatrano RS, McDaniel SF, Khandelwal A, Perroud P-F, Cove DJ (2007) Physcomitrella patens: mosses enter the genomic age. Current opinion in plant biology 10:182–189

Rensing SA, Ick J, Fawcett JA, Lang D, Zimmer A, van de Peer Y, Reski R (2007) An ancient genome duplication contributed to the abundance of metabolic genes in the moss Physcomitrella patens. BMC evolutionary biology 7:130

Schaefer DG, Zrÿd JP (1997) Efficient gene targeting in the moss Physcomitrella patens. The Plant journal : for cell and molecular biology 11:1195–1206

Sparkes I, Hawes C, Frigerio L (2011) FrontiERs: movers and shapers of the higher plant cortical endoplasmic reticulum. Current opinion in plant biology 14:658–665

Staehelin LA (1997) The plant ER: a dynamic organelle composed of a large number of discrete functional domains. The Plant journal : for cell and molecular biology 11:1151–1165

Terasawa K, Odahara M, Kabeya Y, Kikugawa T, Sekine Y, Fujiwara M, Sato N (2007) The mitochondrial genome of the moss Physcomitrella patens sheds new light on mitochondrial evolution in land plants. Molecular biology and evolution 24:699–709

Tolley N, Sparkes I, Craddock CP, Eastmond PJ, Runions J, Hawes C, Frigerio L (2010) Transmembrane domain length is responsible for the ability of a plant reticulon to shape endoplasmic reticulum tubules in vivo. The Plant journal : for cell and molecular biology 64:411–418

Tolley N, Sparkes IA, Hunter PR, Craddock CP, Nuttall J, Roberts LM, Hawes C, Pedrazzini E, Frigerio L (2008) Overexpression of a plant reticulon remodels the lumen of the cortical endoplasmic reticulum but does not perturb protein transport. Traffic (Copenhagen, Denmark) 9:94–102

Ueda K, Matsuyama T, Hashimoto T (1999) Visualization of microtubules in living cells of transgenicArabidopsis thaliana. Protoplasma 206:201–206

Umezu N, Umeki N, Mitsui T, Kondo K, Maruta S (2011) Characterization of a novel rice kinesin O12 with a calponin homology domain. Journal of biochemistry 149:91–101

van Bruaene N, Joss G, van Oostveldt P (2004) Reorganization and in vivo dynamics of microtubules during Arabidopsis root hair development. Plant Physiol. 136:3905–3919

Vidali L, Rounds CM, Hepler PK, Bezanilla M (2009) Lifeact-mEGFP reveals a dynamic apical F-actin network in tip growing plant cells. PloS one 4:e5744

Wang D, Weaver ND, Kesarwani M, Dong X (2005) Induction of protein secretory pathway is required for systemic acquired resistance. Science (New York, N.Y.) 308:1036–1040

Waterman-Storer CM, Salmon ED (1998) Endoplasmic reticulum membrane tubules are distributed by microtubules in living cells using three distinct mechanisms. Current biology : CB 8:798–806

Wu S-Z, Bezanilla M (2014) Myosin VIII associates with microtubule ends and together with actin plays a role in guiding plant cell division. eLife 3

Wu S-Z, Ritchie JA, Pan A-H, Quatrano RS, Bezanilla M (2011) Myosin VIII regulates protonemal patterning and developmental timing in the moss Physcomitrella patens. Molecular plant 4:909–921

Yu Q, Ren J-J, Kong L-J, Wang X-L (2018) Actin filaments regulate the adhesion between the plasma membrane and the cell wall of tobacco guard cells. Protoplasma 255:235–245

Zal T, Zal MA, Lotz C, Goergen CJ, Gascoigne NRJ (2006) Spectral shift of fluorescent dye FM4-64 reveals distinct microenvironment of nuclear envelope in living cells. Traffic (Copenhagen, Denmark) 7:1607–1613

Appendix

Supplementary data 1: 3D reconstructions and time lapse movies

1: maximum projection 3D reconstruction ER cell line bud cell GFP channel

2: maximum projection 3D reconstruction ER cell line leaflet GFP, chloroplast and Transmission channel

3: time lapse of ER movement ER cell line leaflet GFP, chloroplast and Transmission channel

4: average projection 3D reconstruction ER cell line chloronema GFP, chloroplast and Transmission channel

5: movie of a Z-scan through cell ER cell line chloronema GFP channel

6: maximum projection 3D reconstruction ER cell line caulonema GFP channel

7: maximum projection 3D reconstruction Life-act cell line leaflet and protonema GFP channel

8: maximum projection 3D reconstruction Life-act cell line leaflet GFP channel

9: maximum projection 3D reconstruction GFP-Tub cell line chloronema GFP channel

10: maximum projection 3D reconstruction GFP-Tub cell line chloronema at branching point GFP channel

11: maximum projection 3D reconstruction Myosin VIII cell line leaflet GFP, chloroplast, Transmission channel

12: maximum projection 3D reconstruction ER cell line chloronema FM4-64 channel labelled with FM4-64

13: maximum projection 3D reconstruction ER cell line chloronema FM4-64 channel labelled with FM4-64

14: maximum projection 3D reconstruction *M. elongata* cell line caulonema FM4-64 channel labelled with FM4-64

15: maximum projection 3D reconstruction *P. drummondii* cell line leaflet FM4-64, chloroplast, Transmission channel labelled with FM4-64

16: maximum projection 3D reconstruction *P. drummondii* cell line developing chloronema cell FM4-64, chloroplast, Transmission channel labelled with FM4-64

17: maximum projection 3D reconstruction *P. patens control* cell line leaflet FM1-43, chloroplast, Transmission channel labelled with FM1-43

18: maximum projection 3D reconstruction ER cell line chloronema GFP, FM1-43, chloroplast and Transmission channel plasmolysis with 0,4 M Mannitol

19: maximum projection 3D reconstruction *P. drummondii* cell line caulonema FM1-43 and chloroplast channel labelled with FM1-43

20: maximum projection 3D reconstruction *P. drummondii* cell line caulonema plasmodesmata FM1-43 and Transmission channel labelled with FM1-43

21: time lapse of vesicle movement *A. cepa* inner epidermis PBS RHPH conventional fluorescence (Rhodamine in red) labelled with PBS Rhodamine phalloidin

22: time lapse of vesicle movement *A. cepa* inner epidermis Rhodamine phalloidin channel labelled with PBS Rhodamine phalloidin

23: maximum projection 3D reconstruction ER cell line leaflet GFP channel plasmolysis with 0,4 M Mannitol

24: maximum projection 3D reconstruction GFP-Tub cell line chloronema GFP, chloroplast and Transmission channel plasmolysis with 0,4 M Mannitol

25: maximum projection 3D reconstruction GFP-Tub cell line chloronema GFP channel plasmolysis with 0,4 M Mannitol

26: maximum projection 3D reconstruction GFP-Tub cell line chloronema GFP channel plasmolysis with 0,4 M Mannitol

27: maximum projection 3D reconstruction GFP-Tub cell line chloronema GFP, chloroplast and Transmission channel plasmolysis with 0,4 M Mannitol

28: maximum projection 3D reconstruction Reticulon cell line leaflet GFP channel plasmolysis with 0,4 M Mannitol

29: maximum projection 3D reconstruction Calnexin cell line leaflet GFP, chloroplast and Transmission channel plasmolysis with 0,4 M Mannitol

30: maximum projection 3D reconstruction ER cell line new developing chloronema cell at a branching point GFP channel plasmolysis with 0,5 M Mannitol

31: maximum projection 3D reconstruction ER cell line chloronema cell at a branching point GFP, chloroplast and Transmission channel plasmolysis with 0,5 M Mannitol

32: maximum projection 3D reconstruction GFP-Tub cell line leaflet GFP channel plasmolysis with 0,5 M Mannitol

33: maximum projection 3D reconstruction GFP-Tub cell line chloronema cell at a branching point GFP, chloroplast and Transmission channel plasmolysis with 0,5 M Mannitol

34: maximum projection 3D reconstruction ER cell line leaflet GFP, chloroplast and Transmission channel plasmolysis with 0,6 M Mannitol

35: maximum projection 3D reconstruction ER cell line chloronema GFP channel plasmolysis with 0,8 M Mannitol

36: maximum projection 3D reconstruction ER cell line chloronema end cell GFP, chloroplast and Transmission channel plasmolysis with 0,8 M Mannitol

37: time lapse ER movement during plasmolysis ER cell line leaflet GFP, chloroplast, Transmission and overlay of all channels plasmolysis with 0,8 M Mannitol

38: maximum projection 3D reconstruction Life-act cell line leaflet GFP channel plasmolysis with 0,8 M Mannitol

39: time lapse actin movement during plasmolysis Life-act cell line leaflet GFP, chloroplast and overlay of all channels plasmolysis with 0,8 M Mannitol

40: maximum projection 3D reconstruction Life-act cell line chloronema GFP channel plasmolysis with 0,8 M Mannitol

41: maximum projection 3D reconstruction Life-act cell line chloronema GFP, chloroplast and Transmission channel plasmolysis with 0,8 M Mannitol

42: maximum projection 3D reconstruction Life-act cell line chloronema GFP channel plasmolysis with 0,8 M Mannitol

43: maximum projection 3D reconstruction Life-act cell line chloronema GFP, chloroplast and Transmission channel plasmolysis with 0,8 M Mannitol

44: maximum projection 3D reconstruction GFP-Tub cell line leaflet GFP channel plasmolysis with 0,8 M Mannitol

45: time lapse tubulin movement during plasmolysis GFP-Tub cell line leaflet GFP, chloroplast and overlay of all channels plasmolysis with 0,8 M Mannitol

46: maximum projection 3D reconstruction GFP-Tub cell line leaflet GFP channel plasmolysis with 0,8 M Mannitol

47: maximum projection 3D reconstruction GFP-Tub cell line caulonema GFP, chloroplast and Transmission channel plasmolysis with 0,8 M Mannitol

48: maximum projection 3D reconstruction Myosin VIII cell line leaflet GFP, chloroplast and Transmission channel plasmolysis with 0,8 M Mannitol

Supplementary Data 2: statistics of growth measurement

day 0	3M	Area	Control	ER	Calnexin	Reticulon	Life-act	GFP-Tub	Myosin VIII	Pohlia	Mielichhoferia
		1	8311	12353	7680	5978	4938	2244	10587	18546	7236
		2	3470	20762	4959	9021	3989	8020	2803	10845	15395
		3	4875	10756	11183	11364	5628	8051	9666	4619	3731
		4	3815	7788	6459	4320	4731	12771	8050	5350	5285
		5	5646	5217	10643	11139	12964	4750	8678	7976	4139
		6	8573	16327	13244	4856	8487	16100	5158	14851	2783
		7	11856	10669	9416	8385	10517	11518	10928	10323	5584
		8	12086	5151	4950	6926	10897	11610	1173	15714	5687
		9	11381	6587	11443	7790	7344	9221	19559	8990	4867
		Median	8311	10669	9416	7790	7344	9221	8678	10323	5285
		standard deviation	3271,488339	4964,78468	2836,9146	2369,37839	3002,15078	3974,91744	5071,20981	4471,46983	3508,163372
day22	3M	Area	Control	ER	Calnexin	Reticulon	Life-act	GFP-Tub	Myosin VIII	Pohlia	Mielichhoferia
		1	63676	86583	111774	58770	6279	64703	73145	205662	43473
		2	61819	91191	82860	81678	44448	50934	29478	74866	112488
		3	50612	84979	69846	113137	41777	70677	78158	27655	14109
		4	66384	71344	32205	84383	34185	102460	76381	84557	11175
		5	53198	67009	59139	52328	63473	44660	49207	65922	32960
		6	98150	80353	144858	55123	52531	69177	86272	89907	8419
		7	98072	83394	115845	77091	65480	67506	88212	59070	38026
		8	83893	63702	32382	58645	79455	63939	27155	187131	33331
		9	89544	66634	101342	60282	60343	73234	86877	76796	25360
		Median	66384	80353	82860	60282	52531	67506	76381	76796	32960
		standard deviation	17621,98998	9571,8187	36443,4303	18627,6637	20170,8201	15219,0781	23025,3907	56023,1196	29615,56567
		t-test Control/GFP		0,64818515	0,52273007	0,77326072	0,0215927	0,44495091	0,45688861	0,29678799	0,007571506
		t-test Control/GFP		65%	52%	77%	2%	44%	46%	30%	1%
day 0	Parafilm	Area	Control	ER	Calnexin	Reticulon	Life-act	GFP-Tub	Myosin VIII	Pohlia	Mielichhoferia
		1	14271	6733	4249	6217	10984	25272	7891	3487	2992
		2	9022	6866	3101	5013	15107	3075	5931	2961	2134
		3	9465	11928	1847	5679	7543	8478	3645	5229	6240
		4	10797	2637	7864	2257	10467	9212	4376	8208	3289
		5	8817	7484	6065	10022	6988	7213	6996	7828	2682
		6	6821	5643	2333	8681	3505	12263	5569	25887	10349
		7	7639	3095	4354	7308	16450	6314	13820	11116	7266
		8	7122	7984	7228	22593	2791	15216	13304	12881	11845
		9	17133	3853	5374	2986	3308	12667	10170	17734	
		Median	9022	6733	4354	6217	7543	9212	6996	8208	4764,5
		standard deviation	3269,904816	2718,32694	1981,57983	5709,88766	4767,36496	6095,95225	3496,2467	7002,0425	3480,480317
day22	Parafilm	Area	Control	ER	Calnexin	Reticulon	Life-act	GFP-Tub	Myosin VIII	Pohlia	Mielichhoferia
		1	35463	15739	3657	32206	7372	53617	12854	9732	9985
		2	39656	26056	2426	26346	19402	23636	7633	7764	3605
		3	45571	51075	5584	40170	48087	59533	2904	19491	17941
		4	52754	16472	90122	30330	24268	19765	10996	10406	5347
		5	50278	39634	19304	34134	55494	38396	9108	25204	6432
		6	26479	28522	7675	16500	13895	50948	7402	78804	50822
		7	29246	2548	25463	36376	12523	71695	17163	30570	22243
		8	31370	30984	30911	68468	1526	45255	14584	36678	47380
		9	19645	23090	11310	2635	1292	37747	32323	56011	
							1092				
							3189				
		Median	35463	26056	11310	32206	12523	45255	10996	25204	13963
		standard deviation	10595,41679	13334,9131	25922,0653	16857,7119	17987,4753	15708,5014	7986,20496	22419,0081	17589,29146
		t-test Control/GFP		0,09543268	0,1618005	0,50594835	0,01056393	0,2641573	0,00013297	0,49362459	0,056284542
		t-test Control/GFP		10%	16%	51%	1%	26%	0%	49%	6%

Table 3: Statistics of growth measurement for 3M tape and Parafilm at day 0 and day 22: measured areas in pixel^2, median of areas and standard deviation; T-test values for significance of control (*P. patens*) to other cell

	cell lines with Parafilm		Control	ER	Calnexin	Reticulon	Life-act	GFP-Tub	Myosin VIII	*Mielichhoferia*	*Pohlia*
mean	area ratio	day 0	10120,78	6247,00	4712,78	7861,78	8571,44	11078,89	7966,89	5849,63	10592,33
		day 22	36718,00	26013,33	21828,00	31907,22	17103,64	44510,22	12774,11	20469,38	30517,78
		difference	26597,22	19766,33	17115,22	24045,44	8532,19	33431,33	4807,22	14619,75	19925,44
	percentage of area	day 0	100,00	100,00	100,00	100,00	100,00	100,00	100,00	100,00	100,00
		day 22	362,80	416,41	463,17	405,85	199,54	401,76	160,34	349,93	288,11
		difference	262,80	316,41	363,17	305,85	99,54	301,76	60,34	249,93	188,11
	multiplication of area		3,63	4,16	4,63	4,06	2,00	4,02	1,60	3,50	2,88
median	area ratio	day 0	9022,00	6733,00	4354,00	6217,00	7543,00	9212,00	6996,00	4764,50	8208,00
		day 22	35463,00	26056,00	11310,00	32206,00	12523,00	45255,00	10996,00	13963,00	25204,00
		difference	26441,00	19323,00	6956,00	25989,00	4980,00	36043,00	4000,00	9198,50	16996,00
	percentage of area	day 0	100,00	100,00	100,00	100,00	100,00	100,00	100,00	100,00	100,00
		day 22	393,07	386,99	259,76	518,03	166,02	491,26	157,18	293,06	307,07
		difference	293,07	286,99	159,76	418,03	66,02	391,26	57,18	193,06	207,07
	multiplication of area		3,93	3,87	2,60	5,18	1,66	4,91	1,57	2,93	3,07

Table 4: Statistics of growth measurement mean and median values for Parafilm: measured area ratio in pixel^2 of day 0 and day 22, difference of area ratio between day 0 and day 22; percentage of areas and their difference between day 0 and day 22, and multiplication factor for area after 22 days

	cell lines with 3M tape		Control	ER	Calnexin	Reticulon	Life-act	GFP-Tub	Myosin VIII	*Mielichhoferia*	*Pohlia*
mean	area ratio	day 0	7779,22	10623,33	8886,33	7753,22	7721,67	9365,00	8511,33	6078,56	10801,56
		day 22	73927,56	77243,22	83361,22	71270,78	49774,56	67476,67	66098,33	35482,33	96840,67
		difference	66148,33	66619,89	74474,89	63517,56	42052,89	58111,67	57587,00	29403,78	86039,11
	percentage of area	day 0	100,00	100,00	100,00	100,00	100,00	100,00	100,00	100,00	100,00
		day 22	950,32	727,11	938,08	919,24	644,61	720,52	776,59	583,73	896,54
		difference	850,32	627,11	838,08	819,24	544,61	620,52	676,59	483,73	796,54
	multiplication of area		9,50	7,27	9,38	9,19	6,45	7,21	7,77	5,84	8,97
median	area ratio	day 0	8311,00	10669,00	9416,00	7790,00	7344,00	9221,00	8678,00	5285,00	10323,00
		day 22	66384,00	80353,00	82860,00	60282,00	52531,00	67506,00	76381,00	32960,00	76796,00
		difference	58073,00	69684,00	73444,00	52492,00	45187,00	58285,00	67703,00	27675,00	66473,00
	percentage of area	day 0	100,00	100,00	100,00	100,00	100,00	100,00	100,00	100,00	100,00
		day 22	798,75	753,14	879,99	773,84	715,29	732,09	880,17	623,65	743,93
		difference	698,75	653,14	779,99	673,84	615,29	632,09	780,17	523,65	643,93
	multiplication of area		7,99	7,53	8,80	7,74	7,15	7,32	8,80	6,24	7,44

Table 5: Statistics of growth measurement mean and median values for 3M tape: measured area ratio in pixel^2 of day 0 and day 22, difference of area ratio between day 0 and day 22; percentage of areas and their difference between day 0 and day 22, and multiplication factor for area after 22 days

Supplementary Data 3: statistics of cisternae measurement

0 minutes	area	1	2	3	4	5	6	7
	1	19	27	16	176	36	83	98
	2	88	32	62	186	152	67	91
	3	69	46	16	39	182	29	201
	4	66	47	40	44	46	336	190
	5	24	21	16	65	32	57	20
	6	58	45	43	81	90	31	56
	7	44	61	27	18	33	44	75
	8	93	128	26	19	38	16	49
	9	17	92	158	42	25	25	69
	10	20	51	54	30	26	18	16
	11	53	97	71	62	148	39	168
	12	38	90	29	99	22	32	22
	13	39	107	138	97	82	70	25
	14	20	60	52	82	71	116	42
	15	34	85	19	116	34	25	34
	16	20	152	15	31	63	25	25
	17	58	766	23	16	117	76	39
	18	39	39	176	83	103	54	164
	19	72	52	102	55	30	40	74
	20	23	18	18	131	88	48	17
	21	83	90	750	84	76	80	41
	22	58	112	17	112	26	19	1088
	23	102	106	44	18	108	28	61
	24	38	33	41	22	213	46	49
	25	54	32	48	28	49	31	30
	26	958	97	50	22	1094	21	87
	27	62	29	72	34	225	35	76
	28	92	30	102	39	56	15	35
	29	76	108	43	68	75	19	29
	30	129	18	74	42	15	20	22
	31	83	37	119	58	353	22	81
	32	17	61	20	16	16	41	27
	33	31	44	24	27	57	48	51
	34	109	76	52	56	45	35	26
	35	32	18	53	32	47	61	57
	36	20	108	47	16	291	23	138
	37	30	76		34	33	70	153
	38	21	29		101	75	123	19
	39	60	85		25	94	32	113
	40	26	20		22	51	86	28
	41	26	39			25		70
	42	23	35			167		15
	43	119	56			129		31
	44	81	42			25		133
	45	25	32					21
	46	19	48					26
	47	33	48					37
	48	87	86					63
	49	72	17					41
	50	40	20					
	51		25					
	52		77					
	53		105					
	54		17					
	55		181					
	sum of area	3500	4053	2657	2328	4763	2086	4123
	number	50	55	36	40	44	40	49
	mean	70	73,6909091	73,8055556	58,2	108,25	52,15	84,1428571
	standard deviation	131,61	102,14	122,90	42,72	169,30	53,13	154,21
signficance	t-test	0,13738766	0,21210093	0,11009712	0,45252064	0,40493383	0,4822762	0,32799451
	t-test %	14%	21%	11%	45%	40%	48%	33%

Table 6: Statistics of cisternae measurement for the first measured leaflet at 0 minutes: measured areas in pixel^2, sum of area, number of measured areas, mean of areas and standard deviation; T-test values for significance of 0 minutes and after 15 minutes

First leaflet

15 minutes	area	1	2	3	4	5	6
	1	16	36	15	53	64	18
	2	206	281	77	413	64	192
	3	17	167	146	19	62	17
	4	454	127	69	235	71	2509
	5	2815	37	25	79	55	57
	6	34	1635	274	401	69	95
	7	504	122	44	47	161	214
	8	59	64	16	153	79	247
	9	18	16	219	179	66	35
	10	47	66	77	24	19	80
	11	266	51	169	20	23	31
	12	629	56	1008	1652	26	131
	13	63	51	108	43	31	17
	14	72	37	371	18	56	32
	15	16	65	81	48	203	105
	16	194	109	20	103	24	299
	17	303	121	18	110	48	19
	18	47	216	91	274	122	92
	19	28	59	58	32	44	24
	20	17	63	29	70	21	21
	21	22	35	32	17	25	24
	22		113	19	105	18	129
	23		111	786	39		48
	24		250	235	44		
	25		70	86	19		
	26		134	19			
	27		32				
	28		112				
	29		33				
	30		27				
	31		150				
	32		45				
	33		39				
	sum of area	5827	4530	4092	4197	1351	4436
	number	21	33	26	25	22	23
	mean	277,47619	137,272727	157,384615	167,88	61,4090909	192,869565
	standard deviation	609,37	276,60	237,98	329,30	46,9950951	511,367001

Table 7: Statistics of cisternae measurement for the first measured leaflet after 15 minutes: measured areas in pixel^2, sum of area, number of measured areas, mean of areas and standard deviation

Second leaflet

0 minutes	Area	1	2	3	4	5	6
	1	448	72	155	67	132	96
	2	23	32	44	43	19	302
	3	56	26	21	52	14	372
	4	34	18	10	30	22	732
	5	14	13	102	308	20	29
	6	276	23	10	128	65	68
	7	44	59	35	155	24	183
	8	76	247	18	95	64	53
	9	144	365	369	120	42	106
	10	31	15	28	59	30	99
	11	117	359	58	12	120	141
	12	89	146	390	24	84	42
	13	15	43	139	52	17	26
	14	10	34	39	197	27	87
	15	13	293	13	31	51	68
	16	139	32	8	60	28	43
	17	19	22	49	34	39	
	18	59	48	23	22	12	
	19	117	293	25	72	35	
	20	28	49	55	95	67	
	21	175	22	42	24	36	
	22	52	34	64	65		
	23	16	32	368			
	24	390	48	158			
	25	132		88			
	26	21		15			
	27	44		76			
	28	33		40			
	29	203					
	30	91					
	31	65					
	32	45					
	33	93					
	34	236					
	sum of area	3348	2325	2442	1745	948	2447
	number	34	24	28	22	21	16
	standard devi	105,6045325	117,342424	110,089982	69,4038467	33,2900672	182,492546

Table 8: Statistics of cisternae measurement for the first measured leaflet at 0 minutes: measured areas in pixel^2, sum of area, number of measured areas and standard deviation

32 minutes	Area	1	2	3	4	5	6
	1	806	241	367	354	68	104
	2	84	29	109	124	62	668
	3	125	94	95	40	40	51
	4	223	407	146	1283	28	63
	5	87	39	550	84	28	153
	6	1700	57	49	196	43	457
	7	85	190	111	31	65	61
	8	60	104	290	557	133	20
	9	72	206	106	64	376	27
	10	1190	111	51	676	185	255
	11	600	165	1657	298		38
	12	84	125	65			49
	13		393	27			19
	14		135	38			179
	15		297	23			38
	16		469	39			45
	17		60	40			72
	18		203	200			114
	19			33			42
	20			94			
	21			189			
	22			41			
	23			68			
	24			56			
	sum of area	5116	3325	4444	3707	1028	2455
	number	12	18	24	11	10	19
	standard devi	542,5242908	131,541005	337,508347	380,220988	108,177632	168,026314
	T-test	0,061088872	0,03151827	0,18466081	0,04907969	0,13078498	0,69391026
	T-test	6%	3%	18%	5%	13%	69%

Table 9: Statistics of cisternae measurement for the first measured leaflet after 32 minutes: measured areas in pixel^2, sum of area, number of measured areas and standard deviation; T-test values for significance of 0 minutes and after 32 minutes